Karlsruher Institut für Technologie

The virulence factor EinA (expressed in nematode) of *Arthrobotrys flagrans* induces self-digestion in *Caenorhabditis elegans*

Zur Erlangung des akademischen Grades einer

DOKTORIN DER NATURWISSENSCHAFTEN

(Dr. rer. nat.)

von der KIT-Fakultät für Chemie und Biowissenschaften

des Karlsruher Instituts für Technologie (KIT)

genehmigte

DISSERTATION

von

Master of Science

Meihang Du

1. Referent: Prof. Dr. Reinhard Fischer

2. Referent: Prof. Dr. Jörg Kämper

Tag der mündlichen Prüfung: 20.07.2023

Declaration

I hereby declare that I did all the work independently. All of samples, methods and sentences that were used or cited from sources were identified by specifying the respective source.

The regulation at the Karlsruhe Institute of Technology (KIT) to ensure appropriate scientific practice was read intensively. Furthermore, the submission and archiving of the primary data complied with the requirements at KIT to ensure good scientific practice.

Karlsruhe, den 12.06.2023 **Meihang Du**

Contents

Abstract

Nematode-trapping fungi change from a saprotrophic to a predatory lifestyle under low-nitrogen conditions and in the presence of nematodes. *Arthrobotrys flagrans* (formerly *Duddingtonia flagrans*) produces adhesive trapping networks as a result of the interplay of fungal- and nematode-derived low-molecular weight compounds. After trapping, several stages of the attack can be distinguished, penetration, the formation of an infection bulbus underneath the hypodermis, trophic hyphae growing inside the nematode and hyphae growing out of the nematode into the soil again. Bioinformatic analyses of the genome of *A. flagrans* revealed that the NTF secretome contains 249 SSPs. SSPs are well known for their roles in biotrophic or pathogenic microorganisms, but a role in predatory fungi was less obvious. So far, only one small secreted protein called CyrA was reported that it plays a role in virulence. We hypothesize that plenty of specific small-secreted proteins (SSPs) act at each step to enable the attack. Here we studied another possible virulence factor-EinA (Expressed Inside Nematodes).

EinA is a 112 amino acid long protein with a 20 amino acid signal peptide at the N-terminus and a predicted nuclear localization signal in the C-terminal region. The signal peptide was demonstrated to be functional, suggesting that EinA is secreted. Quantitative RT-PCR and a promoter-reporter assay revealed that the *einA* gene is expressed in trophic hyphae inside nematodes after a nematode was trapped. Localization with fluorescent proteins revealed that EinA localizes in vesicle-like structures in the trophic hyphae, suggesting that EinA play a role at later stages of the infection. In comparison to wild type *A. flagrans*, an *einA*-deletion strain took longer for digestion of *Caenorhabditis elegans*, while an *einA*-overexpression strain was faster. These results suggest a function of EinA in the digestion process.

Heterologous expression of EinA, with or without the signal peptide (SP), in *C. elegans* using the all-tissue promoter of *eft-3* and the heat-shock promoter *hsp-16.48* resulted in a reduced lifespan, delayed maturity, and varying degrees of deformity, suggesting toxicity of EinA to *C. elegans*. Heterologous expression of EinAΔSP-GFP in *C. elegans* under the *eft-3* promoter revealed nuclear localization. EinA-GFP lacking the SP and the NLS regions localized not to nuclei in *C. elegans* anymore and rendered the protein non functional. Hence, there was no influence on lifespan or the morphology of *C. elegans*. RNAseq analysis of *C. elegans* expressing EinA-GFP under the *eft-3* promoter and *hsp-16.48* promoter revealed upregulation of many genes associated with digestion pathways and involved in the transportation and secretion of hydrolases, including lysosomes, peroxisome, and phagosomes.

In conclusion, we hypothesize that EinA is secreted mainly from trophic fungal hyphae to target the nucleus of the surrounding *C. elegans* cells, potentially reprogramming the genome to induce self-digestion and facilitate hydrolysis of the prey. This may be a general principle for small predators who attack larger preys, such as spiders and insects.

Zusammenfassung

Unter stickstoffarmen Bedingungen und in Anwesenheit von Nematoden wechseln Nematoden-fangende Pilze (NFP) von einem saprotrophen zu einem räuberischen Lebensstil. *Arthrobotrys flagrans* (ehemals *Duddingtonia flagrans*) produziert durch das Zusammenspiel niedermolekularer Verbindungen von Pilzen und Nematoden adhäsive Fangnetzwerke. Nach dem Fang können mehrere Stadien des Angriffs unterschieden werden: Eindringen, die Bildung eines Infektionsbulbus unter der Hypodermis, trophische Hyphen, die innerhalb der Nematoden wachsen, und Hyphen, die wieder aus dem Nematoden heraus in den Boden wachsen. Bioinformatische Analysen des Genoms von *A. flagrans* ergaben, dass das NFP Sekretom 249 SSPs (small secreted proteins) enthält. SSPs sind für ihre Rolle bei biotrophen oder pathogenen Mikroorganismen bekannt, eine Rolle bei Nematoden-fangen Pilzen wurde noch nicht beschrieben. Bisher wurde nur über ein kleines sekretiertes Protein namens CyrA berichtet, welches eine wichtige Rolle bei der Virulenz einnimmt. Ich haben die Hypothese aufgestellt, dass bei jedem Schritt zahlreiche spezifische kleine Proteine wirken, um den Angriff zu ermöglichen. Hier haben wir einen weiteren möglichen Virulenzfaktor untersucht – EinA (Expressed Inside Nematodes).

EinA ist ein 112 Aminosäuren langes Protein mit einem 20 Aminosäuren langen Signalpeptid am N-Terminus und einem vorhergesagten Kernlokalisierungssignal im C-terminalen Bereich. Es wurde gezeigt, dass das Signalpeptid funktionsfähig ist, was darauf hindeutet, dass EinA sekretiert wird. Quantitative RT-PCR und ein Promotor-Reporter-Assay ergaben, dass das *einA*-Gen in trophischen Hyphen innerhalb von Nematoden exprimiert wird, nachdem ein Nematode gefangen wurde. Die Lokalisierung mit fluoreszierenden Proteinen ergab, dass EinA in vesikelartigen Strukturen in den trophischen Hyphen lokalisiert, was darauf hindeutet, dass EinA in späteren

Stadien der Infektion eine Rolle spielt. Im Vergleich zum Wildtyp *A. flagrans* benötigte ein Stamm mit *einA*-Deletion länger für die Verdauung von *C. elegans*, während ein Stamm mit *einA*-Überexpression schneller war. Diese Ergebnisse legen eine Funktion von EinA im Verdauungsprozess nahe.

Die heterologe Expression von EinA mit oder ohne Signalpeptid (SP) in *C. elegans* unter Verwendung des gewebeübergreifenden Promotors von *eft-3* und des Hitzeschock-Promotors *hsp-16.48* führte zu einer verkürzten Lebensdauer, einer verzögerten Reife und unterschiedlichem Ausmaß einer Deformität, was auf eine Toxizität von EinA gegenüber *C. elegans* schließen lässt. Die heterologe Expression von EinAΔSP-GFP in *C. elegans* unter dem *eft-3*-Promotor zeigte eine Kernlokalisation (NLS). EinA-GFP, dem das SP- und die NLS-Region fehlten, lokalisierte sich mehr in den Kernen von *C. elegans* und machte das Protein funktionsunfähig. Daher gab es keinen Einfluss auf die Lebensdauer oder die Morphologie von *C. elegans*. Die RNAseq-Analyse von *C. elegans*, der EinA-GFP unter dem *eft-3*-Promotor und dem *hsp-16.48*-Promotor exprimiert, ergab eine Hochregulierung vieler Gene, die mit Verdauungswegen verbunden sind und am Transport und der Sekretion von Hydrolasen beteiligt sind, einschließlich Lysosomen, Peroxisomen und Phagosomen.

Zusammenfassend gehen wir davon aus, dass EinA hauptsächlich aus trophischen Pilzhyphen ausgeschüttet wird, um auf den Zellkern der umgebenden *C. elegans*-Zellen abzuzielen und möglicherweise das Genom neu zu programmieren, um die Selbstverdauung zu induzieren und die Hydrolyse der Beute zu erleichtern. Dies könnte ein allgemeines Prinzip für kleine Raubtiere sein, die größere Beutetiere angreifen, wie Spinnen und Insekten angreifen.

1. Introduction

1.1 Nematode-trapping Fungi (NTF)

Nematophagous fungi (NF), an important group of carnivorous microorganisms, suppress the population of plant and animal parasitic nematodes (Nordbring-Hertz *et al*., 2001). They can be classified into four major classes according to their infective strategies: (1) nematode-trapping fungi (NTF) capture, kill, and digest nematodes as nitrogen resource using adhesive or mechanical hyphal traps, when the nematodes are present, or under nitrogen-limiting conditions (Barron, 2003); (2) endoparasitic fungi using their spores; (3) opportunistic fungi using appressoria with the accumulation of mucilaginous materials as adhesives and penetrate nematode's eggs (Niu *et al*., 2011); (4) fungi that immobilize nematodes by using toxins before invasion (Hyde *et al*., 2014). Among that, NTF, as a potential biological control agent of nematodes, has been extensively studied and researched. To capture nematodes, NTF form hyphal rings and five types of adhesive traps (sessile adhesive knobs, stalked adhesive knobs, adhesive nets, adhesive columns, and non-constricting rings) **(Fig. 1)** (Jiang *et al*., 2017)**.** NTF belong to a heterogeneous group of asexual ascomycetes based on conidia and the type of conidiogenesis (Li *et al*., 2005). According to the trap devices nematode-trapping fungi have been classified as *Arthrobotrys*, *Dactylella*, *Dactylaria*, and some other genera (Pfister, 1994). With the development of phylogenetic studies based on rDNA sequence analysis, a new genus concept for predatory *Orbiliaceae* fungi was proposed by Scholler (Hagedorn & Scholler, 1999). I studied *Arthrobotrys flagrans* which belongs to the *Athrobotrys* section and is closely related to *Arthrobotrys oligospora* (Baral *et al*., 2018; Youssar *et al*., 2019).

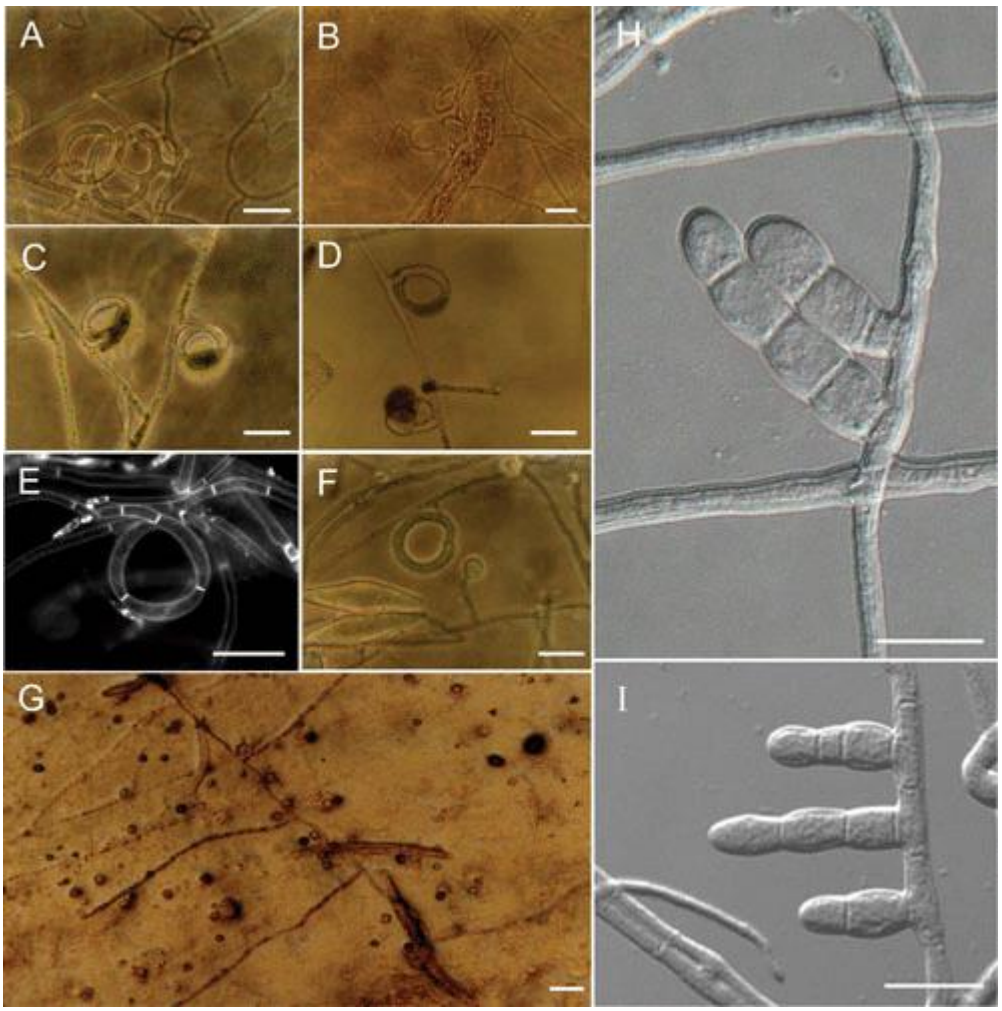

Fig. 1: Structures of traps in nematode-trapping fungi (Jiang *et al*., 2017)**. (A, B)** Adhesive networks of *Arthrobotrys oligospora*. Bar, 20 µm. **(C–E)** Constricting rings of *Drechslerella stenobrocha*. Bar, 20 µm. **(F)** Adhesive knobs and nonconstricting rings of *Dactylellina haptotyla*. Bar, 20 µm. **(G)** Nematode trapped by *D. haptotyla*. Bar, 40 µm. **(H, I)** Adhesive columns of *Gamsylella cionopaga*. Bar, 20 µm.

1.2 Life cycle and trap formation of *A. flagrans*

Arthrobotrys flagrans was first characterized by Duddington in 1948. This fungus was characterized by hyaline and septate hyphae with a diameter of 3-5 µm. Duddington described its conidia, the length of 20-200 µm, as obconical to ellipsoidal, one septate, and with broadly truncate proximal cell **(Fig. 3 D)** (Duddington, 1949). *A. flagrans* also can produce some chlamydospores that are spherical, non-hyaline and intercalate, manifesting numerous globular

protuberances on their surface **(Fig. 3 E - G)** (Balbino *et al*., 2022). The typical adhesive network trap produced by *A. flagrans* consists of one to several loops attached to each other. An initial branch forms from a parental hypha and curves around to meet the parent hypha to develop a loop typically containing three cells, which have special organelles called dense bodies and have the ability to capture nematodes (Haj *et al*., 2022; Nordbring-Hertz & Stålhammar-Carlemalm, 1978). Another feature that is unique to trap cells is the presence of extensive layers of extracellular polymers that consists of proteins and carbohydrates, which have been considered to be important for the attachment of the traps to nematode surfaces and carry many extracellular toxic compounds with nematicidal effects (Tunlid, & Jansson, 1991; Liang *et al*., 2013). Apart from that, it was also found that the traps always accumulated a higher K^+ content than hyphae, which might be responsible for the pronounced turgidity of the traps (Veenhuis *et al*., 1985).

How does *A. flagrans* determine the exact time to develop the traps? In the absence of nematodes, *A. flagrans* produces some chemicals, like polyketide-derived arthrosporols and 6-MSA, to inhibit trap formation (Zhang *et al*., 2012; Yu *et al*., 2021). When nematodes are present, a family of small-molecule pheromones called ascarosides are produced by nematodes, which mediate distinct behaviors of the nematode, such as olfactory plasticity, avoidance, and long-range gender attraction (Hsueh *et al*., 2013; Pungaliya *et al*., 2009; Golden & Riddle, 1982; Yamada *et al*., 2010; Srinivasan *et al*., 2012; Edison, 2009). This kind of product caused the downregulation of arthrosporols synthesis. Subsequently, the trap formation also would be activated **(Fig. 2)** (Yu *et al*., 2021). That is why nematodes could be recognized by fungi without contact (Choe *et al*., 2012). Trap formation, as the most important indicator, requires biotic and abiotic stimulation. The presence of nematodes and a nutrient-defective environment are the prerequisites for switching from a saprotrophic to a predatory lifestyle (Yang *et al*., 2011; Tunlid *et al*., 1992).

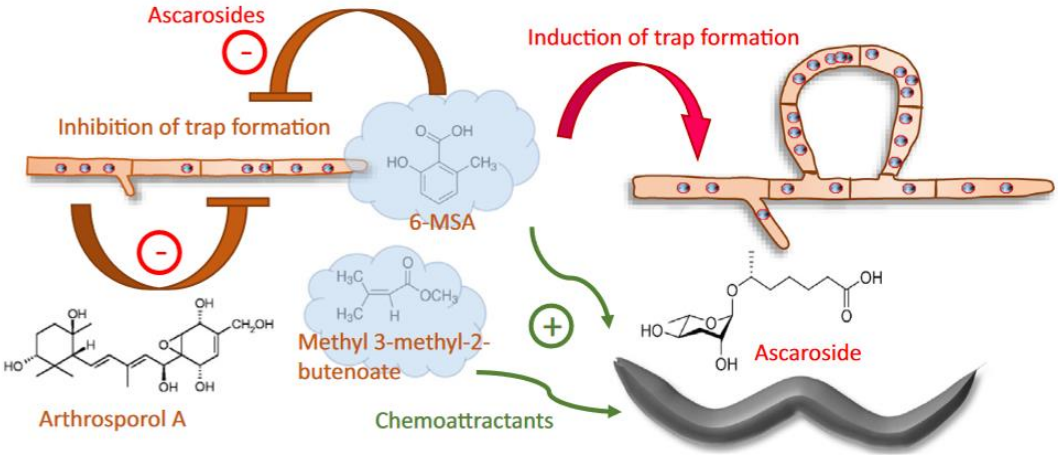

Fig. 2: Scheme for the trap initiation (Fischer & Requena, 2022)**.** Arthrosporols and 6-MSA inhibit trap formation in *A. flagrans*. 6-MSA and other small volatiles, such as methyl-3-methyl-2-butenoate, attract *C. elegans*, and nematode-derived ascarosides inhibit the production of the trap-inhibiting molecules, thereby inducing trap formation. Another prerequisite for the transition from saprotrophic growth to a predatory lifestyle is nutrient starvation.

Once traps are shaped, some attractive and sticky substances will be produced to capture nematodes during their soil migration (Nordbring-Hertz *et al*., 2001; Fischer & Requena, 2022). It only takes about one to four hours from adhesion to penetration, depending on the fungal or nematode species. Here, the cuticle is penetrated by mechanical pressure or destroyed by some lytic enzymes, with a rounded penetration structure being formed. After the nematode is paralyzed, trophic hyphae grow throughout the nematode body and absorb the nutrients by degrading the host cells. After a few hours, the worm is digested completely **(Fig. 3 A - C)** (Jin *et al*., 2011; Dijksterhuis *et al*., 1994). Unlike adhesive traps, constricting rings kill nematodes via mechanical pressure, composing the rings swell inward rapidly and closing around the nematodes (Liu *et al*., 2012). It has been suggested that this release of wall pressure is caused by a rapid uptake of water, followed by expansion of the elastic inner wall of the ring cells (Yang *et al*., 2007; Nordbring-Hertz & Mattiasson, 1979).

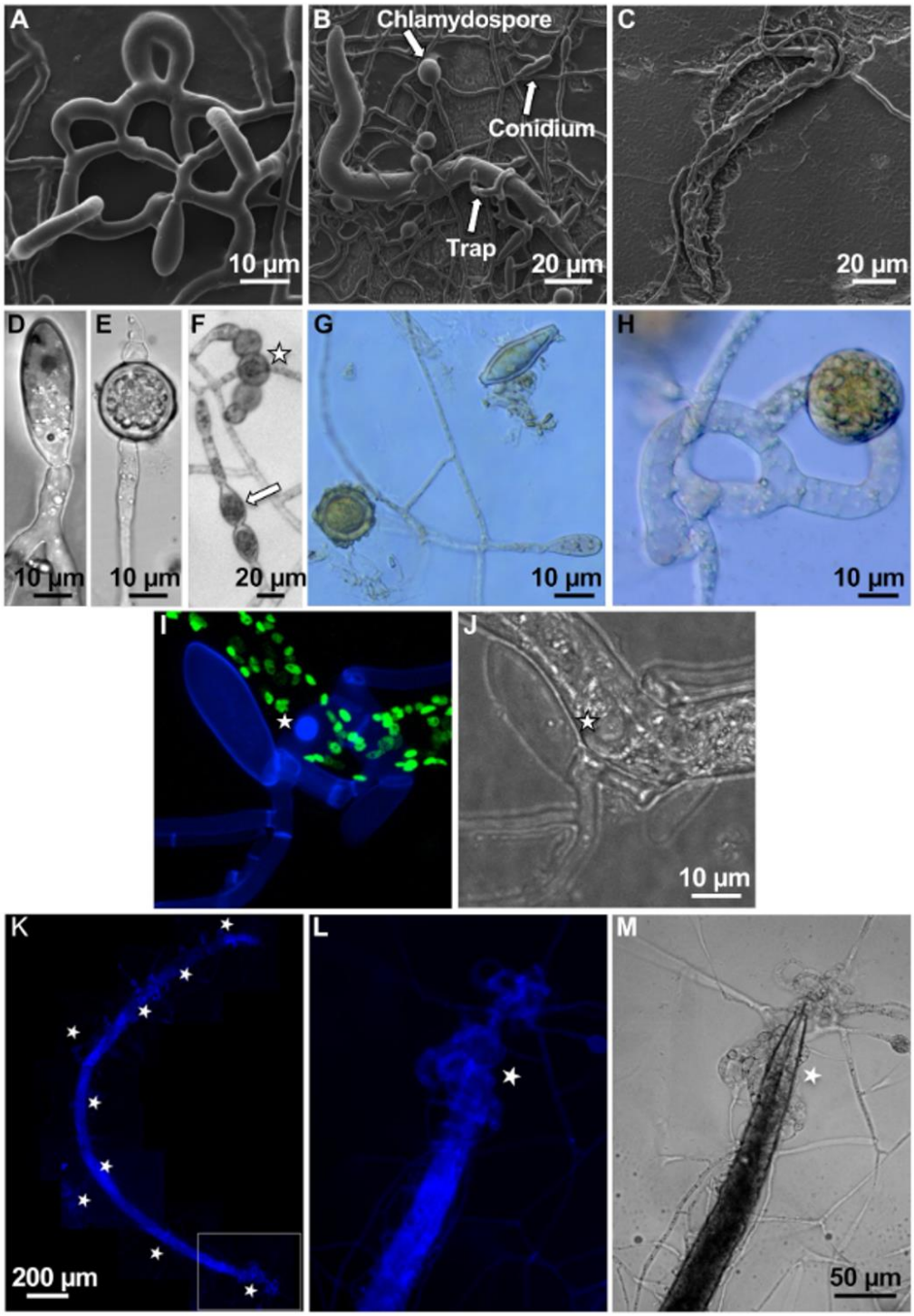

Fig. 3: The nematode-trapping fungus *A. flagrans* produces adhesive traps, spores, and chlamydospores (Youssar *et al*., 2019)**. (A)** Formation of a three-dimensional trapping network. **(B)** Trapped nematode *C. elegans*. Chlamydospores, normal spores and traps are labelled with arrows. **(C)** Complete degradation of *C. elegans* and fungal growth inside the nematode. **(D)** Asexual spore. **(E)** Chlamydospore. **(F)** Conversion of single trap-compartments into chlamydospores (star) compared to the conversion of

vegetative cells (arrow). **(G, H)** Glycogen staining with Lugol‘s iodine. **(I, J)** Visualization of ringlike accumulation of chitin (star) at the contact zone of trap cells with the nematode cuticle. **(K)** A *Xiphinema index* adult trapped in multiple *A. flagrans* networks. **(L, M)** Magnification of the framed area in **(I).**

The infection processes have been studied with some techniques, such as light and low-temperature electron microscopy and bioassays, and have been supported by biochemical, physiological, immunological, and molecular techniques (Thorn & Barron, 1979; Murray & Wharton, 1990; Jansson *et al*., 2000). Nematophagous fungi have been reported to produce nematotoxins that immobilize or kill nematodes. Some kinds of extracellular hydrolytic enzymes, like chitinases, collagenases, and proteases, are involved in the penetration of the nematode cuticle based on ultrastructural and histochemical studies (Schenck *et al*., 1980). When nematodes come into contact with adhesive hyphae, chitin accumulates in trap cells that are in contact with the nematode cuticle **(Fig. 3 I - J)**. In this adhesive process, lectins are also important for binding to carbohydrates on the surface of the nematodes (Zhang *et al*., 2020). Subsequently, the glucose metabolism and the pentose phosphate pathway were activated, and a great number of neutral sugars like mannose, galactose, and glucuronic acid were produced, which contributes to the adhesive process (Liang *et al*., 2019). In the next step of the fungus-nematode interaction, the secretion of proteases, with emphasis on the peptidases of the serine family, occurred in large quantities, to facilitate the penetration of the fungal hyphae (Zhang *et al*., 2020; Braga *et al*., 2012). On the other hand, some secondary metabolites participate in the infection process. For *A. flagrans*, three polyketide synthases (PKS) and three non-ribosomal peptide synthases (NRPS), and these proteins are responsible for the production of most secondary metabolites that correspond to polyketides and peptide derivatives are activated (Youssar *et al*., 2019). For nematodes, sphingolipid metabolites that affect the nervous system of nematodes and the formation of the stratum corneum epidermis are triggered and cause nematode death (Chiang *et al*., 2014; Liang *et al*., 2019).

1.3 Regulatory mechanisms of trap formation in nematode-trapping fungi

The molecular basis of trap formation is still largely unexplored. However, comparative genomics and multi-omics results showed that trap formation likely requires the coordination of multiple pathways **(Fig. 4)** (Zhu *et al*., 2022). The G-protein signaling pathway was important for trap formation by reception and transduction of signals from nematodes. The deletion *gdb1* and *fus3* genes abolished trap formation because of the lack of phosphorylation signals (Chen *et al*., 2021). Deletion of regulators of G protein signaling (*rgs*) genes increased the intracellular cAMP levels and decreased the transcription levels of G-protein signaling genes, suggesting that G-protein regulates the cAMP/PKA and MAPK signaling pathways to participate in the trap formation (Ma *et al*., 2021). In addition, some small GTPases family act as switches in the signaling hub of molecular circuits (Takai *et al*., 2001). For instance, the deletion of *cdc42* and *rac* genes downregulated the expression level of genes encoding regulator subunits of PKA, MAPK, and P21-activated kinases in *A. oligospora* (Yang *et al*., 2022). HOG1 (hyperosmolarity pathway) downregulated effectors of RHO GTPases in *A. oligospora*. STE50 affect MAPK signaling directly by interacting with RAS GTPases and regulate MAPK, TOR, and cAMP/PKA indirectly (Yang *et al*., 2021). Meanwhile, reverse genetics suggested that the MAPK cascade activated STE12 in *A. oligospora* to trigger trap formation (Chen *et al*., 2021). These results indicated that multiple signaling pathways co-regulate trap formation (Zhu *et al*., 2022). Apart from that, some gene deletions have already identified some of the factors involved. In a previous study, the deletion of an NADPH oxidase, NoxA, in *A. oligospora* led to a reduction in trapping, suggesting an important role in reactive oxygen species (ROS) production (Li *et al*., 2017). The deletion of peroxisome biogenesis proteins encoded by *PEX1* and *PEX6* genes induces trap formation and lifestyle switching in *A. oligospora*

(Liu *et al*., 2022). The deletion of STRIP1/2 ortholog SipC in *A. flagrans* resulted in a reduction of septa and trap compartments of very different sizes (Wernet *et al*., 2022). The *sofT* and *makB* genes were identified as important in the ring closure step. The deletion of the *sofT* and *makB* genes prevented the formation of spiral hyphae and inhibition of anastomoses in vegetative hyphae (Youssar *et al*., 2019; Hammadeh *et al*., 2022).

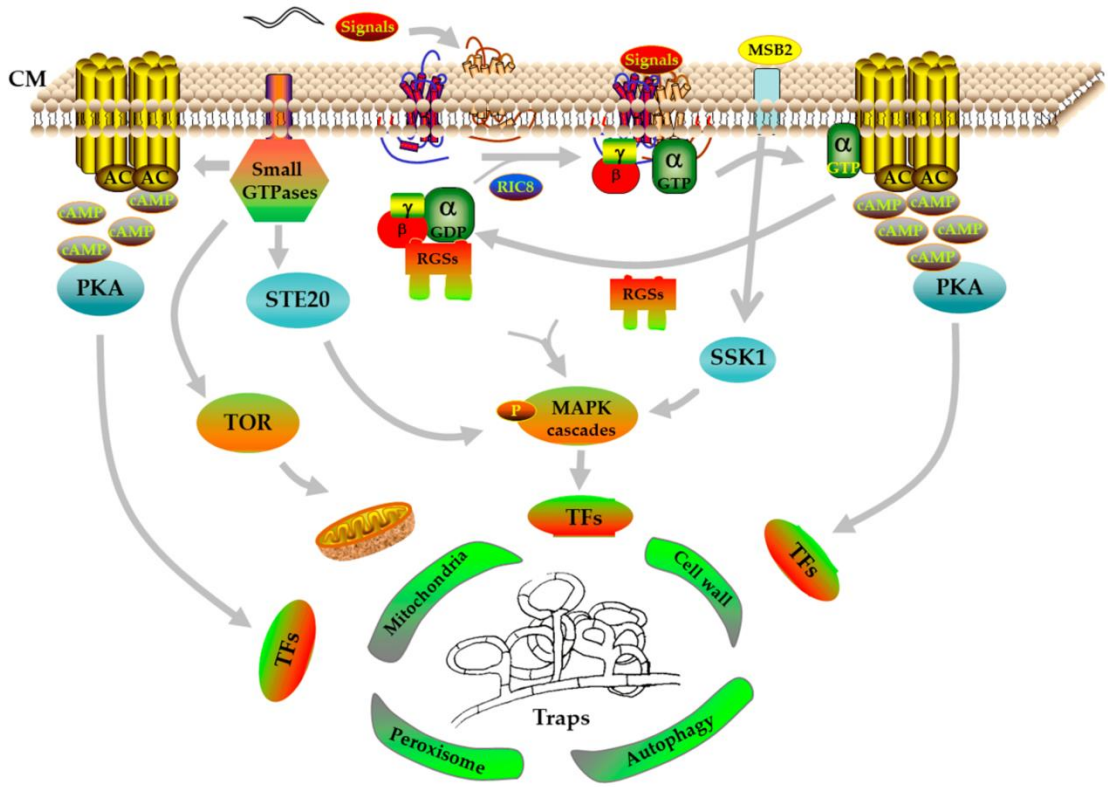

Fig. 4: Proposed model for trap formation in NT fungi using *A. oligospora* as an example (Zhu *et al*., 2022)**.** CM, cell membrane; α, β, and γ, G-protein subunits; AC, adenylate cyclase; cAMP, cyclic adenosine monophosphate; PKA, protein kinase A; RGSs, regulators of G-protein signaling; RIC8, resistance to inhibitors of cholinesterase; MAPK, mitogen-activated protein kinase; STE20, serine/threonine protein kinase; TOR, mammalian target of rapamycin; MSB2, mucin family signaling protein; SSK1, response regulator; TFs, transcription factors; P, phosphorylation.

1.4 Application of *A. flagrans* as a biocontrol agent in agriculture and domestic settings

Due to the extensive distribution and parasitic range, plant-parasitic nematodes (PPNs) pose a considerable global threat to agriculture (Ansari *et al*., 2012; Abd-Elgawad & Askary, 2015; Abd-Elgawad, 2014; Abd-Elgawad, 2020). It is estimated that the economic losses in crop yield due to plant-parasitic nematodes amount to approximately $ 170 billion globally (Coyne *et al*., 2018; Jone *et al*., 2013; Singh & Singh, 2015). Besides causing damage individually to crops, PPNs can collaborate with other micro-organisms, exacerbating the extent of crop losses (Singh & Singh, 2015). The conventional approach of utilizing chemical insecticide agents, like methyl bromide and dibromochloropropane, for control and management has been banned due to their adverse effects on human health and the environment (López-Robles *et al*., 2013; Kumari, S., 2017). Alternative measures against nematode diseases should be considered, such as the utilization of clean nematode-free planting, the cultivation of resistant varieties, crop rotation, and the application of environmentally friendly biocontrol agents (Amer-Zareen *et al*. 2004; Singh *et al*., 2015; Brand *et al*., 2010; Abd-Elgawad, 2020). Some reasons demonstrate that *A. flagrans* is the most promising biological nematicide. Firstly, *A. flagrans* form a three-dimensional trap network to capture nematodes. Secondly, *A. flagrans* live worldwide; it has been isolated from continental Europe (Larsen *et al*., 1991), Austria (Larsen *et al*., 1994), North and South America (Mahoney & Strongman, 1994), and Asia (Wang *et al*., 2015), which avoids destroying the local ecological balance. Thirdly, *A. flagrans* can produce resistant chlamydospores with a thick-walled structure and reserve of substances (glycogen), which give the fungus an advantage in survival-adverse environments (Silva *et al*., 2010). Based on this, chlamydospores were incorporated into food pellets as a means to control nematode infestations

(Vilela *et al*., 2016; Vilela *et al*., 2012). These spores have the remarkable ability to pass through the gastrointestinal tract of domestic animals unscathed, subsequently only germinating in the dung, which ensures the animals remain unharmed during the control intervention (Epe *et al*., 2009; Silva *et al*., 2009). For instance, in a laboratory setting, sodium-alginate pellets containing *A. flagrans* spores were introduced into vineyard soil, resulting in a significant reduction in the population of *Xiphinema index* juveniles within pot cultures of *Ficus carica* (Wernet & Fischer, 2023). These advantages indicate that *A. flagrans* is robust, facilitating its use in crops and domestic industry. There are cases where the products based on *A. flagrans* have been successfully marketed as biocontrol agents. In 2019, the first product (Bioverm) was registered in Brazil for testing nematodes in sheep, chickens, equines, and llamas by providing sodium alginate pellets containing conidia and chlamydospores (Balbino *et al*., 2022).

1.5 Effector proteins and virulence factors of pathogenic fungi

In the case of NTF it was assumed that the attack does not require small effector proteins or virulence factors but that lytic enzymes are secreted which dissolve the cuticle of the nematode and after penetration hyphae produce lytic enzymes for digestion (Pires *et al*., 2022; Al-Ani *et al*., 2022). However, genome analyses in several NTF revealed the presence of many SSPs, i.e., 312 SSPs in the nematode endoparasite *Dr. coniospora*, 695 SSPs in the nematode-trapping fungus *Da. Haptotyla*, and 249 SSPs, in the *A. flagrans* (Zhang *et al*., 2016; Andersson *et al*., 2013; Youssar *et al*., 2019). there is speculation regarding the presence of stage-specific effectors that aid in the infection process **(Fig. 5)** (Fischer & Requena, 2022) The function of most SSP is still unknown. However, many functions can be envisioned if the interaction is as sophisticated as in the case of other organismic interactions.

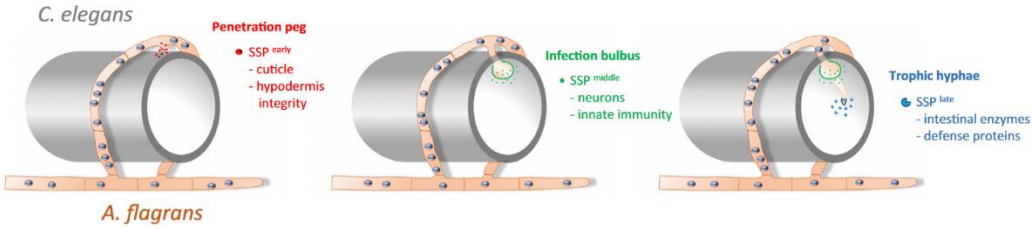

Fig. 5: Scheme for the penetration process. The fungal small-secreted proteins (SSPs) may be divided, according to their time of action, into early-, middle-, and late-stage SSPs. Putative targets of the virulence factors are named. Species: *A. flagrans*, *Arthrobotrys flagrans*; *C. elegans*, *Caenorhabditis elegans*.

The dynamic coevolution between effector proteins of the pathogen and host target genes contributes to the complexity and intricacy of their interactions. The genetic evolution of effector proteins is achieving optimal toxicity and evading host detection. Meanwhile, the long-term evolution of pathogens relies on the continual emergence of novel effector proteins, which can replace those that have become less competitive infections (Lo Presti *et al*., 2015).

Secreted effector proteins from genome sequences could be identified with general criteria and bioinformatics approaches. Frequently, effector proteins are defined as small, secreted, cysteine-rich proteins containing ⩽300 amino acids (Duplessis *et al*., 2011; Chin *et al*., 2016; Martin *et al*., 2008; Martin *et al*., 2010; Sperschneider *et al*., 2015). A criterion frequently used to define effectors is the absence of detectable orthologous proteins outside the genus (O'Connell *et al*., 2012; Godfrey, 2010; Wicker *et al*., 2013). Another frequent criterion is specific expression during the infection process, including stage-specifically and organ-specifically expressed (Axmacher *et al*., 2010; O'Connell *et al*., 2010; Skibbe, 2000; Farman, & Leong, 1998). However, nothing is absolute in the world. Some proteins are defined as effector proteins, even though they do not meet these criteria. For instance, the AvrLm1 effector from the hemibiotrophic

pathogen *Leptosphaeria maculans* that colonizes the apoplast has only one cysteine (Gout *et al*., 2006). Some effectors discovered from plant pathogens always have the conserved domain, which often exhibits a specific structural motif or functional motif that enables their interaction with host proteins or cellular components. For instance, it was demonstrated that the effector of Ecp6 with three LysM domains to prevent chitin-triggered immunity in plants (De Jonge *et al*. 2010), the effector of AVR3a from the oomycete pathogen *phytophthora infestans* has the RxLR domain on N-terminus that is required for host-cell entry (Yaeno *et al*., 2011). Many large proteins can also be defined as effector proteins (Djamei *et al*., 2011). Due to the rapid divergence and host specialization, our knowledge of effector proteins' general features is limited, so effector protein prediction via machine learning approaches remains challenging. Molecular studies have identified more than 60 fungal effector proteins from different species with a broad spectrum of activity. The protein described so far represents only the tip of the iceberg. Its number continues to increase with sequenced pathogen genomes and the possibility of bioinformatic prediction of these proteins (Sperschneider *et al*., 2013). Apart from their molecular feature, effectors can be classified according to their site of action in the host. For instance, in the plant, apoplastic or intracellular. Effector proteins localized in the latter prefer to target host proteins in the cytoplasm and cell organelles, like the nucleus, mitochondria, ER, or chloroplasts **(Fig. 6)** (Kamoun, 2006; Lo Presti *et al*., 2015; Rocafort *et al*., 2020; Figueroa & Henningsen, 2021). Furthermore, some effectors may be specific to some strains or isolation of a species, making them race-specific effectors. In contrast, other effectors that are found in distantly related species are referred to as “core effectors” (Schulze-Lefert & Panstruga, 2011; Hoang *et al*., 2021; Bourras *et al*., 2019).

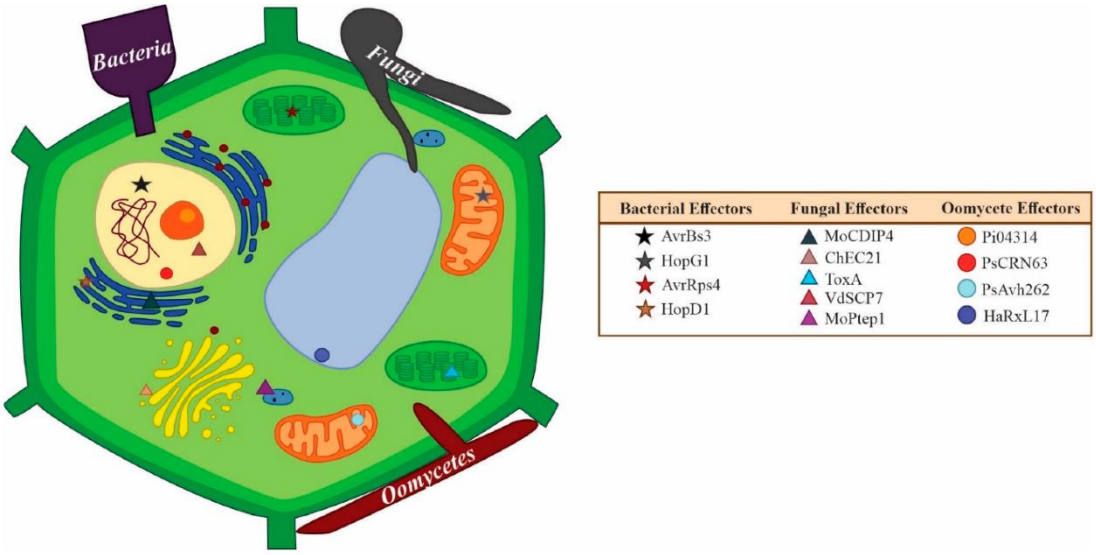

Fig. 6: Examples of effectors and their intracellular targets. Secreted effectors enter the cell apoplast before they reach the interior of the cell; some are retained in the apoplast if their targets are apoplastic while others traverse the cell membrane to reach their targets inside the cell. In the intracellular, the effectors AvrBs3, HopG1, AvrRps4, and HopD1 from bacterial target the nucleus, mitochondria, chloroplast, and endoplasmic reticulum (ER), respectively. The effectors AvrSr35, ChEC21, ToxA, VdSCP7, and MoPtep1 from fungi target the ER, Golgi, chloroplast, nucleus, and peroxisomes, respectively. The oomycetes effectors Pi04313 and PsCRN63 target the nucleus while PsAvh262 targets the mitochondria and HaRxL17 associates with the plant tonoplast (vacuolar membrane).

The molecular functions of effectors and virulence factors are diverse based on the infection strategy; they can change the cell biology of the host, inhibit stress and defense mechanisms, alter metabolism, or interfere with immune signaling cascades (Lanver *et al*., 2017). Apoplastic effectors may inhibit plant lytic enzymes, such as proteases, chitinases, or glucanases, to stop the release of fungal elicitors, like cell wall fragments, or detoxify antimicrobial compounds produced during the infection (Doehlemann & Hemetsberger, 2013). LysM effectors can bind to soluble chitin oligomers to prevent their recognition by plant immune receptors (Sánchez-Vallet *et al*., 2013). Pit2 can inhibit four cysteine proteases that are directly associated with salicylic acid-associated plant defenses (Asadulghani *et al*., 2009). The translocated effector, Tin2,

interacts with the cytoplasmic maize protein kinase ZmTTK1 to prevent its ubiquitylation and proteasome-dependent degradation (Tanaka *et al*., 2014). See1, the localization in cytoplasm and nucleus of plant cells, contributes to tumor progression in maize leaves by activating host DNA synthesis and cell division in leaf tissue (Redlkar *et al*., 2015). SP7, an effector protein secreted from *Glomus intraradices* to the nucleus of plant root cell, contributed to develop the biotrophic status by counteracting the plant immune program (Kloppholz *et al*., 2011). In a comparative study of effector targets of bacterial, oomycetes, and fungi, 95% of bacterial effectors, 65% of oomycetes effectors, and 61% of fungal effectors of targets are in the cell membrane, cytoplasm, and nucleus. It was also found that 28% of effectors in fungi localized in the nucleus to have a function (Khan *et al*., 2018). It suggests that three main strategies were applied to effect host transcription for the nuclear-target effectors (Canonne *et al*., 2012): (1) mimic transcription factors that directly activate transcription in host cells. For instance, AvrBs3 from *Xanthomonas campestris pv vesicatoria* bind to *UPA20* promoter to induce the expression of *UPA20* and result in cellular hypertrophy (Canonne & Rivas, 2007). (2) alter histone packing and chromatin configuration. The bacterial effector OspF from the animal pathogen *Shigella flexneri* can suppress the expression of specific immunity-related genes by inducing histone dephosphorylation and deacetylation to inactivate MAPKs. (3) target or compete with transcription factors directly. PopP2 from *R solanacearum* can target and affect the transcriptional activity of RRS1-R involved in plant disease resistance (Arbibe *et al*., 2007). Nuclear RD19, with the function of a transcriptional activator, may complete with RRS1-R to affect the expression of some defense-relative genes (Beck *et al*. 2012).

During the interaction with nematode-trapping fungi and nematodes, genome and transcriptome analyses of these fungi during the infection represent the most important point of characterization of effectors or virulence factors (Ahren *et al*., 2005; Andersson *et al*., 2014). An analysis with the transcriptome data of

three nematode-trapping fungi *Monacrosporium ciinopagum*, *Arthrobotrys dactyloides* and *A. oligospora* performed a BLAST search of the 500 most highly regulated transcripts in the pathogen-host interaction protein database (PHI-base), including virulence, pathogenicity and effector genes from fungi, oomycetes, and bacterial pathogens (Andersson *et al*., 2014). Proteins with Pfam domains (protein families) associated with known fungal virulence factors, such as the CFEM or DUF domain, were upregulated (Meerupati *et al*., 2013). Orthologs of the Gas1 and Gas2 which contain DUF3129 domain from *Magnaporthe grisea* were identified. RBT4 orthologous proteins with a CAP domain from *Canadida albicans* also were identified (Andersson *et al*., 2014). Apart from that, some small secreted novel proteins were found to upregulate during the infection. 249 SSPs from *Arthobotrys flagrans*, 695 SSPs from *Dactylellina Haptotyla*, and 312 SSPs from *Drechslerella coniospora* were identified. In *A. flagrans*, only 24 SSPs had Pfam annotations in InterProScan. 14 SSPs contained at least five cysteines. 110 SSPs were predicted effectors or virulence factors (Youssar *et al*., 2019). Among that, CyrA was identified as the first example of a virulence factor in *A. flagrans*, which is required for full virulence of the fungus (Wernet *et al*., 2021).

1.6 Nematodes

Caenorhabditis elegans was found worldwide, often on rotting fruit, where it likely consumes nutrient-rich substrates and bacteria (Kiontke & Sudhaus, 2006; Kiontke *et al*., 2011). It was selected as an experimental model for animal developmental by Sydney Brenner in the early 1960s (Culetto & Sattelle, 2000). Because of the transparent body, simple but integrity organelle, short lifespan, and the availability of a detailed and precise genetic map (Brenner, 1974; Kiontke & Fitch, 2013). It has a short lifespan. The average lifespan of *C. elegans* at a standard temperature of 20 °C is approximately 2-3 weeks. It just takes three days developing from embryo to adulthood. A single adult

hermaphrodite gives birth to a large number of progeny (>300) by self-fertilization facilitating the establishment of a large animal population (Culetto & Sattelle, 2000). Another advantage of making *C. elegans* as a model is that mutagenesis can be easily operated by feeding worms on bacteria with expression of respective gene-specific dsRNAs. The aspects of host-pathogen interaction can be studied in this simple metazoan due to containing the highly complex immunity of vertebrates but simple ancestral signaling networks (Ermolaeva & Schumacher, 2014). *C. elegans* can also be used to investigate human diseases because the orthologue of a large fraction of human disease genes was found in *C. elegans* (Mushegian *et al*., 1997). At least 38% of protein-coding genes have orthologs in the human genome, and 40% of genes associated with human diseases have an ortholog in the *C. elegans* genome (Campbell & Fares, 2010; Zhu *et al*., 2016).

C. elegans can be maintained cost-effectively on agar plates typically containing *Escherichia coli* OP50 strain as a food source (Sydney, 1974). The main organelle of *C. elegans* comprises a simple nervous system, pharynx, intestine, and gonad **(Fig. 7)**. The nervous system of the adult hermaphrodite is composed of only 302 neurons. Based on their structure, these neurons could be classified as sensory neurons, interneurons, and motor neurons (Bargmann, 1993). A particular neuron structure called the nervous ring receives processes from about three-quarters of neurons (White *et al*., 1986; Chalfie & Sulston, 1981). These neurons regulate many behaviors. Mechanosensory neurons mediate an escape response to light touch. Egg-laying and feeding require one pair of motor neurons (Chalfie *et al*., 1985; Thomas, 1990). At the posterior end of the pharynx is the grinder, a cuticular structure that mechanically breaks up food particles. At the posterior end of the grinder is the intestine. Partially broken-down food enters the intestine lumen that gets exposed to enzymes that break down membranes and lipid constituents, such as lysozymes, saponins, and lectins (Gravato-Nobre *et al*., 2016; Tarr, 2012). The intestine is a simple

tube containing 20 cells arranged as rings, which lack the capacity to replace somatic cells. At the anterior, four cells form the ring int1. The remaining 16 cells are arranged in pairs, with each pair forming rings int2 through int9. On the apical side of gut cells is the lumen, with weakly acidic around pH 4.4, which is lined with membranous microvilli that form the brush border (Allman *et al*., 2009). Its function is not only to digest and absorb nutrients but also to have roles in immunity, longevity, pathogen infection, and detoxification of metals (Dimov & Maduro, 2019; Block *et al*., 2015; Ezcurra *et al*., 2018; Pukkila-Worley & Ausubel, 2012).

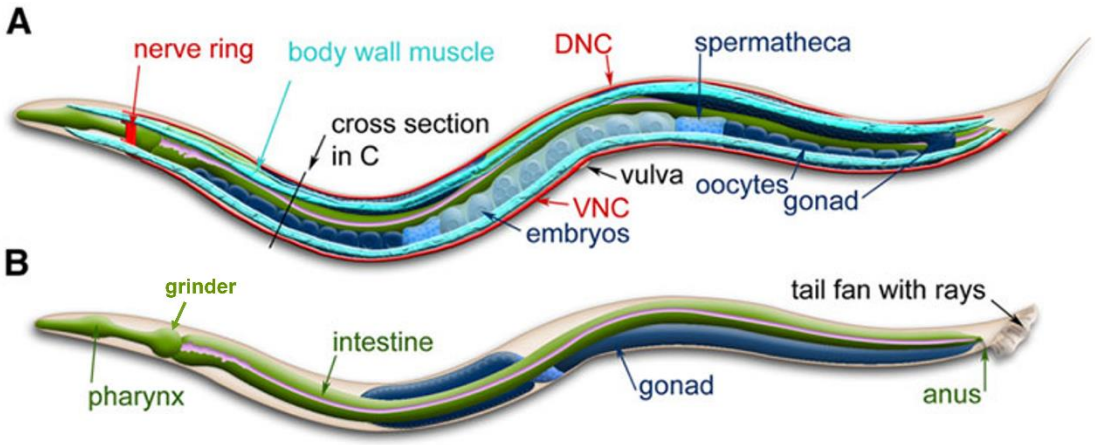

Fig. 7: *C. elegans* anatomy (Corsi *et al*., 2005)**.** Major anatomical features of a hermaphrodite **(A)** and male **(B)** viewed laterally.

1.7 Immune system of *C. elegans*

The immune defense of *C. elegans* lacks cellular immune mechanisms based on phagocytosis of microorganisms and encapsulation of larger foreign bodies (Hoffmann *et al*., 2003; zou *et al*., 2002; Ewbank, 2002). Meanwhile, like many other invertebrates, *C. elegans* does not have an adaptive immune system; instead, the nematode must rely entirely on innate immunity. It is of great relevance for the free-living terrestrial organism since it feeds on bacteria and is thus constantly exposed to potential pathogens. Four main strategies are

available to *C. elegans* for defense against microbial attacks. (1) Avoidance behavior: *C. elegans* can distinguish between pathogen bacterial and bacterial as a food source by odors (Zhang *et al*., 2005). (2) like human beings with skin as a physical barrier, *C. elegans* can utilize cuticles to prevent pathogen invasion. In addition, the pharynx grinder can destroy orally bacterial, and the intestine lumen space and outside of the microvilli is the glycocalyx which is a glycoproteins-rich region that provides a physical barrier from pathogens, serves as the interface between digestive enzymes and macromolecules, and allows filtering of lumen contents entering gut cells (McGhee, 2007; Kurz & Tan, 2004). (3) One mechanism for detecting and discriminating microbes involves the recognition of pathogen-associated molecular patterns (PAMPs) or a more accurate strategy of microbe-associated molecular patterns (MAMPs) (Ishii *et al*., 2008; Jones & Dangl, 2006). Apart from that, more elegant immune responses, like virulence detection and surveillance pathway, that has familiar with effector-trigger immunity (ETI) in plants have been described (Boyer *et al*., 2011; Münter *et al*., 2009). For example, *C. elegans* responds to *P. aeruginosa* infection by detecting Exotoxin A-triggered translational inhibition, which leads to activation of the *zip-2/irg-1* pathway, which functions not only for mRNA translation but also in surveillance of essential host processes to provide defense (Dunbar *et al*., 2012). There are still complex mechanisms of the antimicrobial defense system, such as mitogen-activated protein kinase signaling pathway, Toll and Imd pathway (Kurz & Ewbank, 2003), and some other pathways involving transforming growth factor-β, insulin-like growth factor (Millet & Ewbank, 2004). For instance, the p38 MAP kinase-related signaling pathway is an essential player in anti-microbial defense, which is orthologous to mammalian apoptosis signal-regulating kinase 1 (ASK1) – MAPK kinase 3/6 (MKK3/6) – p38 MAPK cascade involved in triggering the innate immune response. This pathogen-activated linear phosphorylation cascade consists of neuronal symmetry family member 1 (*nsy-1*), SAPK/ERK kinase 1 (*sek-1*), and p38 MAPK family member 1 (*pmk-1*) (Kim *et al*., 2002; Kim *et al*., 2004). For

innate immune response caused by cell-restricted damage and systemic stress, DNA damage in nematodes germ cells leads to activate of MPK-1 that induces immune peptides in the germline, which in turn leads to enhanced proteostasis in somatic tissues through activation of the ubiquitin-proteasome system (Ermolaeva *et al*., 2013; Ermolaeva & Schumacher, 2014). For immunity and stress response pathways, the transcription factor HSF-1 was required for normal tolerance to a variety of *C. elegans* (Singh & Aballay, 2006). For immunity and aging pathway, the activation of DAF-2 resulting in inactivation of DAF-16 was proposed to play a role in pathogen tolerance in addition to aging (Murphy *et al*., 2003; McElwee *et al*., 2003). On the other hand, the anti-viral response of the nematode relies on the intracellular RNA interference (RNA) machinery. The most prominent example of how viral proteins escape the RNAi surveillance through inhibiting the RNAi machinery in *C. elegans* is the Flock house virus protein B2 which significantly downregulates exogenous RNAi and enhances the susceptibility of worms to the Orsay virus infection without having any effect on the endogenous physiological micro-RNA pathway (Guo & Lu, 2013).

For neuronal regulation of immunity, three neuroendocrine signaling pathways modulate stress tolerance in *C. elegans*, including the insulin-like growth factor (IGF)/insulin-like signaling (ILS) pathway, the transformation growth-β (TGF-β), pathway and the nuclear hormone receptor (NR) pathway **(Fig. 8)** (Baumeister *et al*., 2006; Henderson & Johnson, 2001; Lightle *et al*., 2000; Antebi, 2016). They all regulate development, growth, body size, reproduction, fecundity, metabolism, and behavior (Prahlad & Morimoto, 2009). In *C elegans*, the decision to enter a developmentally arrested dauer larval stage is triggered by a combination of signals from sensory neurons in response to environmental cues, which include a dauer pheromone. These sensory inputs are coupled to the parallel DAF-2/insulin receptor-like and DAF-7/TGFβ-like signaling pathways (Li *et al*., 2003).

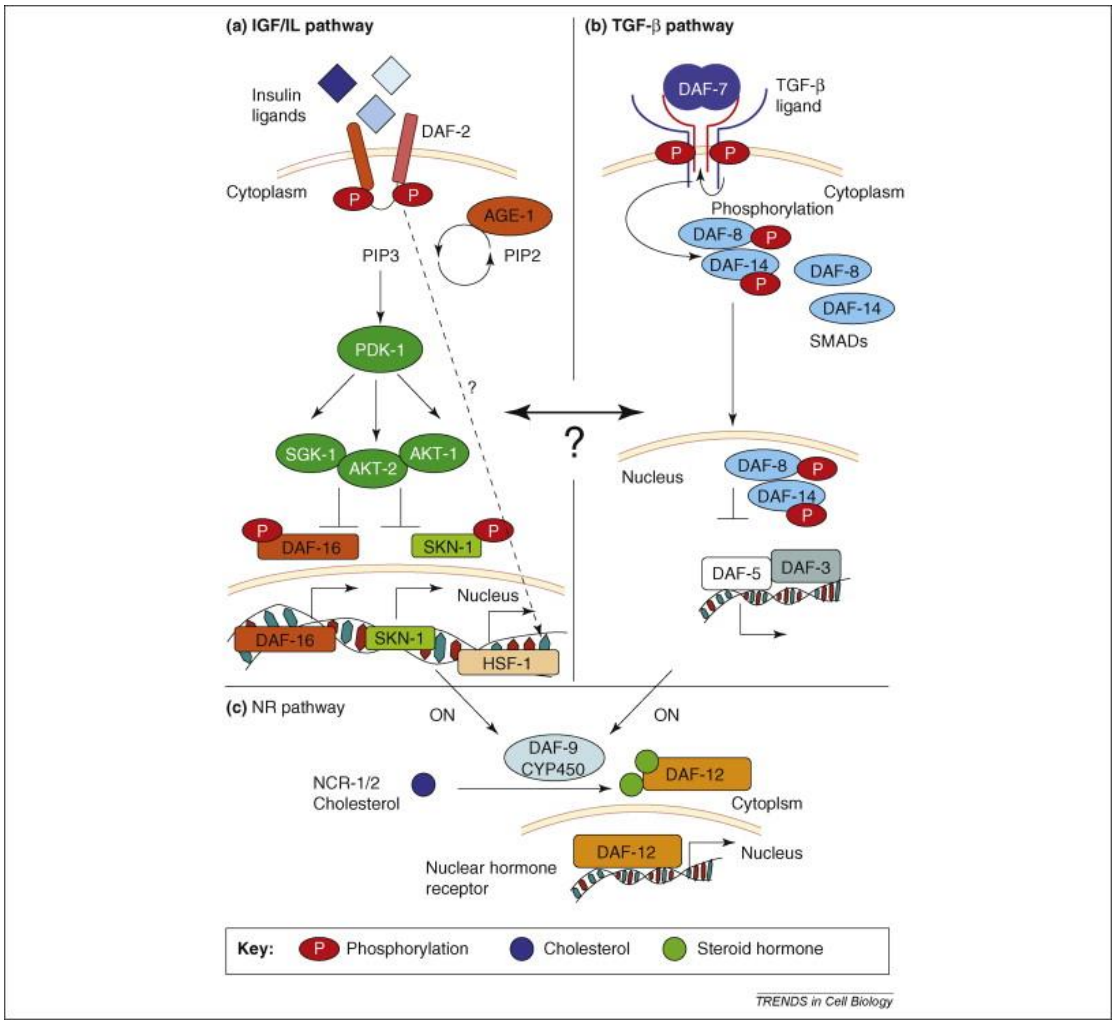

Fig. 8: Neuroendocrine pathways regulate stress tolerance in *C. elegans* (Prahlad & Morimoto, 2009). Schematic depiction of the three neuroendocrine pathways that regulate stress responses in *C. elegans*. **(a)** The IGF/IL signaling pathway. IL ligands bind the IL receptor DAF-2 to activate a phosphorylation cascade, which then activates the PI3 kinase AGE-1. This results in the phosphorylation of the ACG kinases, AKT-1 AKT-2 and SGK-1, which ultimately phosphorylate DAF-16 and SKN-1. Phosphorylated DAF-16 and SKN-1 are cytoplasmic and inactive. Unphosphorylated DAF-16 and SKN-1 are active and translocate to the nucleus to transcribe their target genes. IL signaling also modulates the activity of HSF1 in manner yet to be characterized. **(b)** The TGF-β signaling pathway in C. elegans has all the components of the canonical TGF-β signaling pathway. The TGF-β ligand DAF-7 binds the type I and type II receptors DAF-1 and DAF-4 to modulate the phosphorylation state of the downstream SMAD proteins DAF-8 and DAF-14. DAF-8 and DAF-14 inhibit the function of a DAF-3, a co-SMAD and DAF-5, a protein homologous to the Sno/Ski family of oncogenes. Phosphorylated DAF-8 and DAF-14 translocate to the nucleus where they transcribe its target genes involved in the development of dauer larvae. **(c)** The nuclear hormone receptor (NR) signaling

pathway. Insulin/IGF-I and TGF-β peptide signals converge on the nuclear receptor branch of the dauer pathway. NCR-1/2, a Niemann-Pick C1 homolog, delivers cholesterol to DAF-9, presumably triggering the synthesis of steroid hormone. In the presence of hormone, DAF-12 directs expression of genes involved in reproductive development and the animals are not stress tolerant. In unfavorable environments, hormonal pathways are suppressed and unliganded DAF-12 specifies dauer development and stress resistance.

1.8 Aim of this work

SSPs are well-known for their roles in biotrophic or pathogenic microbial interactions, but their involvement in predatory fungi, such as *A. flagrans*, has been less evident. The aim of this work was to investigate the role of the virulence factor EinA, as a member of the small-secreted proteins (SSPs), in the interaction between NTF and nematodes. For this purpose, the subcellular localization of EinA during the infection process will be analyzed by employing temporal-spatial organization techniques, which will shed light on its potential functions at certain stages of infection. Furthermore, the role of EinA towards *C. elegans* will be assessed by establishing an *einA*-deletion strain. these investigations provide clues regarding the contribution of EinA as a virulence factor in the pathogenicity of *A. flagrans* towards nematodes. Lastly, the potential impact of EinA on *C. elegans* will be explored through heterologous expression strategies. Expressing *einA* in *C. elegans* using various promoters, its effects on nematode physiology, including lifespan, maturation, and possible phenotypic abnormalities will be assessed. This analysis will provide further evidence of the toxic properties of EinA and its ability to modulate host physiology. In conclusion, by conducting these comprehensive investigations, we aim to gain a deeper understanding of the mechanisms underlying the EinA-mediated interaction between *A. flagrans* and *C. elegans*. This research will contribute to our broader knowledge of the predatory strategies employed by nematode-trapping fungi and their implications for host-pathogen interactions.

2. Results

2.1 EinA is a small, lysine-rich secreted protein and is up-regulated during the infection

Small-secreted proteins (SSPs) are important virulence factors in many pathogenic interactions, like some race-specific avirulence proteins (Avrs)(Avr2, Avr4, Avr4E, and Avr9) secreted in the interaction between fungal pathogen *Cladosporium fulvum* and tomato (Laugé *et al*., 2000; Luderer *et al*., 2001; Luderer *et al*., 2002; Westerink *et al*., 2002). Such SSPs (117 predicted with EffectorP) were also predicted in the genome of the nematode-trapping fungus *A. flagrans* and it was speculated that they play a role in the predatory lifestyle (Youssar *et al*. 2019). Ten genes (*dfl_006404*, *dfl_003626*, *dfl_008309*, *dfl_004148*, *dfl_000022*, *dfl_008266*, *dfl_005398*, *dfl_002544*, *dfl_003429*, and *dfl_009366*) among them were selected according to the effector possibility score. One criterium for SSPs to play a role during nematode attack is their expression, which would expect induction of the genes in the presence of nematodes. To test this, quantitative real-time RT-PCR was performed. Conidia of wild-type strain were inoculated on LNA medium on the surface of cellophane membranes and grown at 28 °C for 24 h. Subsequently, 300 µl of fresh adult *C. elegans* washed from the same petri dish were applied to the medium with germinating conidia in order to induce trap formation, and the same volume of water was added as a control. After 24 h, mycelia were scraped off until a multitude of traps could be observed with the microscope, and RNA was extracted for quantitative RT-PCR. Relative expression was calculated using the gene encoding gamma-actin (*dfl_002353*) as an internal reference. The result showed that the relative expression level of *dfl_008309* was dramatically increased when the fungus was induced by nematodes **(Fig. 9 B)**. It indicated that *dfl_008309* was induced, especially during the pathogenic life phase.

Therefore, *dfl_008309* was chosen as a target gene for further analysis.

This virulence factor candidate DFL_008309 (was named as EinA: Expressed inside nematodes) was predicted as a putative effector among 117 proteins by effector P (Youssar *et al*., 2019). EinA is a 112 amino acid small protein that is predicted to contain a 20-amino acid signal peptide at the N-terminus by signal 4.1 (https://services.healthtech.dtu.dk/services/SignalP-4.1/) and a 29-amino acid nuclear localization signal at the C-terminus by NLS Mapper (https://nls-mapper.iab.keio.ac.jp/cgi-bin/NLS_Mapper_form.cgi) **(Fig. 9 A)**. There are four cysteines and twelve lysines in the EinA protein. The average PI is 9.44. Analysis of the protein with the "Rapid Automatic Detection and Alignment of Repeats (RADAR)" tool revealed that there are no repeat structures within the protein (https://www.ebi.ac.uk/Tools/pfa/radar/). A BLAST search resulted in only one hit, revealing 63% identity to the hypothetical *Orbilia oligospora* TWF751_009605 (E value = 6e-43). Secondary structure prediction with the NPS@ server, revealed that EinA mainly consists of random coils (54.35%), extended strand (33.7%), beta turn (7.61%), and alpha helix (4.35%) (https://npsa-prabi.ibcp.fr/cgi bin/npsa_automat.pl?page=/NPSA/npsa_sopma.html).

Another important property of virulence factors can be their secretion. The functionality of the bioinformatically predicted signal peptide should be investigated to know whether EinA can be secreted or not. For this purpose, *einA* or *einAΔSP* was fused with the encoding gene of laccase C (*A. nidulans*) were expressed in the wild-type strain of *A. flagrans*, respectively. The vector was constructed using the modified plasmid backbone of the expression vector pOF018, which contains the gene *lccC*, which codes for laccase C, under the control of the *gpdA* promoter and, in addition, the hygromycin resistance cassette (*trpC(p)::hph:: trpC(t)*) for the selection of *A. flagrans*. The plasmid with *einA* was transformed into wild type of *A. flagrans*, and EinA without the signal

peptide as the negative control with the same operation. If this fusion protein is secreted, the laccase would have an oxidation reaction with ABTS present in the PDA medium to the more stable radical cation, which would cause a green-blue color coming around the colony on the medium. After 48 h incubation of the transformants on PDA with 1 mM ABTS at 28 °C, the result showed that there was a blue-green color visible on the medium inoculating the mutant strain expressing the fusion protein of EinA-Laccase C, but the negative control strain did not show the color change, which indicated EinA could be secreted out of the cell, and the predicted signal peptide is functional **(Fig. 9 C)**.

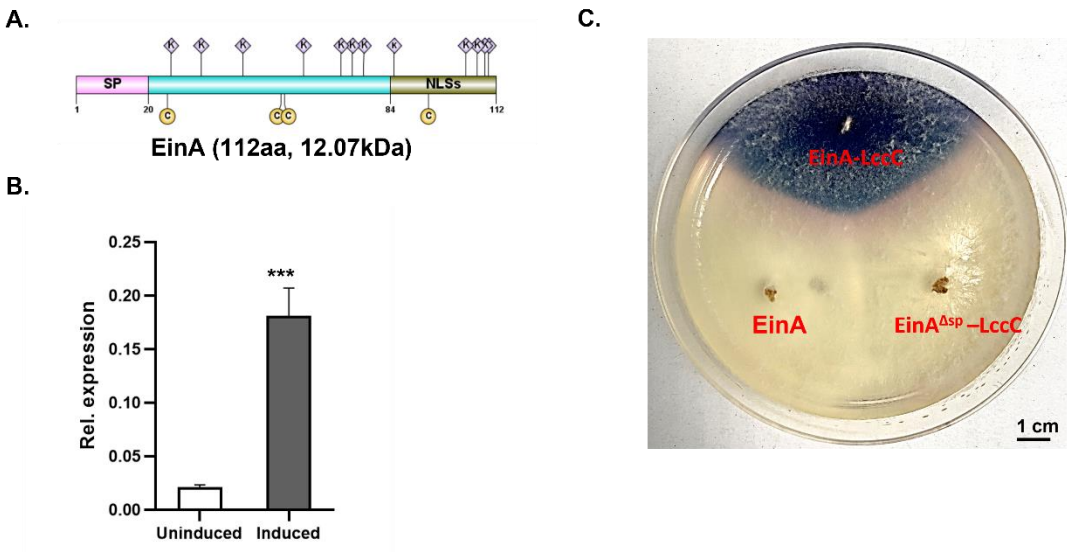

Fig. 9: EinA is lysine rich, contains four cysteines and is secreted. (A) Scheme of EinA. The 112 amino acid long protein is lysine-rich and 4 amino acids of cysteines and contains a 20 amino acid long signal peptide at the N-terminus, a predicted nuclear localization signal at the C-terminus. **(B)** Quantitative real time PCR analysis of *einA* expression in *A. flagrans* hyphae on LNA 24 h with the actin as the reference gene for normalization and hyphae were co-cultivated with *C. elegans*. The error bar indicates the standard diviation of three technical replicates. Asterisks (*) indicate significant differences (*p<0.05, **p<0.01) based on unpaired two-tailed Student's t test. p-value=0.000438. **(C)** EinA-LccC and EinAΔSP-LccC expression in wild type and were grown on PDA with 1 mM ABTS for 48 hours.

2.2 *einA* is expressed in trophic hyphae inside nematodes

The quantitative method used in this study was unable to provide detailed information regarding the timing of *einA* expression or the subcellular localization of EinA during the infection process. This limitation arose due to the isolation of RNA from a mixture of vegetative mycelia and traps. To overcome this, we established a reporter assay to visually observe the precise localization of EinA when it is expressed. The fusion protein consisting of the histone H2B and mCherry under the control of the *einA* promoter (1 kb upstream of the *einA* ORF) was expressed in *A. flagrans*. The same reporter under the control of the constitutive *h2b* promoter served as a positive control. The mCherry signal was localized in the cell nuclei because histone H2B is involved in the structure of chromatin; this helps us to clearly distinguish the fluorescence signal from background fluorescence. The fluorescent intensity of the cell nuclei can be directly correlated with the promoter activity and the gene expression.

Plasmids constructed were transferred into protoplasts of *A. flagrans* via protoplast transformation. After one week, the same number of conidia of transformants were inoculated on slides with a thin layer of LNA medium and incubated for 24 h at 28 °C. A mixed population of *C. elegans* wide-type N2 was also added to the slides to induce trap formation. Fluorescence microscopy revealed that the reporter strain with *einA* promoter had a strong fluorescent signal from nuclei in the trophic hyphae inside nematodes **(Fig. 10 A, iii)**. Vegetative mycelia **(Fig. 10 A, i)** and traps without trapping nematodes **(Fig. 10 A, ii)** had no fluorescent signal observed. Correspondingly, the strain under the control of *h2b* promoter showed an evenly strong signal ubiquitously, be it in traps with nematodes **(Fig. 10 B, i)** without nematodes **(Fig. 10 B, ii)**, or in vegetative mycelia **(Fig. 10 B, i)**. The average fluorescence of individual cell

nuclei of strains labeling nuclei with mCherry under the control of *einA* promoter **(Fig. 10 C)** and *oliC* promoter **(Fig. 10 D)** were analyzed with ImageJ. The data suggested a higher fluorescence intensity in the trophic hyphae inside the nematodes' body compared to the empty traps or vegetative mycelia for the *einA*-promoter reporter strain, but equal fluorescence signals in all hyphae for the strain with *h2b* promoter control. Since the intensity of the reporter's fluorescence directly reflects and visualizes the activity of the promoter, this result confirms the spatial expression of *einA* in the trophic hyphae inside nematodes.

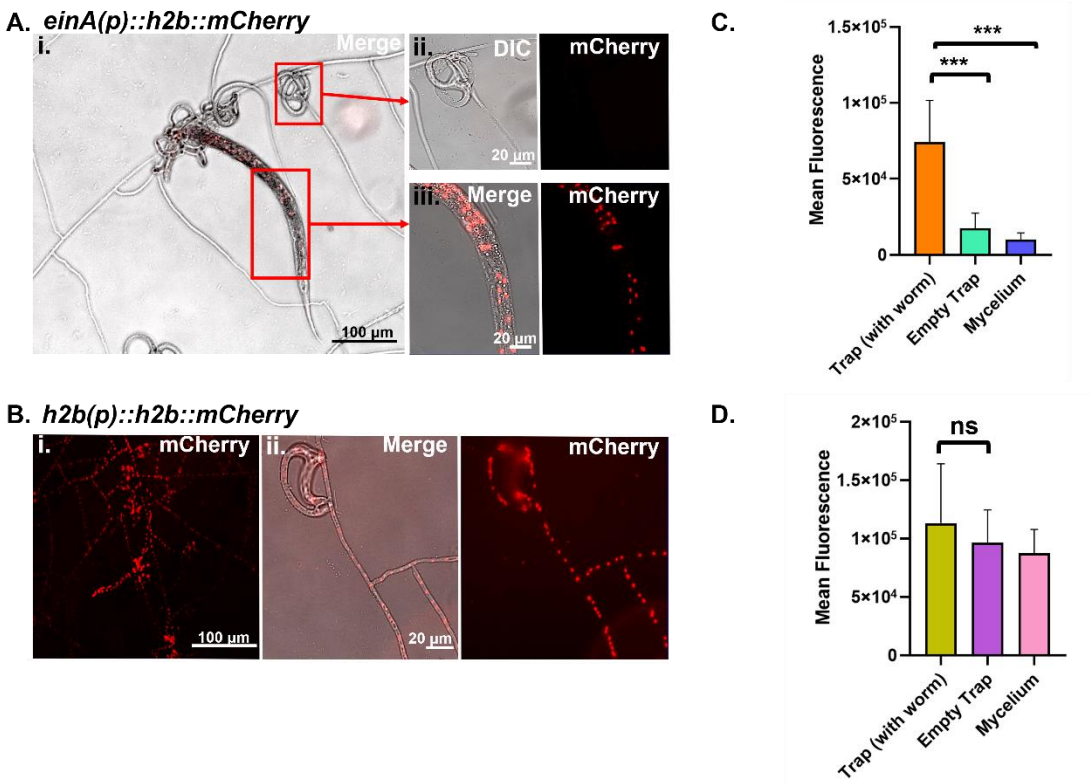

Fig. 10: The expression of *einA* is induced in trophic hyphae inside nematode. (A) Spatial expression of *einA* gene. H2B-mCherry was expressed with the *einA* native promoter. Pictures were taken after co-cultivation of strains with *C. elegans* at 28 °C for 24 h. **(i)** Different kinds of traps and vegetative hyphae are pictured. The enlargement shows the EinA-mCherry localization in the trophic hyphae inside the nematode **(iii)** But not the empty trap **(ii)**. **(B)** Spatial expression of the *einA* gene. H2B-mCherry was expressed with *h2b* promoter. Pictures were taken after co-cultivation of strains with *C. elegans* at 28 °C for 24 h. **(i)** Vegetative mycelia and traps with nematodes, **(ii)** An empty trap. **(C, D)** Mean fluorescence of *einA* expression with *einA* **(C)** and *h2b* **(D)**

promoter, respectively. In different positions of strains were measured with the same setting using Image J. n=40. [***] P-value < 0.0001.

After studying the *einA* promoter activity, the EinA protein should be visualized with microscopy with the help of the fluorescent protein GFP. For this purpose, EinA was C-terminally fused to GFP, and this construct was expressed both under the constitutive *A. nidulans oliC* promoter (*oliC(p)::einA::GFP::trpC(t)*) **(Fig. 11 A, i)** and under the native promoter (*einA(p)::einA::GFP::trpC(t)*) **(Fig. 11 B, i)** expressed. The signal accumulation - whatever *einA* promoter or *oliC* promoter- on the margin of hyphae indicates a tendency for secretion of the protein. EinA was fused to GFP and expressed under the control of the constitutive *oliC* promoter. In this case, the protein was ubiquitously localized in dynamic dots ubiquitously, the trophic hyphae inside the nematodes **(Fig. 11 A, ii)**, traps without trapped worms **(Fig. 11 A, iii)** and the vegetative mycelia **(Fig. 11 A, iv)**.

To further investigate the localization of the protein, the transgenic strain harboring GFP-labelled EinA under the control of the *einA* native promoter was performed **(Fig. 11 B, i)**. The signal could be observed in dynamic puncta in the trophic hyphae inside the nematode's body **(Fig. 11 B, ii / iii)**. In traps without nematodes **(Fig. 11 B, iv)** and vegetative mycelia **(Fig. 11 B, v)**, there were no fluorescence signals observed. This indicates that the temporal distribution of EinA is consistent with the spatial expression of EinA.

Considering that EinA was predicted to have a signal peptide (1-20 amino acid, SP) and a nuclear localization signal (84-117 amino acid, NLS), to check whether the SP contains the information for the correct localization of the protein and if NLS has a localization function or not, EinA without a signal peptide was fused to GFP and expressed with *oliC* promoter in *A. flagrans* **(Fig. 11 C, i)**. Fluorescence micrographs showed that EinA without SP did not

localize in the margins, but instead accumulated in nuclei of fungi **(Fig. 11 C, ii)**, which indicates EinA without SP lost the secretion ability, and that the NLS is fully functional.

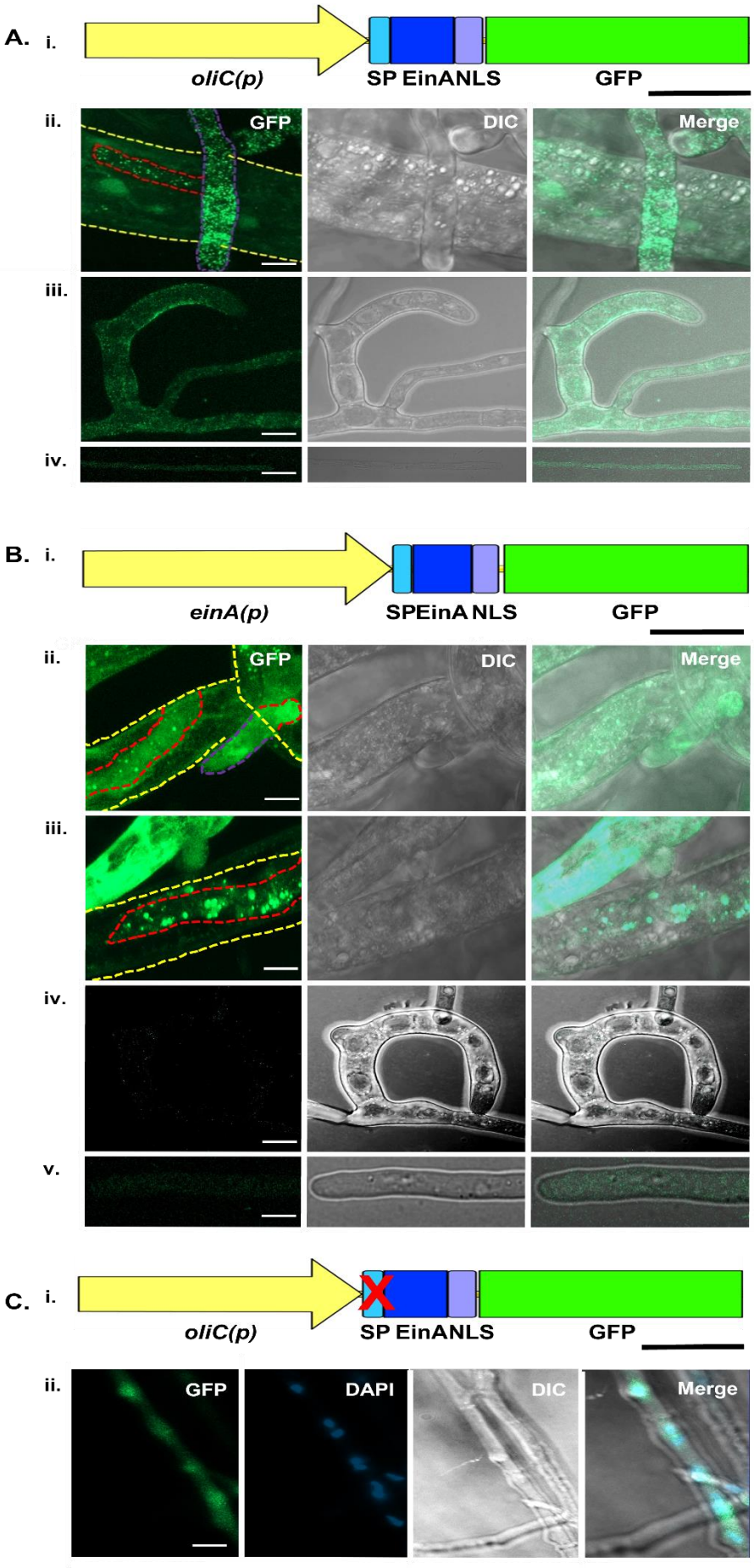
A.
i.
oliC(p)
SP EinANLS
GFP
ii.
GFP
DIC
Merge
iii.
iv.
B.
i.
einA(p)
SPEinA NLS
GFP
ii.
GFP
DIC
Merge
iii.
iv.
v.
C.
i.
oliC(p)
SP EinANLS
GFP
ii.
GFP
DAPI
DIC
Merge

Fig. 11: EinA localizes at trophic hyphae inside nematodes. (A) The EinA-GFP expressing strain was co-cultivated with *C. elegans* on LNA slides at 28 °C for 12 h to induce trap formation. *einA::GFP* was expressed under the *oliC* promoter. Scale bar = 5 µm. **(i)** Schematic representation of the *oliC* promoter fusion *einA::GFP* construct. Scale bar = 100 aa. **(ii)** A trap with the nematode. **(iii)** An empty trap. **(iv)** A vegetative mycelium. **(B)** The EinA-GFP expressing strain was co-cultivated with *C. elegans* on the LNA slides at 28 °C for 12 h to induce trap production. *einA::GFP* was expressed under the *einA* native promoter. Moreover, the fusion protein signal occurred in the trophic hyphae growing inside the worm's body. Scale bar = 5 µm. **(i)** Schematic representation of the *einA* promoter fusion *einA::GFP* construct. Scale bar = 100 aa. **(ii)** Shows a worm during early digestion by the fungus. **(iii)** Shows a worm almost completely digested. More vesicles with EinA-GFP were observed. **(iv)** A trap without trapped worms. **(v)** A vegetative mycelium. **(C)** The EinAΔSP-GFP expressing strain was co-cultivated with *C. elegans* on the LNA slides at 28 °C for 12 h to induce trap production. *einA*ΔSP*::GFP* was expressed under the *oliC* promoter. Scale bar = 20 µm. **(i)** Schematic representation of *einAΔSP::GFP* fusion with *oliC* promoter. Scale bar = 100 aa. **(ii)** GFP and DAPI signals in the mycelium co-localized in nuclei. Nuclei of mycelium were stained by DAPI for 5 min in the dark. Yellow lines region: worm body; red lines region: trophic hyphae inside the nematode; purple lines region: trap's region outside the nematode. Scale bar = 20 µm.

2.3 Deletion of *einA* impairs the ability of *A. flagrans* to digest *C. elegans*

The spatial expression and temporal distribution results confirmed that EinA was expressed and accumulated in the trophic hyphae inside the nematodes. In order to characterize its role during the infection process directly, the gene *einA* was knocked out via homologous recombination with the deletion cassette that includes 1 kb upstream and downstream areas of the ORF of *einA* and the geneticin resistance cassette **(Fig. 12 A)**. *A. flagrans* was transformed with this deletion cassette and transformants were checked by PCR and Southern blot. As expected for the deletion, the LB probe hybridized with a 3.3 kb fragment of the restriction enzyme *Xmn*I-cleaved gDNA of the *ΔeinA*-transformants and a 2.2 kb fragment in the wild-type gDNA **(Fig. 12 B)**. Moreover, the PCR products were amplified with primers outside of LB and RB showed the correct

transformation was get (the PCR product of WT = 3.5 kb, the PCR product of *einA*-deletion = 4.6 kb.) **(Fig. 12 C)**. On the other hand, *einA* was rescued in the *einA*-deletion strain. The deletion strain was transformed with a vector containing the *einA* ORF with the 1 kb upstream and downstream; hygromycin resistance cassette was used as the selection maker.

For the morphological phenotype in a saprotrophic phase, the *einA*-deletion strain did not display any dramatic difference **(Fig. 12 D)**. Considering the low expression level of *einA* with a saprobe lifestyle, this result is very reasonable. A microscopic virulence assay was established to identify the virulence ability of the *einA* deletion strain, which could illustrate precisely the period of EinA to work. This experiment was performed using the deletion strain, the overexpression strain (the strain with the expression of EinA-GFP with *einA* promoter), plus the complemented strain and the *A. flagrans* wild type as controls. Spores of the respective strains were inoculated on LNA slides with a mixed population of *C. elegans* N2 and incubated at 28 °C for 24 h to induce trap formation. The N2 worms were then extensively flushed away from the slides with M9, and a plate of the *C. elegans* strain B126 (genotype: *his-72(p)::his-72::GFP*) which were allowed to synchronize until growing to the adult stage was collected and placed on the slides with already induced traps shortly before microscopy. Various trapping networks were observed using a mechanical stage and a confocal microscope, and recordings were made every 2 minutes for 20 hours. Since the cell nuclei are labeled with GFP, this allows the course of the infection to be observed and the point of cell death to be determined by the disappearing fluorescence. For analyzing the recordings, the whole process of infection was divided into two parts: the paralysis time, spanning from when the worm was caught in a trap to the time the worm stopped twisting, and the second part which comprises the digestion period, i.e., from when the worm stops twisting to the point of disappearance of the nuclear GFP fluorescence signal. Analysis of these data revealed that the paralysis time

of the *einA*-deletion strain was 138.92 [SD ± 36.95] min, that of the *einA*-overexpression strain was 118.73 [SD ± 32.93] min, that of the *einA*-complementation strain was 111.83 [SD ± 36.20] min, which showed no significant difference compared to 129.98 [SD ± 41.69] min in the wild-type strain **(Fig. 12 E)**. However, compared with 257.03 [SD ± 55.49] min taken by the wild-type *A. flagrans* to digest worms, the *einA*-deletion strain took a longer time, about 290.71 [SD ± 49.96] min to complete digestion, while the *einA* overexpression strain took shorter time about 143.29 [SD ± n40.72] min to digest. The complemented strain took 236.28 [SD ± 46.95] min to digest the nematodes **(Fig. 12 F)**. The result of delayed digestion suggests EinA might play a role in late processes of the interaction. It may indicate that EinA is directly or indirectly involved in the process of worm digestion.

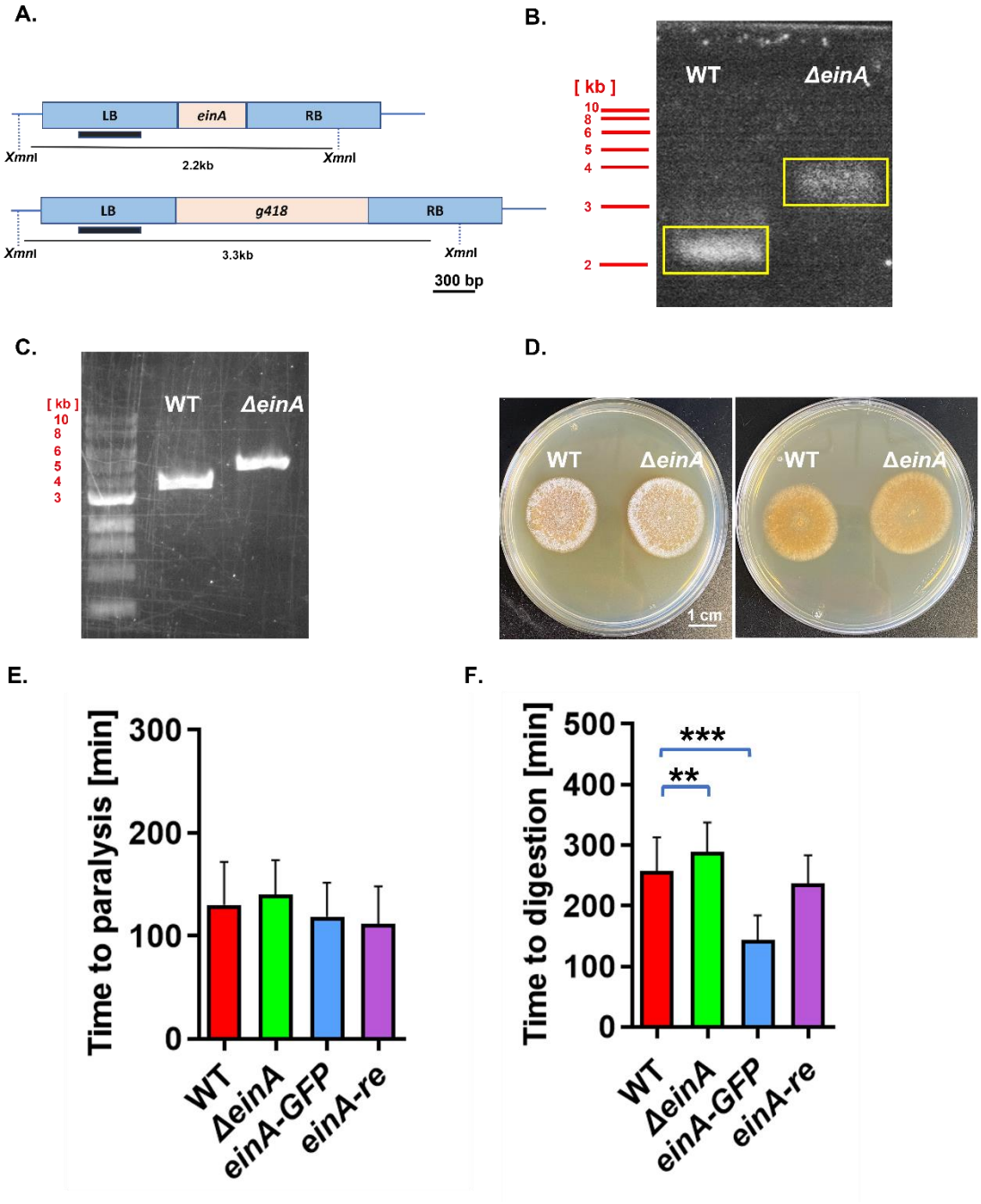

Fig. 12: The *einA* gene is required for digestion. (A) Scheme of the deletion strategy of *einA*. The gene was deleted via homologous recombination flanking geneticin resistance gene with 1 kb upstream of *einA* (LB) and 1 kb downstream of *einA* (RB); LB was used as a probe. The restriction enzyme *Xmn*I was chosen to cleave the gDNA of the *ΔeinA*-transformants. The primers (Ver_pjet_*einA*_F/R) of PCR for transformants verification are upstream of LB and downstream of RB of gDNA. **(B)** Southern blot of genomic DNA of the *ΔeinA*-strain and the WT using the probe indicated in (A). **(C)** PCR of genomic DNA of the *ΔeinA*-strain and the WT using the verification primers mentioned in (A). **(D)** the morphological phenotype of the *einA*-deletion and wild-type of *A.*

flagrans. The same number of conidia (2 x 10^6) were cultivated on PDA at 28 °C for 4 days. The frontside and backside of the colonies are shown. **(E - F)** Virulence assay with the wild type (WT), the *einA*-deletion strain, the *einA*-overexpression strain, and the *einA*-complementary strain. Multiple traps were observed, and the time from the capturing event to complete paralysis and from paralysis to complete digestion was taken. Error bars indicate the standard deviation. A student's t-test was performed for statistical analysis (p-value [**] = 0.0012, p-value [***] < 0.0001; n [WT] = 59, n [KO] = 64, n [OE] = 59, n [*einA*-Re] = 40).

2.4 Heterologous expression of *einA* in *C. elegans*

To elucidate the function of virulence factors during the infection process and to identify possible targets of these effectors in the nematodes, *einA* was expressed heterologously in *C. elegans*. The vectors carrying the particular promoter of the nematode, the target genes, and the marker genes, like *GFP* or *Scarlet*, were transferred into *C. elegans* via the microinjection method. These transgenes would be expressed as an extrachromosomal array. The selection took place via the co-injection with a marker vector, which leads to the expression of a fluorophore in the pharynx, which is controlled by the promoter of the *myo-2* gene (*myo-2(p)::tdTomato* or *myo(p)::GFP*). The plasmids were first linearized by restriction digestion and purified for efficient expression of the array. It is a suitable strategy to inject a mixture with a concentration of 5 ng/µl target vector, 5 ng/µl marker vector, and 150 ng/µl of the 1 kb ladder. Individuals of the F1 generation showing fluorescence in the pharynx were isolated, and the F2 generation was defined as one line.

Since the function of EinA in *C. elegans* is still obscure, different expression vectors were constructed and injected for heterologous expression of the target gene in *C. elegans*. Given that EinA contains a signal peptide at the N-terminus, which is more likely to cause a different influence of the function of EinA in *C. elegans* by localization changes. Therefore, the respective constructs expressing *einA* with and without signal peptide were performed. Our

expectation is that EinA without SP should stay in the cells of the transgenic worms and be imported into nuclei, but EinA with SP should be secreted from the worm cells to the extracellular space.

On the other hand, for the heterologous expression of *einA* in the wild-type strain N2, it is essential to consider a suitable promoter. The target tissue of EinA is unknown. Moreover, there are many promoters that could be chosen in *C. elegans*, such as the all-tissue promoter of *eft-3* and heat shock promoter *hsp-16.48*, the tissue-specific promoters, like the muscle-specific promoter of *myo-3*, the cuticle-specific promoter *col-12*, and the intestine-specific promoter of *ges-1* and so on (Meister *et al*., 2010). The all-tissue promoter *eft-3* was first selected to maximize the negative impact of the heterologous expression of EinA on the morphology or the life expectancy of *C. elegans*. Transgenic lines expressing the constructs of *eft-3(p)::einAΔSP::GFP::unc-54UTR* and *eft-3(p)::einA::Scarlet::unc-54UTR* as an extrachromosomal array were constructed and using *myo-2(p)::tdTomato* or *myo-2(p)::GFP* as a marker vector that can lead to green or red fluorescence of the pharynx for the selection of positive transformants. Accordingly, the fusion protein of EinAΔSP-GFP was expressed under the control of the *eft-3* promoter **(Fig. 13 A, i)**, The signals seem to localize as dots in nuclei, more likely in nuclei of intestine cells **(Fig. 13 A, ii/iii)**. Besides, some worms had a stronger signal intensity, but others did not **(Fig. 13 A, iv)**. There was a different expression level of *einAΔSP* due to genetic mosaicism and mitotic instability of the extrachromosomal array (Yochem & Herman, 2005).

Nuclear staining with Hoechst 33258 was performed to determine the nuclear localization of EinA without SP. However, the impermeability of the nematodes' cuticle and hypodermis to external substances, along with the localization of EinAΔSP-GFP signals in deeper organelles, rendered the use of external staining with Hoechst 33258 impractical. Consequently, an alternative

approach was employed, where mutant strains were stained by feeding them stained OP50 with Hoechst 33258 overnight. Subsequently, these worms were flushed away with M9 buffer and collected. Finally, these stained worms were anesthetized in a urethane solution for 20 minutes. The presence of the urethane solution was crucial for the success of the staining process. The results of staining the worms with EinAΔSP-GFP demonstrated a complete overlap between the GFP signal and the stained nuclei **(Fig. 13 B)**, thereby confirming the nuclear localization of EinAΔSP.

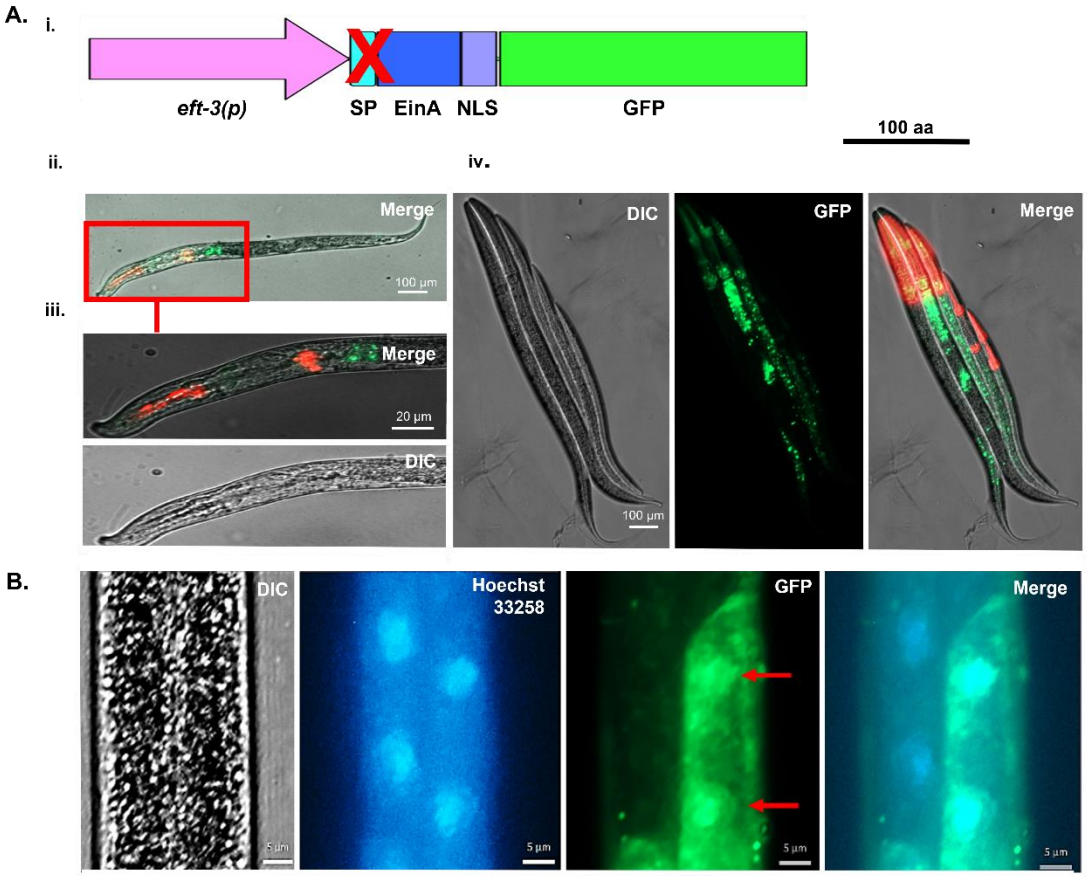

Fig. 13: EinAΔSP localizes in nuclei of *C. elegans*. (A) An N-terminal GFP fusion protein of EinAΔSP expressed in *C. elegans* shows it localized as dots. The gene was expressed using the *eft-3* promoter. The red fluorescence showed the expression of the marker plasmid (*myo-2(p)::tdTomato*) in the pharynx of *C. elegans.* **(i)** Schematic representation of the construct of *eft-3* promoter fusion *einAΔSP::GFP*. **(ii)** A worm with EinAΔSP-GFP in the intestine cells and tdTomato signals at the pharynx with the merge channel. **(iii)** Enlargement of the region of (A-ii) containing signals. **(iv)** Five worms at the

different life stage with EinAΔSP-GFP localization were shown. **(B)** Another individual of *C. elegans* expression an N-terminal GFP fusion protein of EinAΔSP was stained with Hoechst 33258. GFP signals and Hoechst 33258 signals were co-localized. Red arrow: intestine cells with EinAΔSP-GFP signals.

To examine the localization of the full-length of EinA, the N-terminal Scarlet was fused with EinA under the control of *eft-3* promoter **(Fig. 14 A, i)**. I observed that the signal was localized in the cytoplasm **(Fig. 14 B - C and S1 Movie)**.

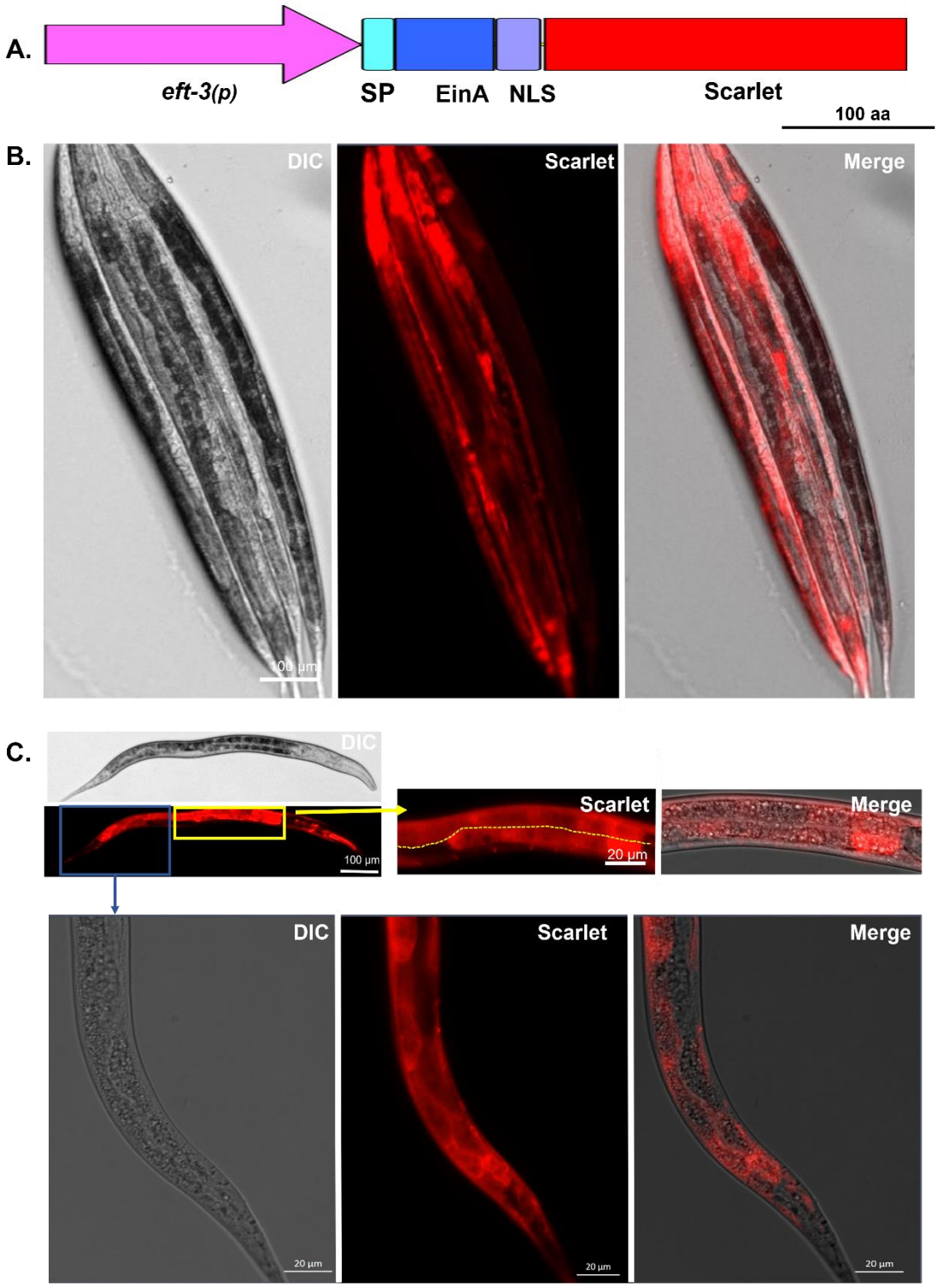

Fig. 14: EinA localizes in the cytoplasm of *C. elegans*. (A) Schematic representation of the *eft-3* promoter fusion *einA::Scarlet* construct. **(B)** Four worms with EinAΔSP-GFP localization ubiquitously were shown. **(C)** Another individual worm expressing EinA-Scarlet. Yellow box: the enlargement of a part of the intestine organ; blue box: the enlargement of a part of the tail; yellow dash line: the intestine lumen.

2.5 Heterologous expression of *einA* in *C. elegans* causes deformation

Upon heterologous expression of *einA* in *C. elegans*, a striking phenotype was observed. At 20 °C, approximately 64% of mutant animals displayed a wild-type morphological phenotype. The remaining approximately 36% of mutant animals, regardless of whether *einA* was expressed with SP or without SP, displayed variable defects in morphology, characterized by swelling or deformities from the inside layer of the worm's body **(Fig. 15 A, B and S2, S3 Movies)**. Notably, unlike the blister phenotype caused by heterologous expression of *nipA* in *C. elegans*, which arises from the hypodermal layer (Jennifer Menzner 04/2020), the deformities observed in worms expressing *einA* consistently manifested as a prominent bag-like protrusion originating from the deeper organelle.

The *einA* expression was detected throughout all development stages, from embryos to adults. However, in the case of eggs expressing *einAΔSP-GFP* during the embryonic stage, they were no longer capable of hatching **(Fig. 15 A, ii)**. Worms exhibiting severe deformities presented a range of developmental defects, including growth retardation and, in some cases, infertility.

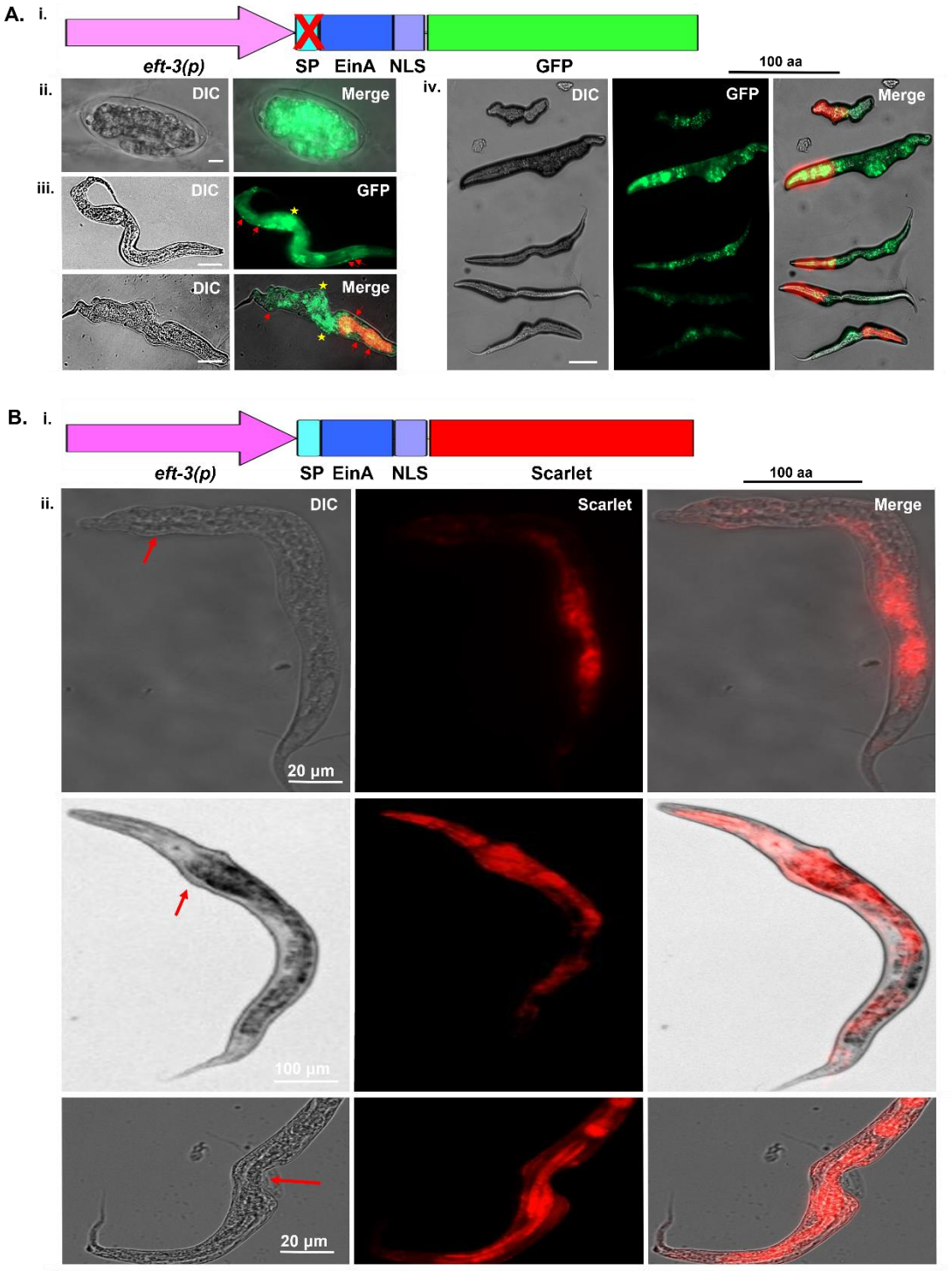

Fig. 15: Transgenic lines of *C. elegans* with the different genotypes of *einA* have the deformity phenotype. (A) Deformed worms at different stages were caused by the expression of the *einAΔSP* gene fused to *GFP* under the all-tissue promoter *eft-3*. **(i)** Genotype scheme of *eft-3(p)::einAΔSP::GFP*. **(ii)** An egg with an expression of *einAΔSP* fused with *GFP* was picked on an NGM plate with OP50 *E. coli* as food to cultivate for one day; it showed that this egg failed to hatched. Scale bar = 5 µm. **(iii)** An individual worm with different

deformation degrees. Red arrows: EinAΔSP-GFP signals into other organelles except for the intestine cell; yellow pentagrams: the deformed position. **(iv)** Five deformed worms with (i) genetic pattern. **(B)** The deformed worm caused by the expression of the *einA* gene fused to *Scarlet* under the all-tissue promoter *eft-3*. **(i)** Genotype scheme of *eft-3(p)::einA::Scarlet*. **(ii)** worms with the deformity phenotype in the head, pharynx, and the dorsal side of body.

To strengthen the evidence of EinA's impact in *C. elegans*, transgenic strain lines expressing *eft-3(P)::einAΔSP* in *unc119* mutant worms that present a movement defect phenotype was established **(Fig. 16 A)**. Whether the phenotype of movement defect was rescued or not served as a marker for selecting of positive transformants. The results showed that 30.67% of worms rescued motility presented a deformity phenotype **(Fig. 16 B)**, thereby indicating that EinA was responsible for the deformity phenotype.

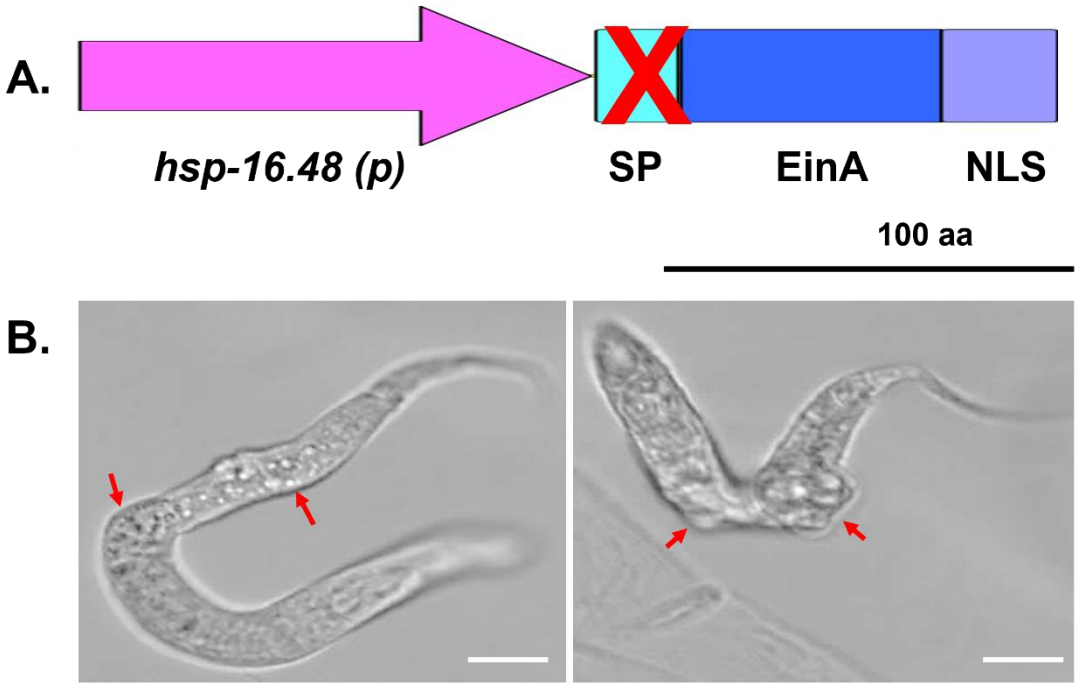

Fig. 16: Heterologous expression of *einAΔSP* in the *unc119* mutant strain causes the deformity phenotype while rescuing movement. (A) Scheme of the expression strategy of *einAΔSP* into the *unc119* mutant. **(B)** The *unc119* rescuing strains with the different deformation range that *einAΔSP* gene was expressed under the all-tissue promoter *eft-3.* Scale bar = 10 µm. Red arrows: deformed positions.

In addition to the previous findings, the deformity phenotype could also be observed in the worms expressing *einA* with SP or without SP under the control of the heat shock promoter *hsp-16.48*. Previous publications reported that the temperature curves of transgenic lines expression were typically between 29 °C and 35 °C (Stringham *et al*., 1992). To assess the expression of *einA* without SP, transgenic lines were subjected to heat shocking at 33 °C for 1 hour on NGM plates spread with OP50 *E. coli* **(Fig. 17, i)**. Subsequently, the worms were allowed recover at room temperature for 30 min before being washed off in distilled water. Notably, worms expressing *einA* without SP showed the deformity phenotype **(Fig. 17 A, ii; indicated by the red arrow and S4 movie)**. Meanwhile, to investigate whether the same phenotype would manifest in transgenic lines expressing einA with SP, worms were heat shocked at 33 °C for three hours and RT at one hour on NGM plates spread with OP50 *E. coli* to induce expression **(Fig. 17 B, i).** Worms with a deformity phenotype were observed **(Fig. 17 B, ii)**.

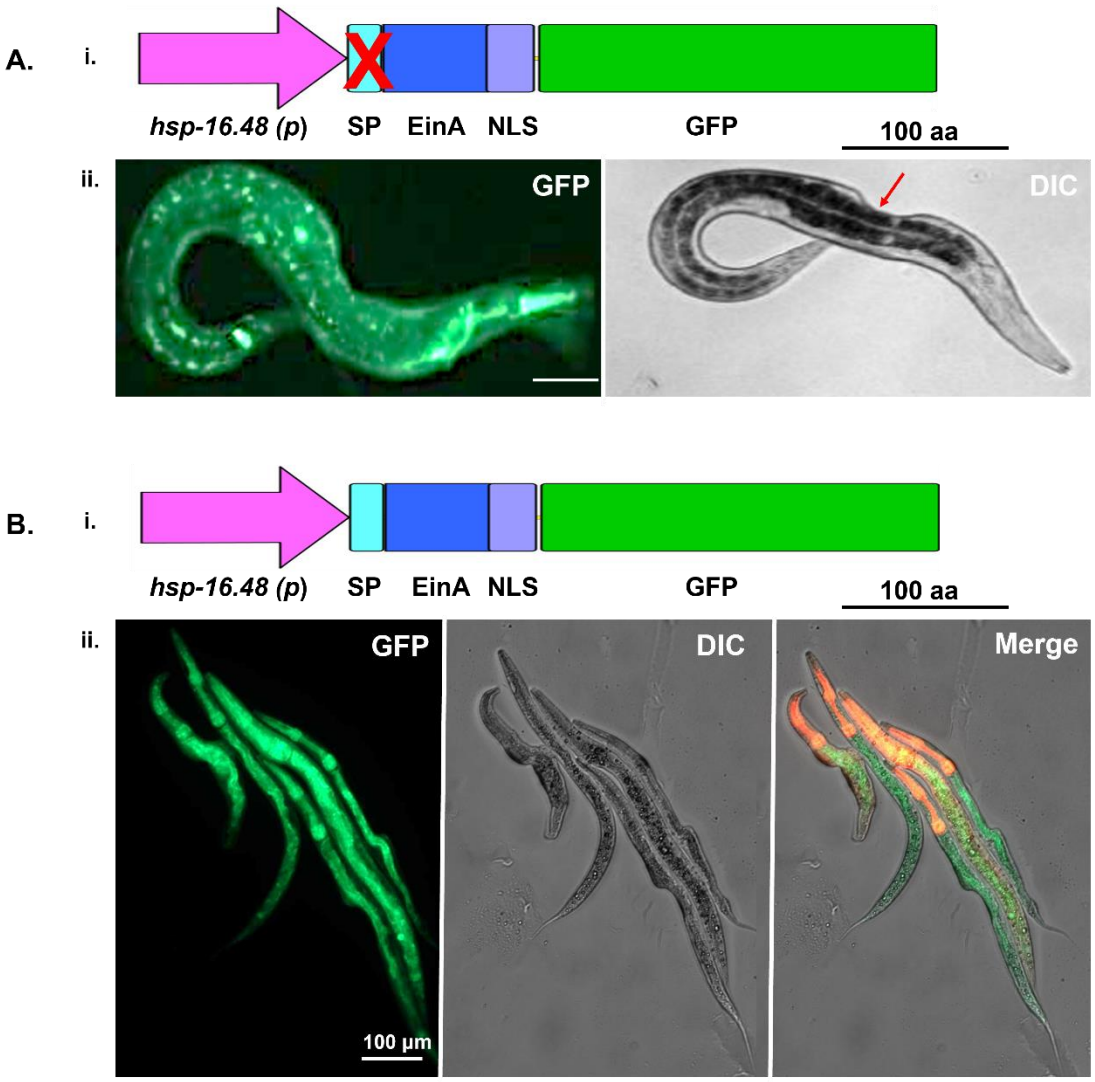

Fig. 17: Morphological phenotype of the transgenic strain expressing EinAΔSP-GFP (A) or EinA-GFP (B) with *hsp-16.48* promoter. (A) Worms expressing EinAΔSP-GFP grown on the NGM medium with OP50 as food was placed at 33 °C for 1 h, and then allowed to recover at RT for 30 min. **(i)** Scheme of the expression strategy of *hsp-16.48*::*einAΔSP::GFP*. **(ii)** A deformed worm carrying with the vector of (i). The red arrow: the deformed position. Scale bar = 10 µm. **(B)** Worms expressing EinA-GFP grown on the NGM medium with OP50 as food was placed at 33 °C three hours and then at RT for one hour for recovery. **(i)** Scheme of the expression strategy of *hsp-16.48*::*einA::GFP*. **(ii)** Five worms carrying with the construct of (B - i), worms represented the different deformed level were shown.

In addition, we assessed the deformity rate in various transgenic lines expressing *einA* with or without the signal peptide (SP). To conduct this analysis,

we synchronized these transgenic worms and obtained twenty adult individuals from each line. We then calculated the deformity rate of the F1 generation of each worm. The findings indicated that both transgenic worm lines, which expressed *einAΔSP::GFP*, *einA::Scarlet*, and *einAΔSP* under the control of the *eft-3* promoter, displayed a deformity rate of 35.65%, 30.78%, and 32.43%, respectively. These rates were significantly higher compared to those observed in worms with an empty vector of *eft-3::GFP* (2.13%) **(Fig. 18)**.

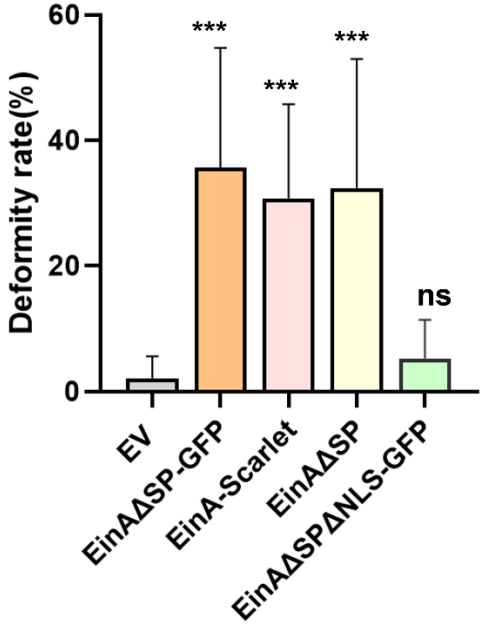

Figure 18: Deformity rate of various transgenic strains. 20 adult worms of each transgenic lines were picked on the NGM medium with OP50 *E. coli*. The number of F1 deformed worms were counted and calculated the deformed rate. [***] P-value < 0.0001.

These transgenic worms represent two distinct phenotypes: the deformity and the wild-type morphology, despite having the same gene expression pattern. The deformity phenotype showed a broader localization of EinA, as observed in the images **(Fig. 16 A, iii, indicated by red arrows)**. This broader localization is likely due to extrachromosomal arrays. It can be inferred that the deformity worms had a higher relative expression of *einA* compared to the

worms with the same gene expression pattern but with wild-type phenotype. A higher expression of *einA* leads to more severe morphological phenotypes. To support this hypothesis, this study investigated the expression of *einA* without the signal peptide under the control of tissue-specific promoters, muscle *myo-3* and cuticle *col-12* promoters in *C. elegans*. The transgenic strain expressing *einA* under the control of *col-12* and *myo-3* promoters did not exhibit any deformities. Additionally, the lifespan of the transgenic strain expressing *einAΔSP* with the *col-12* promoter was similar to that of worms with an empty vector (data not shown). For transgenic worms expressing *einA* under the *myo-3* promoter, the movement ability was assessed by the locomotion assay. Ten worms of the adult mutant strains and N2 were picked and placed on the NGM medium with OP50 *E. coli*. Tracks about the movement of worms were record by using a microscope for a duration of 1 minute **(Fig. 19 A and S5 videos)**. The locomotion assay revealed that the body bend frequency of transgenic worms expressing *einA* (28.1 bends per minute) was not significantly different from that of N2 worms (25.3 bends per minute) **(Fig. 19 B)**. This provides evidence that the presence of *einA* under these tissue-specific promoters does not result in deformity and does not impact the lifespan and movement of the worms.

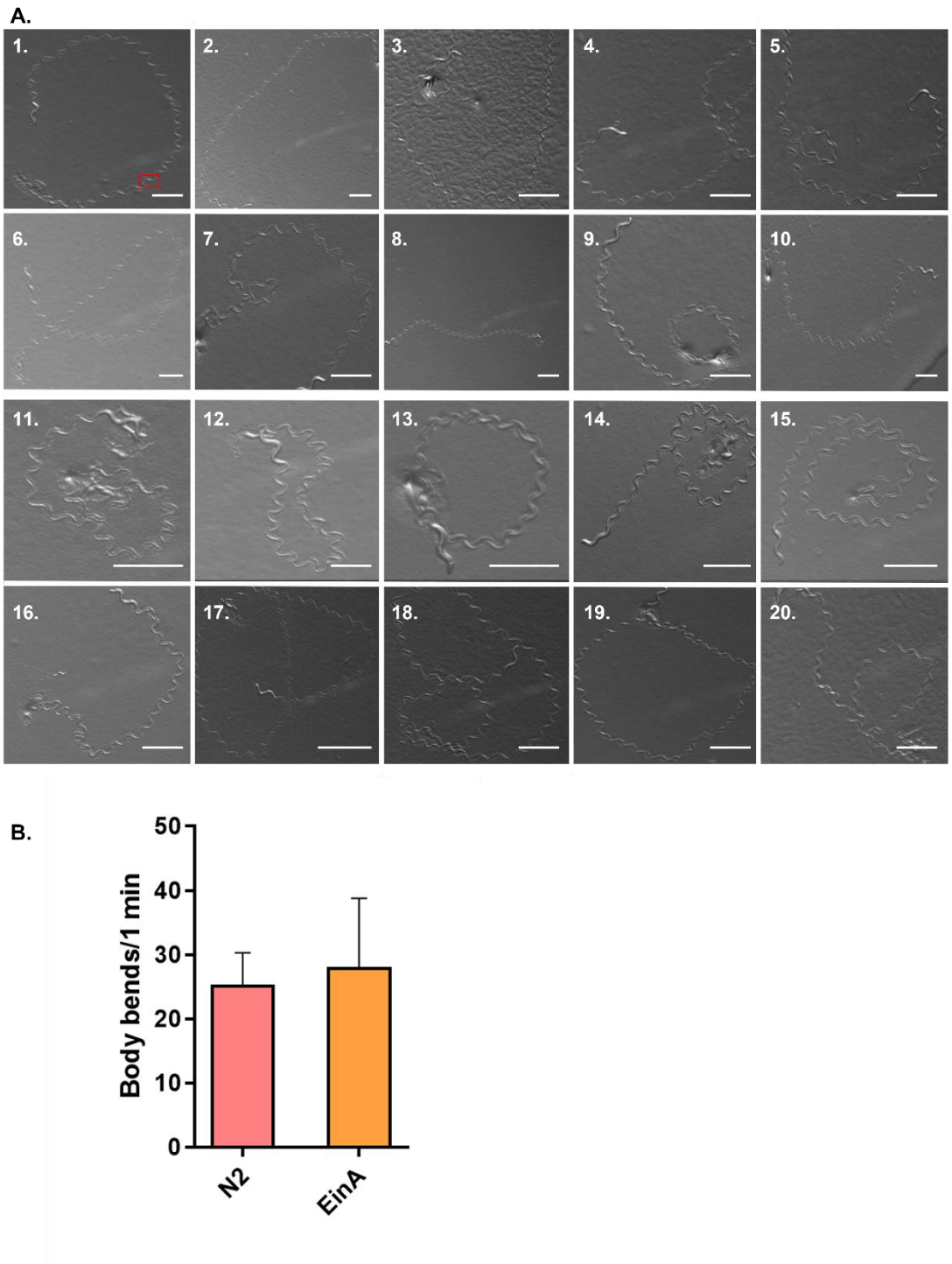

Fig. 19: EinA does not impact locomotion in *C. elegans*. (A) Track records about the cultivation of 20 worms for 1 min at RT. (1-10) N2; (11-20) transgenic worms expressing *einA* under the *myo-3* promoter. the red box contains a body bend. Scale bar = 1 mm. **(B)** The number of body bends was counted for adult worms cultivated on NGM medium with OP50 *E. coli* for 1 min at RT.

2.6 EinA shortens the lifespan and delays maturation process of *C. elegans*

Several transgenic worms with expression of EinAΔSP-GFP and EinA-Scarlet do not exhibit the deformity phenotype, leading us to suspected that the expression of *einA* might have a subset effect that is not reflected in a dramatic morphological phenotype. To explore this further, the longevity analysis of these transgenic strains was performed to investigate a possible influence of heterologous expression of *einA* with or without SP on the lifespan of worms.

For this analysis, N2 nematodes were injected with an empty vector (*eft-3(p)::GFP*) together with the same marker plasmid (*myo-2(p)::tdTomato*) as a negative control. A hundred adult individuals with the wild-type phenotype from each transgenic strain were transferred to three petri dishes with NGM medium and OP50 bacteria as food sources. The medium was supplemented 50 mM 5'fluorodeoxyuridine (FudR) to prevent the formation of offspring. The nematodes were monitored every two days, and worms that no longer responded to touch were considered deceased. Alive nematodes were transferred to the new petri dishes every seven days to guarantee that worms lived in a favorable environment.

Worms in the N2 strain background with an empty vector could survive for approximately 33 days, which was longer than the lifespan of worms expressing *einA*. Notably, the lifespan of worms with SP (25 days) or without SP (25 days) had no difference, indicating that the presence of signal peptide sequence did not influence the lifespan of worms **(Fig. 20)**.

Similarly, 30 individuals with the deformity phenotype from each strain were transferred to two petri dishes with NGM medium and OP50 bacterial as food

sources. The nematodes were checked daily, and worms that no longer responded to touch were determined dead. In comparison to the worms with the control vector, worms with deformity phenotype experienced a significant reduction in lifespan, only 14 days for worms with *einA*-expressing and 16 days for *einAΔSP*-expressing worms. The reduction in lifespan indicated that *einA* expression might have a negative impact on life expectancy by affecting the physiology of the nematodes **(Fig. 20)**.

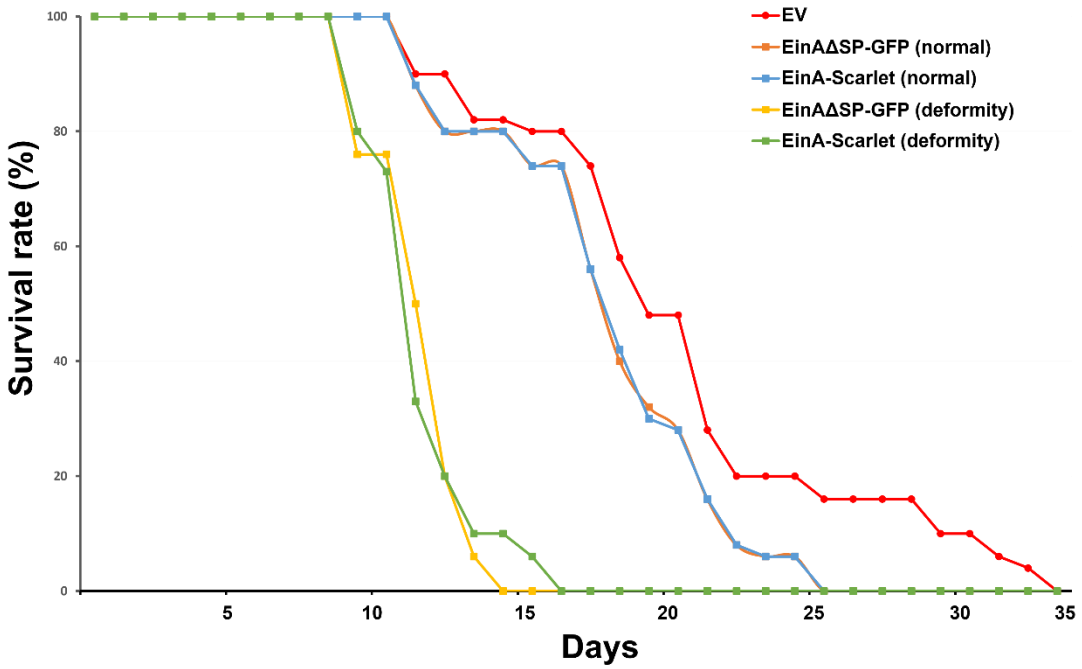

Fig. 20: Lifespan assay with *C. elegans* transgenic strains with wild-type morphological phenotype and deformed phenotype. Survival curves of N2 with empty vector (*eft-3(p)::GFP* & *myo-2(p)::tdTomato*), the strains with different phenotype expressing *einAΔSP::GFP* and *einA::Scarlet*. Lifespan assays were performed on NGM plates with 50 mM FudR at 20 ˚C. n[normal] = 100, n [deformity] = 30.

Mutants with heavy deformity phenotype were largely infertile and showed a significant reduction in lifespan. On the other hand, transgenic worms with the wild-type phenotype look small and scrawny even though they were capable of

developing into adult stage and generating offspring. To investigate whether EinA could be responsible for the growth retardation, we conducted a test to determine the time required for maturation from the L1 stage to the adult stage when the first egg is generated.

As mentioned before, the presence or absence of the signal peptide (SP) did not influence the phenotype induced by EinA. Thus, 40 individuals expressing EinAΔSP-GFP with wide-type phenotype at the L1 stage were picked up to 40 small Petri dishes containing NGM medium and OP50 bacterial as the food source. The nematodes were monitored every 8-10 hours, and the time at which each worm produced the first egg was recorded. The data showed that all N2 worms with the empty vector were able to generate the first egg after 48 hours. In contrast, only 56% of transgenic worms could do. These mutants took more time (72 hours) to develop into the adult stage. These findings indicate that the expression of *einA* in *C. elegans* leads to developmental impairments, resulting in a delayed maturation process **(Fig. 21)**.

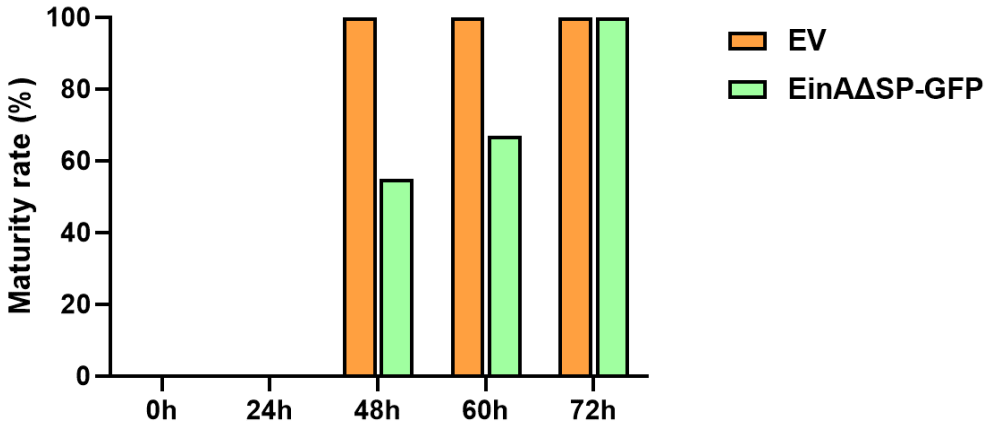

Fig. 21: Heterologous expression of EinAΔSP-GFP in *C. elegans* caused development retardation. The individuals of synchronized transgenic worms and control worms that developed into L1 were picked, respectively. The time developed from L1 larvae to adult worms that generate the first egg was checked. L1 larvae were obtained after two days of synchronization. n [EV] = 40, n [EinAΔSP-GFP] = 40.

2.7 The NLS is critical for EinA distribution and toxicity in *C. elegans*

Taking into consideration the presence of a predicted nuclear localization signal (NLS) within the C-terminal region of EinA (amino acids 85-112), we investigated the functional significance of this NLS. *einA* without SP and NLS was extrachromosomally expressed under the *eft-3* promoter in *C. elegans* **(Fig. 22 A)**. The distribution patterns observed in several transgenic lines clearly indicated that NLS plays a critical role in facilitating the distribution of EinA **(Fig. 22 B)**. the absence of nuclear localization signal effectively stopped EinA from distributing into nuclei **(Fig. 22 C)**, which suggested that the predicted NLS is fully functional for the distribution of EinA. Moreover, only 5.28% of the transgenic strain displayed the deformity phenotype, which was comparable to worms expressing the empty vector (*eft-3::GFP*) (2.13%) **(Fig. 18)**. In comparison with the transgenic strain expressing *einA* with *SP* and without *SP* , the absence of NLS dramatically weaken the toxicity of EinA for *C. elegans*. Likewise, the lifespan assay was preformed to check the impact of EinA without SP and NLS on worms' survival time. A hundred worms with an empty vector could survive for approximately 29 days, which had no difference with the lifespan of worms expressing *einAΔSPΔNLS* (27 days) **(Fig. 22 D)**. It indicated that NLS plays an essential role in not only EinA distribution but also EinA toxicity.

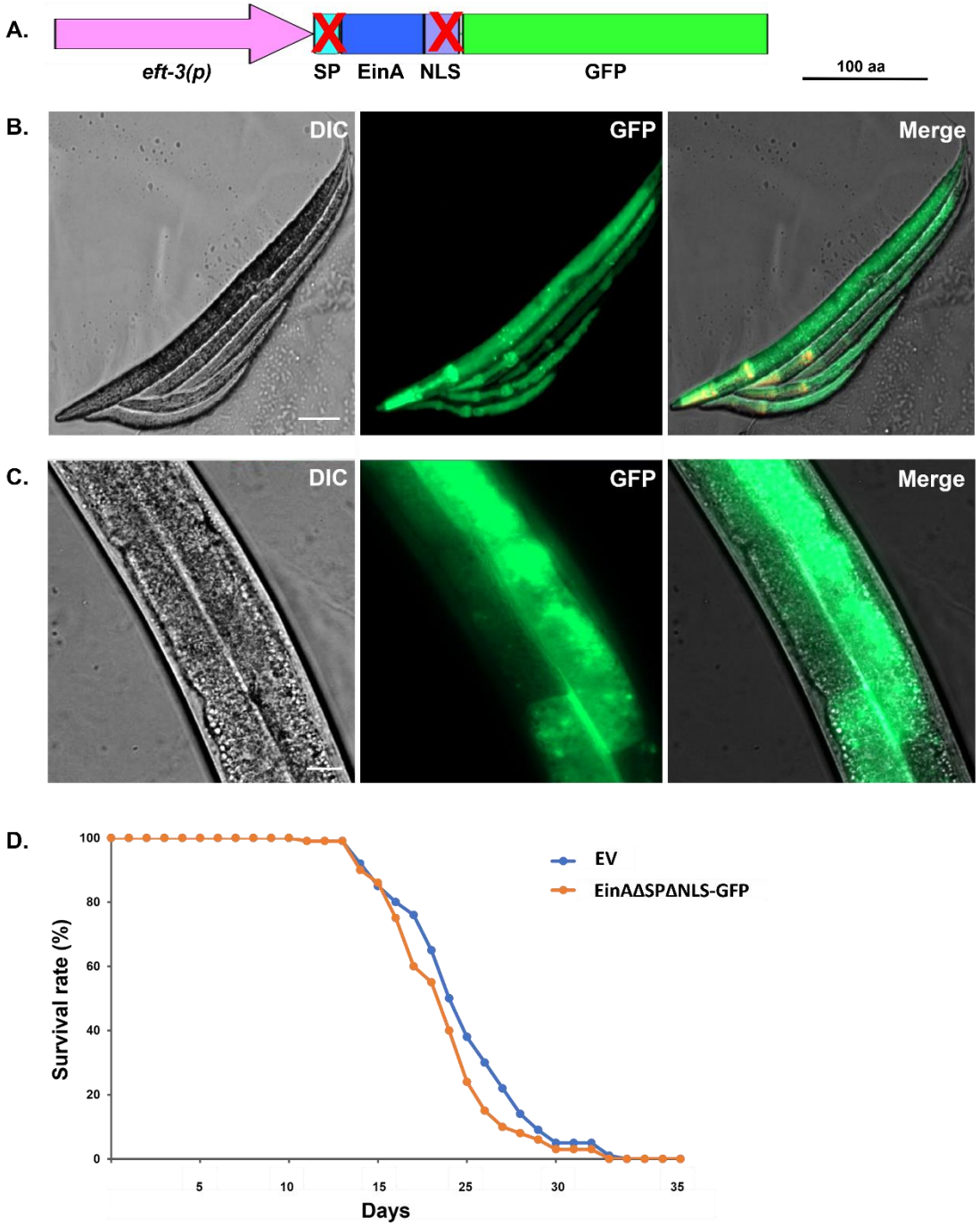

Fig. 22: EinAΔSPΔNLS localizes in the cytoplasm of *C. elegans*. An N-terminal GFP fusion protein of EinAΔSPΔNLS expressed in *C. elegans*. It localized cells ubiquitously. The gene was expressed using the *eft-3* promoter. The red fluorescence showed the expression of the marker plasmid (*myo-2(p)::tdTomato*) in the pharynx of *C. elegans*. **(A)** Schematic representation of the construct of *eft-3* promoter fusion *einAΔSPΔNLS::GFP*. **(B)** Five worms expressing with the plasmid of (A). Scale bar = 20 µm. **(C)** A worm with EinAΔSP&NLS-GFP signals in the cytoplasm. Scale bar = 10 µm. **(D)** Survival curves of N2 with empty vector (*eft-3(p)::GFP* & *myo-2(p)::tdTomato*), the

strains expressing EinAΔSPΔNLS-GFP. Lifespan assays were performed on NGM plates with 50 mM FudR at 20 ˚C. n = 100.

To regulate the expression level of *einA* and mitigate potentially fatal phenotypes, an inducible promoter of *hsp-16.48* was chosen in *C. elegans*. Transgenic lines expressing *hsp-16.48::einA::GFP* **(Fig. 23 A)** and *hsp-16.48::einAΔSP::GFP* **(Fig. 23 C)** were established using *myo-2::tdTomato* as a co-marker. Under non-activated condition at 33 °C, no GFP signal was observed, confirming the dependence on promoter activation. The strains expressing EinA-GFP were subjected to a three hours incubation at 33°C, followed by one hour at RT to recovery, allowing for promoter induction. Microscopic examination revealed ubiquitous localization of the GFP signal **(Fig. 23 B)**. In the strain expressing *einA* without the signal peptide (SP), the GFP signal was observed as distinct dots, more likely in nuclei of specific regions, primarily in intestine, head neuron, central nerve cord and tail ganglia **(Fig. 23 D - F)**.

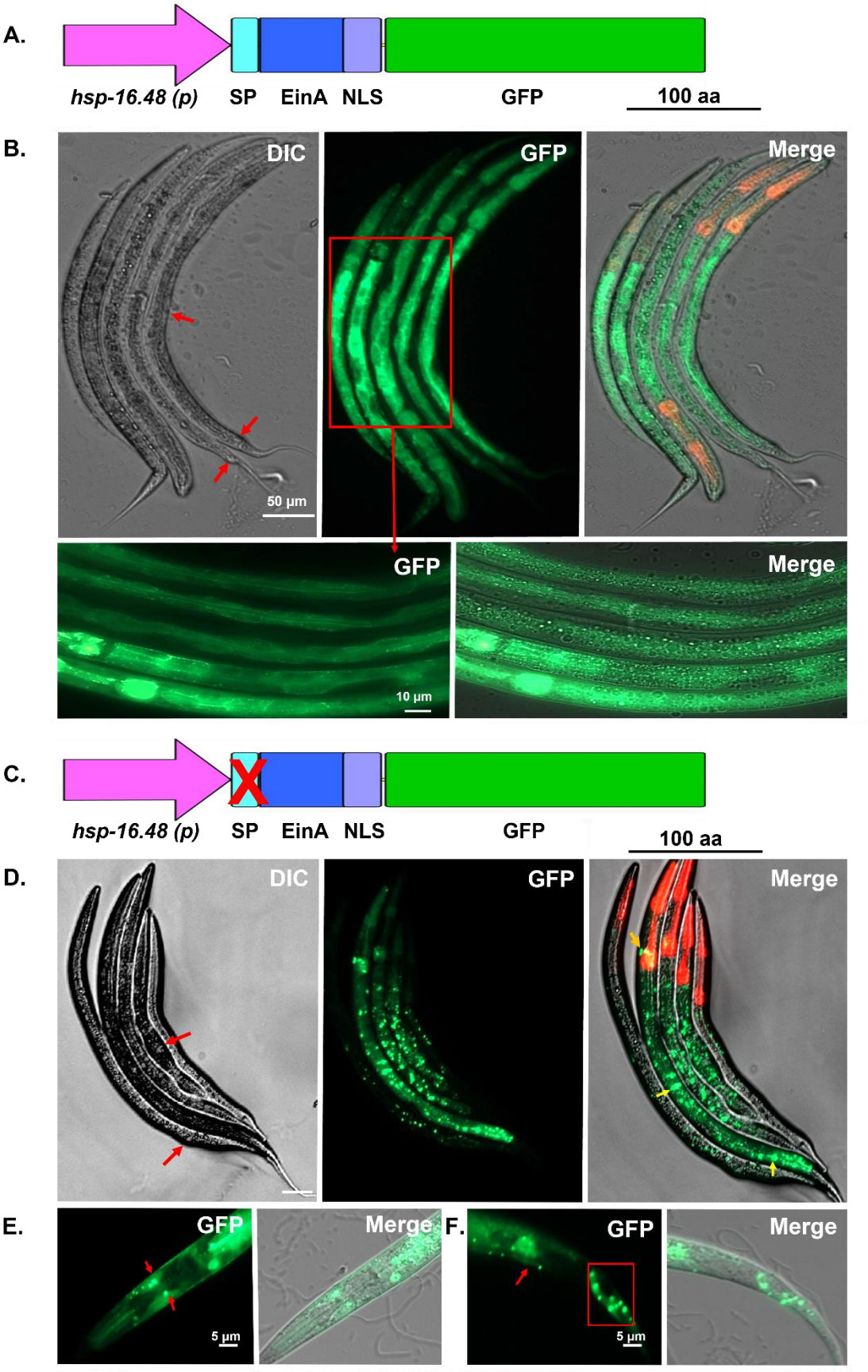

Fig. 23: Localization of EinA-GFP and EinAΔSP-GFP under the control of

the *hsp-16.48* promoter in the N2 strain. (A) Scheme of the vector of *hsp-16.48::einA::GFP*. **(B)** Worms carrying on the construct of (A) were grown on the NGM medium with OP50 as food was placed at 33 °C three hours and then at RT for one hour for recovery. the red signal at the pharynx showed the control plasmid of *myo-2(p)::tdTomato* was transformed into N2 strain successfully. Red arrows: deformed positions. **(C)** Scheme of the vector of *hsp-16.48::einAΔSP::GFP*. **(D)** Transgenic worms with the construct of (C) were placed on the NGM medium with OP50 as food was placed at 33 °C three hours and then at RT for one hour for recovery. the red signal at the pharynx showed the control plasmid of *myo-2(p)::tdTomato*. Red arrows: deformed positions; yellow arrows: signals in nuclei, probably in the neuron and intestine cells. Scale bar = 50 μm. **(E)** Some signals in head. **(F)** Some signals in tail.

2.8 Heterologous expression of *einA* induces immune responses and digestion pathways

As mentioned previously, the heterologous expression of *einA*, with SP or without SP, resulted in a decrease in survival time and development impairment. which probably also triggered some immune response pathways. Furthermore, the distribution of the EinA without SP within the nematode consistently indicated their involvement in nuclei. It is hypothesized that EinA likely binds to DNA, leading to the reprograming of essential genes translation to facilitate digestion. Another possibility is that EinA interacts with some transcriptional factors to suppress the immune response pathway. In order to investigate this further, the relative expression level of certain transcriptional factors associated with the defense system was examined, including *irg-4*, which is controlled by the p38 MAP kinase pathway (Anderson *et al*., 2019); *zip-2*, involved in mRNA translation surveillance for essential host defense processes (Estes *et al*., 2010); *arf-7*, related to aging pathway (Matheu *et al*., 2008); *daf-6*, participating in neuroendocrine signaling pathway (Li *et al*., 2003); *nlp-29*, involved in cellular wound-healing mechanism and the induction of AMP gene expression (Ziegler *et al*., 2009); *spp-5*, which produces antimicrobial peptides against infection (Bogaerts *et al*., 2010).

The result of the relative expression analysis of *einA* showed a significant up-regulation of *einA* expression in the mutant strains expressing *einAΔSP* with the *eft-3* and the *hsp-16.48* promoter, respectively **(Fig. 24 A)**. Consequently, these strains were employed to assess the expression levels of the aforementioned transcriptional factors, which are associated with the immune response. When compared to N2 at 33 °C for 3 hours, the relative expression of *irg-4* **(Fig. 24 B)**, *zip-2* **(Fig. 24 C)**, and *daf-6* **(Fig. 24 E)** showed a slight up-regulation in the mutant expressing *einAΔSP* under the *hsp-16.48* promoter at the same treatment. However, the expression of *nlp-29* **(Fig. 24 F)** and *spp-5* **(Fig. 24 G)** were slightly down-regulated. In Comparison to N2, the expression of *zip-2* **(Fig. 24 C)**, *arf-7* **(Fig. 24 C)**, and *daf-6* **(Fig. 24 E)** were up-regulated in the mutant with the expression of *einAΔSP* under the control of *eft-3* promoter. However, there was no change in the expression of *irg-4* **(Fig. 24 B)**, *nlp-19* **(Fig. 24 F)** and *spp-5* **(Fig. 24 G)**. These results indicated that EinA, as a putative virulence factor, has a subtle impact on the immune response of *C. elegans*, which correspond to the fact that the genetic evolution of effector proteins is achieving optimal toxicity and evading host detection. The differential changes observed in *irg-4*, *nlp-29*, and *spp-5* in mutants with different genotypes suggest the activation of distinct immune responses under different expression conditions. Therefore, EinA appears to exhibit suppressive actions on specific defense pathways triggered by different treatments. This insight implies that heterologous expression of effectors from *A. flagrans* into *C. elegans* may not accurately represent the true infection situation. Consequently, it is crucial to establish a more effective strategy to determine the specific immune responses activated when EinA functions during real infection. For instance, single-cell RNA sequencing (scRNA-Seq) of cells obtained from various organelles could be employed to analyze the invasion of *C. elegans* by *A. flagrans*.

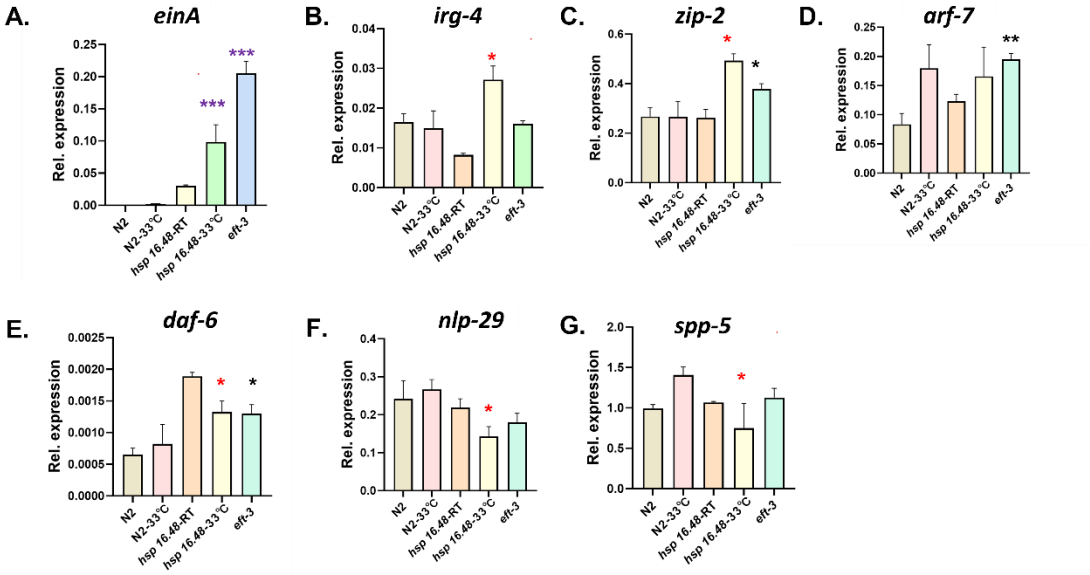

Fig. 24: EinA affects the relative expression level of some genes that are related to the immune response. (A) The relative expression of *einA* in the different transgenic strains. For 33 °C treatment, the worms were kept for 3 h and then recovered for 1 h at RT. **(B-G)** The relative expression of the immune response genes of *irg-4* **(B)**, *zip-2* **(C)**, *arf-7* **(D)**, *daf-6* **(E)**, *nlp-29* **(F)**, and *spp-5* **(G)** in the *einA*-expressing strains with the different promoter, normalized against actin expression. The error bar indicates the standard deviation of three technical replicates. Asterisk (*) markers indicate a significant difference (*p<0.05). Red asterisks indicate a significant difference between transgenic worms expressing *einA* under the *hsp-16.48* promoter at RT and 33 °C; black asterisks indicate a significant difference between transgenic worms expressing *einA* under the *eft-3* promoter and N2.

In this study, I conducted an RNAseq analysis to investigate the molecular changes occurring in *C. elegans* upon expression of EinA-GFP under the control of the *eft-3* promoter, and *hsp-16.48* promoter at 33 °C for 3 hours. As the negative control, N2 worms, and transgenic worms expressing EinA-GFP under the control of the *hsp-16.48* promoter at RT for the same duration were maintained. This analysis revealed significant findings regarding the impact of EinA on *C. elegans*.

The expression of numerous genes was observed to change **(Fig. 25 A - C)** in the worms with *einA* expression. We hypothesize that EinA plays a crucial role

in facilitating *A. flagrans* in digesting *C. elegans*. Therefore, special attention was given to genes associated with digestion pathways involved in protein digestion and absorption; as well as lipid metabolism; and the transportation and secretion of hydrolases, including lysosomes, Peroxisome, and Phagosomes. When comparing the RNAseq data between transgenic worms expressing *einA* under the *hsp-16.48* promoter at RT and 33 °C for three hours, respectively, a substantial total of 50 upregulated genes were observed **(Table S1)**. Considering the significant upregulation of these genes, it is likely attributed to the high temperature. In contrast, when analyzing the data of N2 worms at RT and 33°C for three hours, only two genes (lys-2 and cest-24) upregulated genes associated with the digestive pathway were identified **(Table S2)**, with only the lys-2 gene shared between the two conditions. It suggests that the rest of upregulation of 49 genes observed in the transgenic worms expressing *einA* under *hsp-16.48* promoter at 33 °C for three hours can be primarily attributed to the expression of *einA*, thereby excluding the impact of temperature on the digestive system **(Fig. 25 D, i)**.

Moreover, during the comparative analysis of N2 worms and transgenic worms expressing *einA* under the *eft-3* promoter, a total of 21 upregulated genes related to the digestive system were identified **(Table S3)**. Likewise, only the lys-2 gene mentioned above that were upregulated due to temperature. nine genes were up-regulated when *einA* was expressed under the *hsp-16.48* promoter and the *eft-3* promoter in *C. elegans*, respectively. **(Fig. 25 D, ii)**. These findings provide additional support to the conclusion that the upregulation of genes associated with the digestion pathway is primarily driven by the expression of *einA*.

Likewise, we observed the activation of several immune response pathways in response to *einA* expression, such as the p53 signaling pathway and the insulin signaling pathway, indicating that *C. elegans* activates specific defense

mechanisms to counteract the impact of EinA, suggesting that EinA's virulence factors trigger immune responses in the host **(Fig. 25)**. The upregulation of genes associated with digestion, transportation and secretion of hydrolases, neuroendocrine pathways, and immune response pathways indicates the multifaceted effects of EinA on the host.

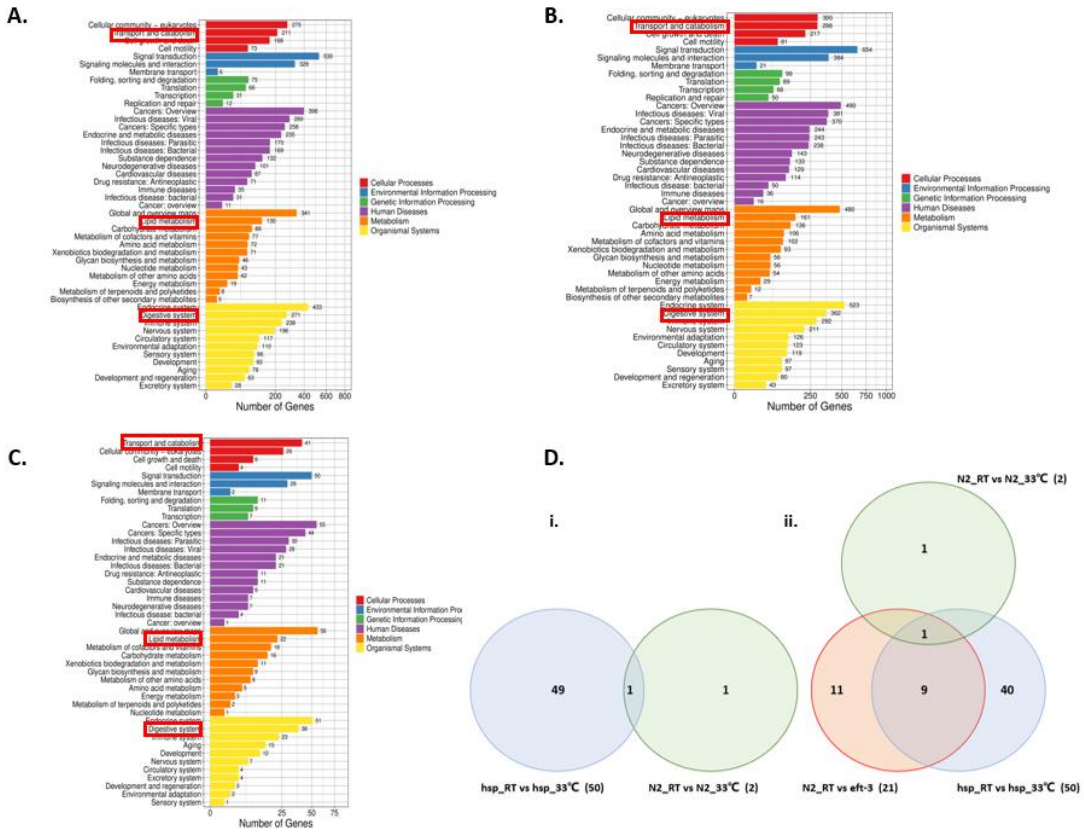

Figure 25: EinA up-regulates genes related to digestion pathways. Pathway classification of differentially Expressed Genes (DEGs) among various transgenic worms. **(A)** Comparison between transgenic worms expressing *einA* under the *hsp-16.48* promoter at RT and worms with the same transgenic pattern at 33 °C for 3 h (hsp_RT vs hsp_33 °C). **(B)** Comparison between N2 worms and transgenic worms expressing *einA* under the *eft-3* promoter (N2_RT vs eft-3). **(C)** Comparison between N2 worms at RT and at 33 °C (N2_RT vs N2_33 °C). Red boxes indicate pathways related to transportation and catabolism, lipid metabolism, and the digestive system. **(D)** Venn diagrams of up-regulation of genes involved in the digestive pathway, and transportation and secretion of hydrolases, including lysosomes, peroxisomes, and phagosomes, both within samples and between groups.

2.9 Analysis of another effector: NipB

Among the ten detected genes mentioned previously, one gene (*dfl_003626*) also capture our attention because of its dramatic up-regulation expression level during the infection process **(Fig. 26 A)**. The bioinformatic analysis of the virulence factor candidate DFL_003626 (NipB: Nematode Induced Protein B) revealed that it is an asparagine-rich small protein consisting 84 amino acids. Signal peptide prediction using signal 4.1 (https://services.healthtech.dtu.dk/services/SignalP-4.1/) indicated the presence of an 18 amino acid predicted signal peptide on the N-terminus. No conserved domain and fewer BLAST hits were found for NipB. The protein contains six cysteines and eight asparagines **(Fig. 26 B)** with an average PI of 8.38. Analysis of the protein with the "Rapid Automatic Detection and Alignment of Repeats (RADAR)" tool revealed that there are no repeat structures within the protein (https://www.ebi.ac.uk/Tools/pfa/radar/). The BLAST search resulted in six hits, revealing 77% identity to the hypothetical *Orbilia oligospora* AOL_s00043g88 (E value = 9e-32), 78% identity to the hypothetical *Orbilia oligospora* TWF788_009668 (E value = 2e-24), 46% identity to the hypothetical *Dactylellina cionopaga* ABW20_dc0108229 (E value = 2e-14), 46% identity to the hypothetical *Arthrobotrys entomopaga* AA313_de0204610 (E value = 4e-13), 44% identity to the hypothetical *Drechslerella dactyloides* Dda_8331 (E value = 3e-05), 44% identity to the hypothetical *Dactylellina haptotyla* H072_7799 (E value =0.001). Secondary structure prediction using the NPS@ server, revealed that NipB predominantly consists of random coils (57.58%), extended strands (7.58%), beta turns (3.03%), and alpha helix (31.82%) (https://npsa-prabi.ibcp.fr/cgi-bin/npsa_automat.pl?page=/NPSA/npsa_sopma.html).

Similar to EinA, the quantitative method employed did not provide any information regarding the phase of the trap formation and infection process

when *nipB* was expressed. Therefore, a reporter assay about NipB was established. With this, A fusion construct containing the coding sequences of histone H2B and mCherry under the control of the *nipB* promoter (2 kb upstream of *nipB* ORF) was expressed in *A. flagrans* **(Fig. 26 C)**. As a control, the same reporter array but *h2b* ORF expressing under the control of the constitutive *h2b* native promoter was generated **(as shown in Fig. 10 B)**. Fluorescence microscopy analysis revealed that strong fluorescence signals from nuclei in the traps and mycelia around traps in the *nipB*(p) reporter strain, and gradually attenuated as the hyphae extended beyond the trap vicinity **(Fig. 26 C)**. The spatial expression of *nipB* has a different expression pattern with *einA* that only expressed in the trophic hyphae inside the nematodes. These spatial expression patterns of *einA* and *nipB* results suggested that these two different effectors are all differently expressed time-wise, as well as spatially.

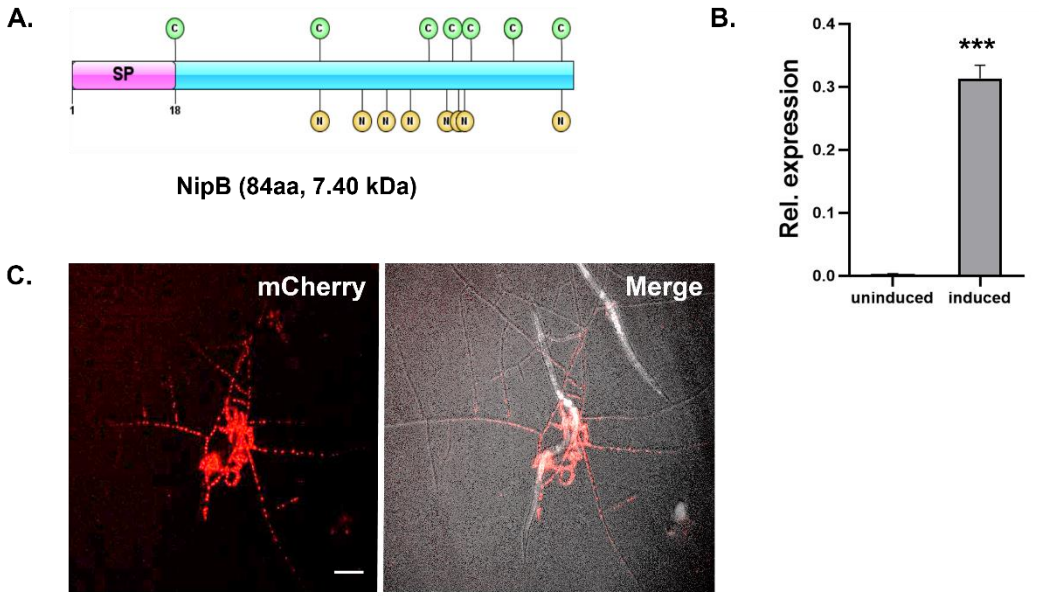

Fig. 26: Expression of *nipB* is induced in traps. (A) Scheme of NipB. The 84 amino acid long protein is asparagine-rich and contains 7 cysteine residues, as well as an 18 amino acid long signal peptide at the N-terminus, **(B)** Quantitative real-time PCR analysis of *nipB* expression in *A. flagrans* hyphae on LNA 24 h with actin as the reference gene for normalization; hyphae were co-cultivated with *C. elegans*. The error bar indicates the standard deviation of three technical replicates. Asterisks (*) indicate a significant difference (*p<0.05, **p<0.01) based on unpaired two-tailed Student's t-test. p-value=0.000014. **(C)**

Spatial distribution of *nipB* gene expression. *h2b::mCherry* was expressed with *h2b* promoter. Pictures were taken after co-cultivation of strains with *C. elegans* at 28 °C for 24 h. Scale bar = 100 µm.

2.10 NipB localizes at the penetration site in the host

To visualize the localization of NipB, a C-terminal fusion of NipB with GFP was generated. This construct was expressed under both the constitutive *A. nidulans oliC* promoter (*oliC(p)::nipB::GFP::trp(c)*) and the *nipB* native promoter (*nipB (p)::nipB::GFP::trpc(t)*). The NipB-GFP fusion protein accumulated in traps, regardless of the presence of worms, particularly at the inner margin of traps **(Fig. 27 A; indicated by the red arrow)**. In contrast, the NipB-GFP fusion protein under the *nipB* native promoter localized at the penetration site inside the nematode's body with a round shape **(Fig. 27 B)**, similar to the distribution observed for CyrA (Wernet *et al*., 2021). Due to strong GFP autofluorescence within the worm body and a relative weak NipB-GFP accumulation signal, a plasmid was constructed with *nipB* fused to *mCherry* under the control of *nipB* promoter. It revealed that NipB-mCherry signals accumulated at the penetration bulb inside the nematodes **(Fig. 27 C)**. Unlike EinA, which distributed in the trophic hyphae inside the nematodes and probably affects the digestion of trapped nematodes, the temporal distribution of NipB at the penetration site suggests its involvement in the middle stage of infection. It is presumed that NipB is more likely to paralyze the nematode and participates in the infection process earlier than EinA.

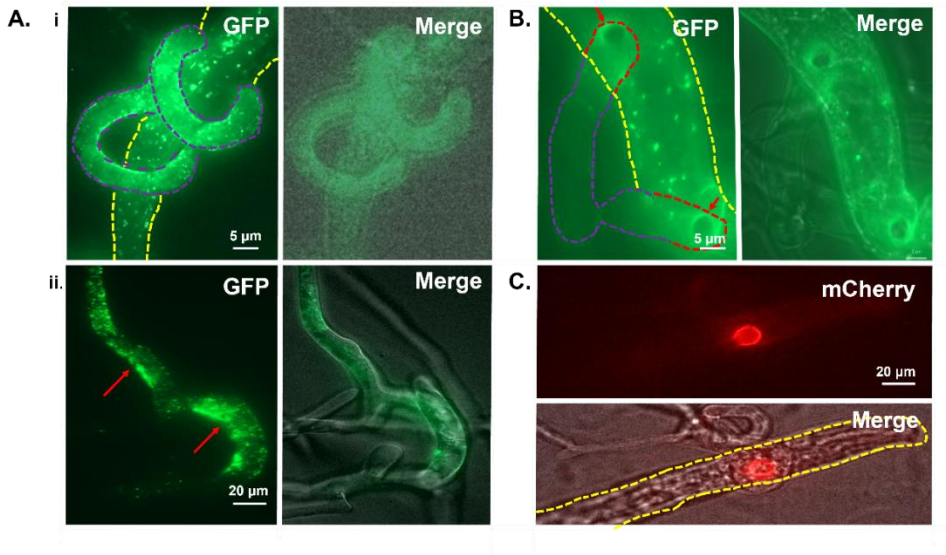

Figure 27: NipB localizes at the penetration site inside nematodes. (A) The *nipB::GFP* expressing strain was co-cultivated with *C. elegans* on the LNA slides at 28 °C for 12 h to induce trap production. *nipB::GFP* was expressed under the *oliC*-promoter. **(i)** A trap with the nematode. Yellow lines region: a worm body; purple lines region: traps. **(ii)** An empty trap. Red arrows: signals in the inner margin of traps. **(B)** The *nipB* expressing strain was co-cultivated with *C. elegans* on the LNA slides at 28 °C for 12 h to induce trap production. *nipB::GFP* was expressed under the *nipB* promoter. And the fusion protein signal occurred in the penetration site inside the worm body. Red arrows: penetration bulbs. Yellow lines region: a worm body; purple lines region: traps outside the worm body; red lines region: trophic hyphae inside the worm body; **(C)** The NipB-mCherry expression strain was co-cultivated with *C. elegans* on the LNA slides at 28 °C for 12 h to induce trap production. *nipB::mCherry* was expressed under the *nipB* promoter. The fusion protein signal occurred at the penetration site inside the worm body. Yellow lines region: a worm body.

3. Discussion

Transcriptome and secretome analysis conducted on *A. flagrans* revealed the production of 638 proteins predicted to possess hydrolase, oxidoreductase, and peptidase activities. Additionally, 117 small-secreted proteins (SSPs) were identified as putative effectors by EffectorP 2.0 (Youssar *et al*., 2019). SSPs are well known for their roles in biotrophic or pathogenic microorganisms, but a role in predatory fungi was less obvious. Therefore, investigating and analyzing these small proteins holds significant promising for understanding the interaction between NTF and nematodes. In this research, we aim to elucidate the potential role of a putative virulence factor called EinA in the virulence of nematode-trapping fungi.

Four out of the 117 putative effector proteins were predicted to localize to the nucleus of the host. Increasing evidence suggests that nuclear localized pathogen effectors play a central role in parasitism, by co-opting the host cell nuclear transport system and hijacking the host transcriptional machinery to suppress the host immunity (Shi *et al*., 2018). For instance, RiNLE1 from *Rhizophagus irregularis* was found to interact with the nucleosome protein histone, resulting in the suppression of defense-related gene expression (Wang *et al*., 2021). Similarly, HopA1 from *Pseudomonas syringae* was shown to interact with RPS6, leading to the suppression of cell death (Kang *et al*., 2021). These findings highlight the advantages that an effector protein with nuclear localization can provide for the survival and dissemination of pathogenic microorganisms.

Considering the properties and sequence-derived features of effectors, such as those discussed in previous studies (Stergiopoulos & de Wit, 2009; Saunders *et al*., 2012; Syme *et al*., 2013), EinA, as a small size of 112 amino acids,

possesses an N-terminal signal peptide (SP), a C-terminal NLS, no conserved domains, and is induced during infection. These characteristics further support the potential significance of EinA as a nuclear-target effector during infection, worth further investigation.

3.1 The localization of virulence factors represents their function classification in the infection process

The spatial-temporal organization of EinA suggests that its expression pattern aligns with its distribution within the trophic hyphae inside the nematode. Notably, EinA accumulates throughout the entire length of the trophic hyphae rather than being localized exclusively at the tip. This distribution ensures the effective release of a sufficient amount of effector proteins, enabling them to regulate the host immune response and manipulate host cell mechanisms.

Moreover, our laboratory has made an intriguing observation regarding another effector, NipA, at different stages of infection. Notably, GFP-fused NipA shows a significant accumulation at the penetration site rather than in the infection bulb (Jennifer Menzner, 04/2020). This finding distinguishes NipA from CyrA, NipB, and EinA. Therefore, the spatial expression and temporal distribution of effectors could serve as indicators for their specific functions during the infection process. These observations highlight that the localization of virulence factors reflects their functional classification in the context of the infection process.

3.2 The presence of cellular physiology is crucial in relation to the role of EinA in the paralyzed *C. elegans*.

During the infection process of *A. flagrans* on nematodes, the later stage involves the growth of trophic hyphae inside the worm and the secretion of

enzymes primarily responsible for tissue breakdown and nutrient uptake. It is reasonable to hypothesize that the proteins secreted during this stage play a crucial role in facilitating the digestion process. The observed spatial and temporal expression patterns of EinA support the hypothesis that it is produced during the final steps of the interaction, potentially serving to suppress defense responses that are activated in the late stage of infection. Additionally, EinA may play a role in facilitating *A. flagrans* in digesting *C. elegans* by modulating the expression levels of specific hydrolytic genes or regulating genes involved in the transportation and secretion of hydrolases in *C. elegans*. Regarding this hypothesis, there is an important point to note. Since EinA functions during the late stages of infection when the worms are in a paralyzed state, it is crucial to determine whether cellular activities are still present in the worm's cells. Many reports have demonstrated the persistence of cellular activities after organismal death. For instance, there is literature suggesting ongoing regulation of transcription, at least in the immediate hours following death. Studies have shown activation of stress responses, DNA damage detection, and relevant repair mechanisms within seven hours after human death (Hadj-Moussa *et al*., 2019; Pozhitkov *et al*., 2017; Ferreira *et al*., 2018). Mitochondria remain functional for up to 10 hours post-mortem in human cerebral cortical tissue (Barksdale *et al*., 2010). This evidence suggests that some cellular functions, such as intracellular enzyme activity, membrane permeability, and ion homeostasis, may continue for some time after death. In addition, some cell types may maintain certain functions after death, for example nerve cells may continue to release neurotransmitters (Mele *et al*., 2019). However, over time, without a supply of nutrients and oxygen, the cells gradually lose their vitality and eventually die. This process can vary depending on tissue type and environmental conditions. Thus, these findings collectively provide compelling evidence supporting the hypothesis that EinA is capable of hijacking the genome of paralyzed worm cells to exert its functional effects.

3.3 Individual effectors with an intelligent strategy of tiny effects in the process of host-pathogen wrestling

Based on the spatial expression and temporal distribution patterns, we can speculate that EinA likely plays a role in later stages of the interaction. The results of this assay showed that the *einA*-deletion strain took longer to complete digestion, while the time of paralysis remained unchanged. This finding could potentially support the assumption that EinA is required for the digestion process. Additionally, the observation that the *einA*-overexpression strain exhibited a shorter digestion time further supports this assumption. Furthermore, the fact that the *einA*-deletion strain displayed a wild-type morphological phenotype suggests that EinA may not participate in any developmental processes. It is worth noting that the deletion of individual effectors, such as EinA, CyrA, and NipB, often has only a slight side effect or even no impact on virulence. This phenomenon has been observed in various other pathogenic organisms, including *Xanthomonas axonopodis* (Lopez *et al*., 2019), *P. syringae* (Liu *et al*., 2019). Effectors with the characteristics of avoiding the activation of the defense system due to being recognized by the host are doomed that they cannot play a significant role individually. That is also the reason why a fascinating feature of these effectors is their lack of sequence identity with known proteins. Additionally, the relative expression results of certain transcriptional factors related to the immune response in transgenic strains with heterologous expression of *einA* showed only slight changes, which could be considered as evidence of EinA's minimal toxicity to *C. elegans*. However, as an old Chinese saying goes, "the fire burns high when everyone brings wood." This saying can be applied to the interaction between hosts and pathogens. Individually, the deletion of *einA* might only cause a slight decrease in virulence. However, deleting *einA* in combination with other effector genes simultaneously or deleting the entire effector cluster could potentially

lead to a significant decrease in virulence impact. For example, the deletion of the largest gene cluster of *19A*, which encodes 24 secreted effectors identified in *Ustilago maydis*, results in a severe attenuation of virulence (Brefort *et al*., 2014). This hypothesis could be further confirmed by employing a more efficient knockout strategy, such as the *CRISPR-Cas9* method. Alternatively, deleting key genes that regulate the secretion of multiple effectors could potentially block the effector-mediated effects. For example, the deletion of *hrp* gene cluster could be strongly reduced in vitro secretion of effector proteins and hypersensitive response triggered by type III (TTS) system (Gürlebeck *et al*., 2006). Understanding how effectors contribute to disease progression and how the host's defense network perceives them remains a significant area of study in the field of host-pathogen interactions.

3.4 Heterologous expression of *einA* activates the immune response and digestion pathway of *C. elegans*

The virulence assay indicate that EinA has only a slight negative impact on *C. elegans* during natural infection due to functional redundancy among effectors (Tan *et al*., 2015; Birch *et al*., 2008). To further analyze the influence of EinA on *C. elegans*, the heterologous expression approach was considered increase the influence of EinA on *C. elegans*. This strategy has been widely used to produce valuable biomolecules in more suitable hosts and to discover novel bioactive compounds through the expression of cryptic gene clusters (Huo *et al*., 2019). This transgenic method has also been extensively employed to investigate the interaction between pathogens and hosts. For instance, in C. elegans, the expression of bacterial pertussis toxin (PTX) has been utilized to identify G proteins as the targets of these toxins (Darby & Falkow, 2001). Heterologous expression of key monoamine receptor agonists in *C. elegans* has been employed to identify ligands for host anthelmintic targets (Law *et al*., 2015). Therefore, this approach may also be suitable for examining the effect

of virulence factors on the immune response of *C. elegans*.

Initially, tissue-specific promoters such as *col-12* and *myo-3* were used to express *einA* in *C. elegans*. However, these mutants did not cause any discernible effects on *C. elegans*. One possible explanation for this observation is that localized *einA* expression within specific organelles is insufficient to induce obvious morphological phenotypes. This hypothesis was supported by the presence of two different phenotypes (wild-type and deformed) within the same transgenic line, attributed to variations in the expression level of *einA* resulting from extrachromosomal arrays. To maximize the production and widespread distribution of EinA, the use of all-tissue promoters, such as *eft-3* and *hsp-16.48*, was considered for expressing *einA* in *C. elegans*. The results demonstrated that EinA caused a deformed phenotype, reduced lifespan, and delayed maturation, indicating its toxicity to *C. elegans*. Furthermore, the NLS was found to be crucial for the toxicity of EinA.

How does EinA impair *C. elegans*? There have many reports showed infection by viruses commonly causes the arrest of host translation to allow viral transcripts privileged access to host translational machinery. For instance, bacterial toxins are known to target host translation, such as diphtheria toxin, ricin toxin, and Shiga toxin (Dunbar *et al*., 2012). Cycloheximide, a translational elongation inhibitor, was originally isolated from the soil bacterium *Streptomyces griseus* (Schneider-Poetsch *et al*., 2010). Considering that EinA contains a nuclear localization signal at the C-terminus, we hypothesized that EinA may (1) act as a transcription factor that directly activates transcription in host cells, or (2) target host transcription factor activity. To investigate this, we measured the expression of several immune response-related transcription factors in the *einA*-expressing strains. The up-regulation of *zip-2*, *arf-7*, and *daf-6* expression levels indicated the mRNA translation regulated by the *zip-2*

pathway; aging pathway regulated by *arf-7*; DAF-7/TGFβ-like signaling pathways regulated by *daf-6* were activated. However, the relative expression of *Spp-5*, which produces antimicrobial peptides against infection, showed no change in the *einA*-expressing strain. It is worth noting that mutants can significantly alter pathogen resistance even if they do not appear to primarily respond to microbial infection (Ermolaeva & Schumacher, 2014).

The slight up-regulation of these transcription factors suggests that EinA may indirectly influence the immune system, or the observed phenotypes resulting from *einA* expression may be a manifestation of a cascade reaction within the immune system, similar to how the signal-regulated kinase (ERK) mitogen-activated protein (MAP) kinase cascade mediates tail swelling and protects *C. elegans* from severe constipation (Nicholas & Hodgkin, 2004).

The activation of the TGF-β signaling pathway and the expression of *daf-6* can induce the dauer program in *C. elegans* (Patterson & Padgett, 2000). Therefore, we suspect that the mutants expressing *einA* may have entered the dauer stage, resulting in further developmental retardation. Dauer worms can exhibit a decreased lifespan due to enhanced tolerance to proteotoxic damage, even at the cost of cell damage, through neuroendocrine regulation under stressful conditions.

In addition to the above findings, an RNAseq analysis was conducted on *C. elegans* expressing EinA-GFP under the control of the *hsp-16.48* promoter and *eft-3* promoter. This analysis revealed the upregulation of numerous genes associated with digestion pathways, including lysosomes, peroxisomes, and metalloproteinase. These findings suggest that the increased production of hydrolases in *C. elegans* may be utilized for self-digestion. Moreover, these results indicate that EinA not only plays a role in activating the immune responses of *C. elegans* but also manipulates the transcriptional machinery of

C. elegans to enhance the production of hydrolytic enzymes, thereby facilitating *A. flagrans* infection in *C. elegans*. This hypothesis can be extended to the dynamics of predator-prey interactions with significant differences in body size, as exemplified by studies involving white-tailed spiders and crickets (Michálek *et al*., 2022), Assassin flies and wasps, bees, and dragonflies (Ghahari *et al*., 2007; Whitfield, 1925). Moreover, a recent study reported that predators may exhibit a response by recruiting additional toxins, consequently leading to an increase in venom complexity (Michálek *et al*., 2022).

3.5 Conclusion and model

My study has demonstrated that EinA, acting as a virulence factor, plays a crucial role in the digestion process. I proposed a hypothesis that upon secretion from *A. flagrans*, EinA enters the nucleus of *C. elegans* through its nuclear localization signal (NLS). Subsequently, EinA might directly bind to DNA or act as a competitor of certain transcription factors, leading to the up-regulation of specific genes associated with the digestion pathway in *C. elegans*. Consequently, a significant increase in the production of hydrolytic enzymes by *C. elegans* is observed, which serves to self-digestion and facilitate *A. flagrans* to digest *C. elegans*. **(Fig. 28)**.

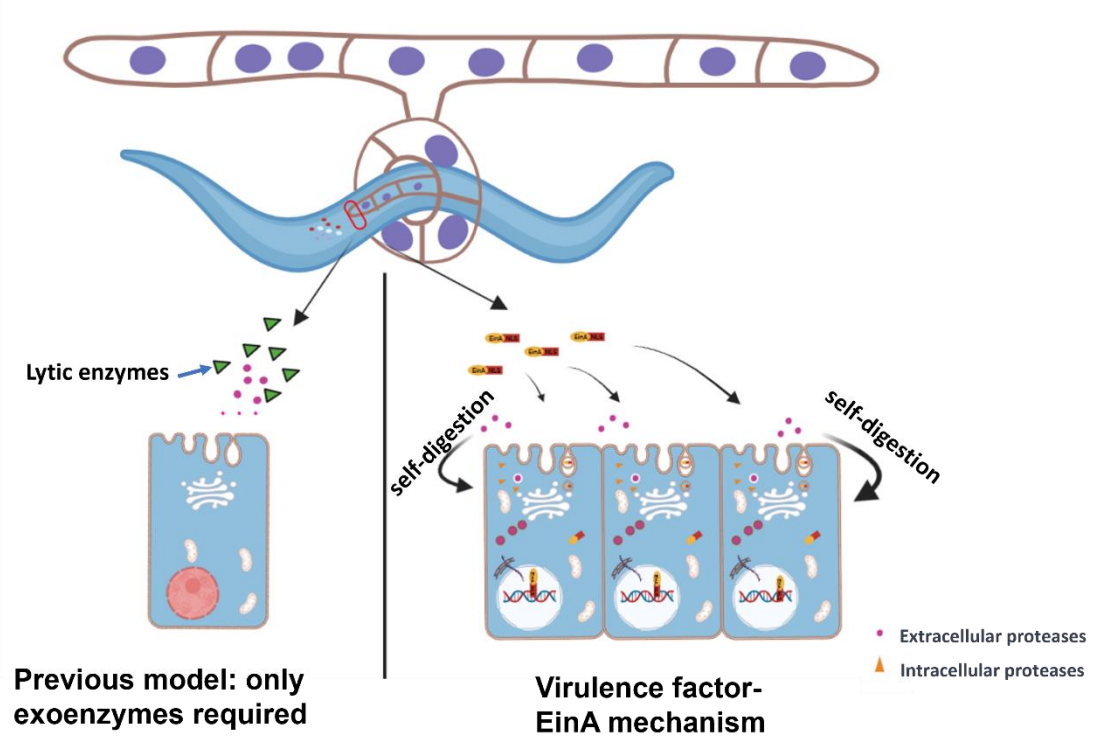

Fig. 28: An illustrative representation of models depicting the toxin-producing mechanism and the virulence factor of EinA mechanism during NTF invasion of the nematodes. On the left side is an old model about the previous mechanism. Extracellular hydrolytic enzymes produced by *A. flagrans,* like chitinases, collagenases, and proteases, degrade the cuticle and then digest nematodes (Pires *et al*., 2022; Al-Ani *et al*., 2022). On the right side is the new model describing the virulence factor – EinA mechanism. During the infection process, EinA is secreted from *A. flagrans* and then enter into the nucleus of *C. elegans* due to the presence of a nuclear localization signal. EinA likely bind to the genome of *C. elegans* or act as a competitor of certain transcription factors, thereby modulating the expression of genes involved in digestive pathways, including non-selective autophagy-lysosome pathway and ubiquitin-proteasome pathway. This modulation accelerates the digestion process. The scheme was created with BioRender.

The upregulation of genes associated with digestion pathways and the transportation of hydrolases provides insights into the molecular mechanisms underlying the interactions between EinA and the host. The hijacking of the transcriptional machinery by EinA implies a sophisticated strategy employed by *A. flagrans* to manipulate the host's cellular processes for its own benefit. These findings broaden our understanding of the complex interplay between

pathogens and hosts, shedding light on the molecular mechanisms underlying nematode infection. Further investigations into the specific genes and pathways involved in the response to EinA will be valuable for unraveling the detailed mechanisms of pathogenesis in this system. This could be a model also valid for other predator-prey interactions.

4. Materials and Methods

4.1 Organisms, plasmids, and oligonucleotides

All *E. coli* strains, *A. flagrans* and *C. elegans* strains are listed below:

Table 1: *E. coli* used in this project.

Strain	Genotype	Resistance	Reference
Top10	F-mcrrA_(mrr-hsdRMSmcrBC) _80lacZ_M15_lacX74 recA1 araD139_(ara-leu)7697 galU galK rpsL(StrR) endA1 nupG	Amp	Invitrogen, Karlsruhe
Op50	Ura-		Institute für Biologie, Bioinformatik und Molekulargenetik, Freiburg

Table 2: *A. flagrans* strains used in this project.

strain	genotype	Resistance	Source
A. flagrans CBS 349.94	Wild type (WT)	-	CBS-KNAW culture & collection
SMH02	*einA(p)::h2b::mCherry::tubT*	hph	This work
SNH04	*h2b(p)::h2b::mCherry::tubT*	hph	(Wernet *et al*., 2021a)
SMH04	*oliC(p)::einA::GFP::gluC(t)*	hph	This work
SMH56	*oliC(p)::einAΔSP::GFP::gluC(t)*	hph	This work
SMH10	*einA(p)::einA::GFP::gluC(t)*	hph	This work
SMH13	*gpd(p)::einA-lccC:: gluC(t)*	hph	This work

SMH14	*gpd(p)::einA-lccCΔSP:: gluC(t)*	hph	This work
SMH20	*ΔeinA*	G418	This work
SMH67	*SMH20 x einA(p)::einA::einA(t); hph; Recomplementation*	hph	This work
SMH68	*SMH20 x einA(p)::einA::einA(t); G418; Recomplementation*	G418	This work
SMH01	*nipB(p)::nipB::GFP::gluC(t)*	hph	This work
SMH03	*oliC(p)::nipB::GFP::gluC(t)*	hph	This work
SMH05	*nipB(p)::h2b::mCherry::tubT*	hph	This work
SMH12	*nipB(p)::nipB:: mCherry::gluC(t)*	hph	This work

Table 3: *C. elegans* strains used in this work.

Strain	Genotype	Source
SMH22	*myo-2(p)::tdTomato hsp-16.48::einA::GFP*	This work
SMH23	*myo-2(p)::tdTomato hsp-16.48::einAΔSP::GFP*	This work
KIT03	*myo-2(p)::tdTomato hsp-16.48::Scalet*	(Wernet *et al*., 2021a)
SMH30	*myo-2(p)::tdTomato eft-3::einAΔSP::GFP*	This work
SMH31	*myo-2(p)::GFP eft-3::einA::Scarlet*	This work
SMH32	*eft-3::einA*	This work
SMH41	*myo-2(p)::tdTomato eft-3::einAΔSP&NLSs::GFP*	This work
SMH34	*myo-2(p)::tdTomato eft-3::GFP*	This work
SMH36	*myo-2(p)::tdTomato col-12::einAΔSP::GFP*	This work
SMH37	*myo-2(p)::tdTomato col-12::GFP*	This work
SMH39	*myo-2(p)::tdTomato myo-3::einA*	This work

All Plasmids are listed in **Table 4**.

Table 4: plasmids used in this work.

Strain	Phenotype	Resistance	Source
PMH01	*nipB(p)::nipB::GFP::gluC(t)*	hph	This work
PMH02	*einA(p)::h2b::mCherry::tubT*	hph, amp	This work

PMH03	*oliC(p)::nipB::GFP::gluC(t)*	hph, amp	This work
PMH04	*oliC(p)::einA::GFP::gluC(t)*	hph, amp	This work
PMH05	*nipB(p)::h2b::mCherry::tubT*	hph, amp	This work
PMH10	*einA(p)::einA::GFP::gluC(t)*	hph, amp	This work
PMH12	*nipB(p)::nipB:: mCherry::gluC(t)*	hph, amp	This work
PMH13	*gpd(p)::einA-lccC:: gluC(t)*	Pyr4, hph, amp	This work
PMH14	*gpd(p)::einA-lccCΔSP:: gluC(t)*	Pyr4, hph, amp	This work
PMH20	*ΔeinA*	G418, amp	This work
PMH22	*hsp-16.48::einA::GFP::unc-54UTR*	amp	This work
PMH23	*hsp-16.48::einAΔSP::GFP::unc-54UTR*	amp	This work
PMH25	*eft-3::einA::GFP::unc-54UTR*	amp	This work
PMH30	*eft-3::einAΔSP::GFP::unc-54UTR*	amp	This work
PMH31	*eft-3::einA::Scarlet::unc-54UTR*	amp	This work
PMH32	*eft-3::einA::unc-54UTR*	amp	This work
PMH33	*eft-3::einAΔSP::unc-54UTR*	amp	This work
PMH34	*eft-3::GFP::unc-54UTR*	amp	This work
PMH35	*col-12::einA::GFP::unc-54UTR*	amp	This work
PMH36	*col-12::einAΔSP::GFP::unc-54UTR*	amp	This work
PMH37	*col-12::GFP::unc-54UTR*	amp	This work
PMH39	*myo-3::einA::unc-54UTR*	amp	This work
PMH41	*eft-3::einAΔSP&NLSs::GFP::unc-54UTR*	amp	This work
PMH56	*oliC(p)::einAΔSP::GFP::gluC(t)*	hph, amp	This work
PMH67	*einA(p)::einA::einA(t)*	hph, amp	This work
PMH68	*einA(p)::einA::einA(t)*	G418, amp	This work

pNH10	*gpd(p)::cyrA::lccCΔAS1-18*	Pyr4, hph, amp	Doctor thesis of Nicole Wernet
pCFJ90	*myo-2(p)::tdtomato*		Phil Frankino UC Berkeley
pEGFPMyo-2	*myo-2(p)::GFP*		Institut für Biologie, Freiburg

All oligonucleotides are listed in **Table 5**.

Table 5: Oligonucleotides used in this work.

Name	Sequence
einA(p)::h2b::mCherry::hph	
BB_einA_h2bmCherry_F	CTCTTTCCCTAAACTCCCC
BB_einA_h2bmCherry_R	GAATTCACTGGCCGTCGTTT
PeinA_mcherry_F	CGACGGCCAGTGAATTCCCCAACCAC AAATTACGG
PeinA_mCherry_R	TGAGTTTATTGGATATATATTTCGACAT GCCACCAAAAGCCG
oliC(p)::einA::GFP::hph	
BB_oliC_GFP_F	ATGGTTTCCAAGGGTGAGGTAAG
BB_oliC_GFP_R	TTGGATCGATTGTGATGTGATGGAG
einA_GFP_F	ATCACATCACAATCGATCCAAATGAAG TTCTCCGCCGTC
einA_GFP_R	CTCACCCTTGGAAACCATATCGTCCTT CTTACCCTTTCC
oliC(p)::einAΔSP::GFP::hph	
BB_oliC_GFP_F	ATGGTTTCCAAGGGTGAGGTAAG
BB_oliC_GFP_R	TTGGATCGATTGTGATGTGATGGAG

einAΔSP_GFP_F	CTTTCCCTAAACTCCCCCCActgcagCCC AACCACAAATTACGG
einAΔSP_GFP_R	CTCACCCTTGGAAACCATATCGTCCTT CTTACCCTTTCC
einA(p)::einA::GFP::hph	
BB_einA_GFP_F	ATGGTTTCCAAGGGTGAGGTAAG
BB_einA_GFP_R	ctgcagTGGGGGGAGT
einA_einA_GFP_F	CTTTCCCTAAACTCCCCCCActgcagCCC AACCACAAATTACGG
einA_einA_GFP_R	CTCACCCTTGGAAACCATAATATTGCA GACCTTGGTCAAC
***EinA* laccase assay**	
BB_Lac_F	accggttcttgggtctttga
BB_Lac_R	tgtgatgtctgctcaagcg
Lac_einA_F	gcagacatcacaggcgcgccATGAAGTTCATC ACCGTCGC
Lac_einA_R	caaagacccaagaaccggtAATATTGCAGACC TTGGTCAACTT
***EinAΔSP* laccase assay**	
BB_Lac_F	accggttcttgggtctttga
BB_Lac_R	tgtgatgtctgctcaagcg
Lac_einAΔSP_F	ccgcttgagcagacatcacaATGGCTGCTCCA GTCGC
Lac_einAΔSP_R	caaagacccaagaaccggtAATATTGCAGACC TTGGTCAACTT
Lcc_mid_R	GTGTCAATGGCGCCGTTGA
***einA* deletion**	
ko_ol_pjet_einA_LB_F	GATGGCTCGAGTTTTTCAGCAAGATAG AGAACGTGGGAATAACGG
ko_ol_pjet_einA_LB_R	CCTCCACTAGCATTACACTTGGATGGA AGCGTCTAGTGT
ko_einA_Gen_F	AACACTAGACGCTTCCATCCAAGTGTA ATGCTAGTGGAGGTC

ko_einA_Gen_R	ATATGCTTTCAATCTATGGCTGGGGGGAGTTTAGGGAA
ko_ol_pjet_einA_RB_F	CTTTCCCTAAACTCCCCCCATTTTGGGAACGACGGGA
ko_ol_pjet_einA_RB_R	AGGAGATCTTCTAGAAAGATGCTAAATTACTCTGCTTGTCACC
Ver_pjet_einA_F	CTTGAAACTTTCGATACGAGAATAATAGG
Ver_pjet_einA_R	CGGGCATGTATCATTTTTCCATG
ko_no ol_einA_LB_F	AGAGAACGTGGGAATAACGG
ko_no ol_einA_RB_F	GCTAAATTACTCTGCTTGTCACC
***einA* recomplementation (*G418*)**	
Re-8309-F	CTCGAGTTTTTCAGCAAGATAGAGAACGTGGGAATAACGGC
Re-8309-R	CCTCCACTAGCATTACACTTGCTAAATTACTCTGCTTGTCACCAAA
BB-Re-8309ko-F	AAGTGTAATGCTAGTGGAGGTCAA
BB-Re-8309ko-R	ATCTTGCTGAAAAACTCGAGCC
***einA* recomplementation (*hph*)**	
Re_einA_F	CTCGAGTTTTTCAGCAAGATAGAGAACGTGGGAATAACGGC
Re_einA_R	CCTCCACTAGCATTACACTTGCTAAATTACTCTGCTTGTCACCAAA
BB_Re_einA_ko_F	AAGTGTAATGCTAGTGGAGGTCAA
BB_Re_einA_ko_F	ATCTTGCTGAAAAACTCGAGCC
hsp-16.48::einA::GFP	
Hsp_einA_GFP_F	attctctaaacttcaagaaATGAAGTTCTCCGCCGTC
Hsp_einA_GFP_R	GAGCCTCCAGATCCACCTGAATCGTCCTTCTTACCCTTTCC
BB_Hsp_GFP_F	TCAGGTGGATCTGGAGGCT

BB_Hsp_GFP_R	ttcttgaagtttagagaatgaacag
hsp-16.48::einAΔSP::GFP	
Hsp_einAΔSP_GFP_F	cattctctaaacttcaagaaATGCCGGCCCCAGAAT
Hsp_einAΔSP_GFP_R	GAGCCTCCAGATCCACCTGAATCGTCCTTCTTACCCTTTCCG
BB_Hsp_GFP_F	TCAGGTGGATCTGGAGGCT
BB_Hsp_GFP_R	ttcttgaagtttagagaatgaacag
eft-3::einA::GFP	
eft-3_einA_F	gttgggaaacactttgctcATGAAGTTCTCCGCCGTCG
eft-3_einA_R	AGCCTCCAGATCCACCTGAATCGTCCTTCTTACCCTTTCCG
BB_elf-3_GFP_F	ATGCCAGCCGCTGC
BB_eft-3_GFP_R	CTCGAGGAATTCCTGCAGGAT
eft-3::einAΔSP::GFP	
eft-3_einAΔSP_F	TCCTGCAGGAATTCCTCGAGgcacctttggtcttttattgtca
eft-3_einAΔSP_R	ACTGGAGCAGCGGCTGGCATgagcaaagtgtttcccaact
BB_elf-3_GFP_F	ATGCCAGCCGCTGC
BB_eft-3_GFP_R	CTCGAGGAATTCCTGCAGGAT
eft-3::einA::Scarlet	
scarlet_F	GTCAGCAAGGGAGAGGC
scarlet_R	cttgtagagctcgtccattcC
BB_eft-3_einA_scarlet_F	gaatggacgagctctacaagTGAgagctccgcatcgg
BB_eft-3_einA_scarlet_R	ACTGCCTCTCCCTTGCTGACTGAGCCTCCAGATCCACC
eft-3::einA	
BB_eft-3_einAΔSP_F	[PHO]gagctccgcatcggcc
BB_eft-3_einAΔSP_R	[PHO]TTAATCGTCCTTCTTACCCTTTCCG

eft-3::einAΔSP	
BB_eft-3_einAΔSP_F	[PHO]gagctccgcatcggcc
BB_eft-3_einAΔSP_R	[PHO]TTAATCGTCCTTCTTACCCTTTCCG
eft-3::einAΔSP&NLSs::GFP	
einA(no SP&NLSs)_F	TCAGGTGGATCTGGAGGC
einA(no SP&NLSs)_R	GTGAGTGACAGTTGCCGTAAC
Ver_eft-3_GFP_F	gaggtcaaacattcagtccca
ver_GFP_R	AGAACTTATGTCCATTTACATCTCCATC
***eft-3* EV**	
peft-3_F	[PHO]gagctccgcatcggcc
peft-3_R	[PHO]gagcaaagtgtttcccaactgaaaaa
col-12::einA::GFP	
col-12_einA_F	TCCTGCAGGAATTCCTCGAGtccacatcgagcacttttcac
col-12_einA_R	CGACGGCGGAGAACTTCATaccttacctgtcactggact
BB_col-12_einA_F	ATGAAGTTCTCCGCCGTCG
BB_col-12_einA_R	CTCGAGGAATTCCTGCAGG
col-12::einAΔSP::GFP	
col-12_einAΔSP_F	TCCTGCAGGAATTCCTCGAGtccacatcgagcacttttcac
col-12_einAΔSP_R	TTGCATTCTGGGGCCGGCATaccttacctgtcactggact
BB_col-12_einAΔSP_F	TCAGGTGGATCTGGAGGCT
BB_col-12_einAΔSP_R	CTCGAGGAATTCCTGCAGG
nipB(p)::nipB::GFP::gluC(t)	
BB_nipB_GFP_F	ATGGTTTCCAAGGGTGAGGTAAG
BB_nipB_GFP_R	TTGGATCGATTGTGATGTGATGGAG
nipB_GFP_F	ATCACATCACAATCGATCCAAATGAAGTTCTCCGCCGTC
nipB_GFP_R	CTCACCCTTGGAAACCATATCGTCCTTCTTACCCTTTCC

oliC(p)::nipB::GFP::gluC(t)	
BB_nipB_oliC_GFP_F	ATGGTTTCCAAGGGTGAGGTAAG
BB_nipB_oliC_GFP_R	TTGGATCGATTGTGATGTGATGGAG
NipB_GFP_F	TCACAATCGATCCAAATGAAGTTCATC ACCGTCGCC
NipB_GFP_R	CTCACCCTTGGAAACCATAATATTGCA GACCTTGGTCAAC
nipB(p)::h2b::mCherry::tubT	
BB_nipB_h2b_mCherry_F	CTCTTTCCCTAAACTCCCC
BB_nipB_h2b_mCherry_R	GAATTCACTGGCCGTCGTTT
nipB_mCherry_F	CGACGGCCAGTGAATTCCCCAACCAC AAATTACGG
nipB_mCherry_R	TGAGTTTATTGGATATATATTTCGACAT GCCACCAAAAGCCG
col-12::GFP	
Col-12(P)_F	[PHO]TCCTGCAGGAATTCCTCGAGtcca catcgagcacttttcac
Col-12(P)_R	[PHO]ACTGGAGCAGCGGCTGGCATacct tacctgtcactggact
myo-3::einA	
myo-3_einA_F	TCCTGCAGGAATTCCTCGAGgtgatcttcttc gcaactgttc
myo-3_einA_R	GCGACGGCGGAGAACTTCATaattgaattg tattgagccttcgg
BB_myo-3_einA_F	ATGAAGTTCTCCGCCGTCG
BB_myo-3_einA_R	CTCGAGGAATTCCTGCAGGATAT
Worm_immune genes_QPCR	
actin_F_worm	ACGACGAGTCCGGCCCATCC
actin_R_worm	GAAAGCTGGTGGTGACGATGGTT
Q_einA_F	ACGCCTTTCACCAGTCCATA
Q_einA_R	TGCTTGTGAGTGACAGTTGC
Q_irg-4_F	ATACAGCGGCAAGTGGCTAT
Q_irg-4_R	TGGTGGAGAGCGTATTTGGAG

Q_zip2_F	CACGACGTTCCCTACCGAAA
Q_zip2_R	CTTCTGGAACCGGTGGGAAA
Q_atf7_F	ACGAGCATGCAGTCGGATT
Q_atf7_R	TCGCTTCTCGGAACTTTGCT
Q_daf-6_F	CCTGCACCGTTCAACTACCT
Q_daf-6_R	CTCCCGGTCCTTGCTCTTTT
Q_nlp-29_F	GTTCTTGTCGTCCTTCTCGC
Q_nlp-29_R	TTCCACGTCCATATCCACCA
Q_spp-5_F	CCTCCTTCCAGCTCGTGAAT
Q_spp-5_R	CGCCGATAAGGATGCCAATG

4.2 Chemicals and equipment

Unless otherwise descripted in the text, the chemicals used come from the companies Roth (Karlsruhe), Merck (Darmstadt), Biozym (Hessisch Oldendorf), Zymo Research (Freiburg), Bio-Rad (Munich), Nippon Genetics (Düren) and MachereiNagel (Düren). DNA fragments were sequenced, and oligonucleotides were synthesized by Eurofins Genomics (Ebersberg). Restriction enzymes and DNA polymerases were purchased from New England Biolabs (Frankfurt).

All antibiotics are listed in **Table 6**.

Table 6: Antibiotics used in this project.

Name	Concentration (mg/L)
Ampilicin	100
Hygromycin	100
Geneticin 418	50

All kits are listed in **Table 7**.

Table 7: all kits used in this project.

Name	Company	Application

Ambion Turbo DNA Free Kit	Invitrogen	DNAse digestion of RNA
Luna One-Step RT-Qpcr Kit	New England Biolabs GmbH	qRT-PCR
ProtoScript® III First Strand cDNA Synthesis Kit	New England Biolabs GmbH	cDNA acquisition
Plasmid Easypure Kit	Macherey-Nagel	Plasmid-DNA-Isolation
Zymoclean Gel DNA Recovery Kit	Zymo Research US	DNA purification from gel
DIG Probe Synthesis Kit	Roche	Probes synthesis for Southern blot analysis

Table 8: Equipment required in this work.

Name	**Type**	**Company**
Autoclave	3870ELV	Tuttnauer, Breda
Freezer (-80 °C)	Innova U101	New Brunswick Scientific, Hamburg
Votex	Vortex-Genie2	Scientific Industry, Inc., New York
incubator	Mintron AL72	Infors HAT, Bottmingen-Basel
	Heraeus 6000	Heraeus, Instruments Hanau
UV/visible spectrophotometer	Nanodrop ND 1000	PeQlab, Erlangen
Gelscanner	SnapScan1236v	Agfa, Cologne
PCR cycler	Labcycler	SensoQuest, Göttingen
Centrifuge	Eppendorf 5415R	Eppendorf, Hamburg
	AccuSpin Micro 17	Fisher Scientific, Schwerte
	Universal 320 R	Hettich, Tuttlingen

UV-cross linker	UV Stratalinker 2400	Stratagene, Heidelberg
pH meter	HHanna HI 208	Hanna, Romania
Microscope	Axio Imager Z1	Zeiss, Jena
	LSM 900	Zeiss, Jena
	Axio Observer Z1	Zeiss, Jena

4.3 Microbiological methods

Cultivation, storage, and transformation of *E. coli*.

E. coli was cultured on the solid LB agar or liquid LB at 37 °C for 16-18 h. For long-term storage, 600 µl of liquid culture for 16-18 h was mixed with 600 µl 50% glycerol well in the 2 ml Eppendorf tube, kept at -80 °C.

For the transformation into *E. coli* Top10, the heat shock method was used. 20 µl Gibson Assembly product was added and incubated on ice for 15-20 min. And then, tubes with the Top10 and plasmid DNA mixture were heat-shocked at 42 °C for 1-2 min. Afterward, the mixture was incubated on ice for 2-4 min. The last step was to pour and spread evenly with the sterile triangle spreader on the LB agar with ampicillin for incubation overnight at 37 °C.

Table 9: Media used for *E. coli*.

Name	**Composition/L**
LB (Lysogeny Broth)	10 g Trypton
	5 g Yeast extract
	5 g NaCl
	15 g Agar
	pH 7.0
Ampicillin (1000 x)	5 g Ampicillin
(Keep in -20 °C)	25 ml ddH_2O
	25 ml 100% Ethanol

Cultivation, storage, and transformation of *A. flagrans*.

A. flagrans was cultured on the solid PDA with agar or liquid PDA at 28 °C. The cultivation days depend on the purpose of the mycelia. For long-term storage, mycelia grown on the normal size plate with PDA and agar for seven days was scraped and suspended with 1.2 ml 25% glycerol in 2 ml Eppendorf tubes.

For transformation of *A. flagrans*, it includes the protoplast preparation and transformation. For the protoplast preparation, the mycelia of A.flagrans cultured for seven days were collected and inoculated in 100-150 ml liquid PDA at 28 °C and 180 rpm. After 24 h, the mycelia were filtered through the sterile two-layer Miracloth and washed with MN buffer and then were transferred to 50 ml falcon containing 5-10 ml MN buffer with 10 mg kitalase and 100 mg Glucanx (Novozyme) and cultured at 28 °C 70 rpm. After 2-2.5 h, the liquid with mycelia was filtered through a sterile two-layer Miracloth, and protoplast was collected. Then 50 ml falcon with filtrate was filled with MN buffer and centrifuged for 18 min at 5000 rpm. The supernatant was poured, and the precipitate was washed with 50 ml KTC buffer and centrifuged again with the same condition at mention before. After pouring the supernatant, the protoplast was resuspended with 500 µl KTC buffer and kept on ice. The concentration was calculated by using the hemocytometer. The counter area is 0.0025 x 0.02 mm^3. 1ml equals 1000 mm^3.

The number of protoplasts/ml = (the number of protoplasts x 1000)/

(0.0025 x 0.02)

For the transformation, 100 µl of the mixture system contains $20x10^6$ protoplasts and a 3 µg DNA fragment always were required. It was incubated on ice for 2 minutes. Then, 1 ml PTC6000 solution was added and mixed gently for several minutes, incubated for 20 minutes at room temperature. Finally, 20-30 ml PDASS was added into 50ml reaction falcon, after inverting several times,

applied to the normal size of petri dish with PDA containing antibiotics. These plates were incubated at 28 °C until colonies arose.

Table 10: Media and buffers used for *A. flagrans.*

Solution	Composition/L
Potato Dextrose agar	24 g potato Dextrose Broth 15 g Agar pH to 6.6
MN buffer	75.8 g $MgSO_4 \cdot 7H_2O$ 17.54 g NaCl
KTC buffer	89.46 g KCl 7.4 g $CaCl_2$ 10 ml Tris-HCl (1 M)
PTC6000 buffer	10 mmol/l Tris-HCl, pH 7.5 50 mmol/l $CaCl_2$ 60 % (w/v) Polyethylenglykol-6000
PDASS top agar	24 g Potato Dextrose Broth 205 g Sucrose 0.3 g Yeast extract 0.3 g Peptone 7.5 g Agar pH to 6.6

Cultivation, storage, transformation of *C. elegans*.

C. elegans were grown on the liquid NGM with *E. coli* OP50 on the surface of plates for 5-7 days. For long-term storage, plenty of *C. elegans* at the stage of L1 and L2 were required. 10ml M9 buffer was added to wash off worms from the plates and then centrifuged at 4 °C for 2 minutes. The supernatant would be discarded and then resuspended the pellet with 10 ml of M9 buffer. Repeat this process 2-3 times. Finally, the nematodes were stored in 2 ml Eppendorf tubes with 1 ml freezing solution.

For the transformation of *C. elegans*, the microinjection method was used. The DNA mix was injected into the distal arm of the gonad, which resultd in the integration of extrachromosomal assay that can be heritage to the offspring. For injection, young, adult, and pregnant worms containing few eggs were transferred to a glass slide covered with a thin pad of LNA medium. During the injection procedure, the worms were maintained in a small volume of Halocarbon oil 700 to prevent desiccation. The injection mixture was transferred to a needle which was connected to a microinjection compressor. The individual injected nematode was diverted to a fresh NGM-OP50 plate. 2µl of M9 buffer was added to the worms for regeneration, and the plates were incubated at 20°C, after three days. The plates should be checked. The positive transformation of the F1 generation could be recognized by the fluorescence of the pharynx and picked to the new plates for subsequence experiments.

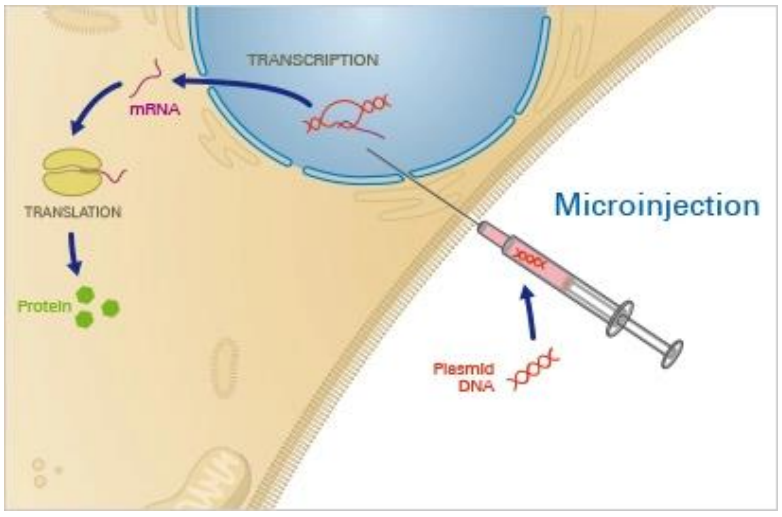

Fig. 29: Transformation of controlled nucleotide amounts into the nucleus of specific target cells.
(https://ibidi.com/img/cms/applications/transfection/TR_M_Microinjection.jpg)

Synchronization of *C. elegans*

The synchronization of *C. elegans* is to maintain all of the nematodes in the

same developmental phase. In addition, this technique also can be used to rid the culture of contamination. The nematodes with eggs were rinsed from the NGM-OP50 agar plate with 15ml sterile water and then collected with a centrifuge for 3.5 minutes at 1500rpm. The pellet was suspended with 500μl NaOH and 1ml NaClO to the lysis nematodes' body wall; after shaking vigorously for 4 minutes, added 15 ml sterile water to stop the reaction. Eggs were collected on the bottom of the falcon with a centrifuge for 2 minutes at 2000rpm. Then, the water-washing step was repeated twice. The supernatants were removed, and 2 ml of M9 buffer was added. Eggs with 2 ml of M9 buffer were transferred into small Petri dishes and incubated at 20 °C. The eggs would take a day to hatch.

Survival assay of *C. elegans*

After three days bleached, thirty larvae of each line of nematodes were transferred into an NGM plate containing 150 μM floxuridine (FudR). Nematodes that no longer respond to touch using a picker would be considered dead. The experiment was performed in biological triplicate.

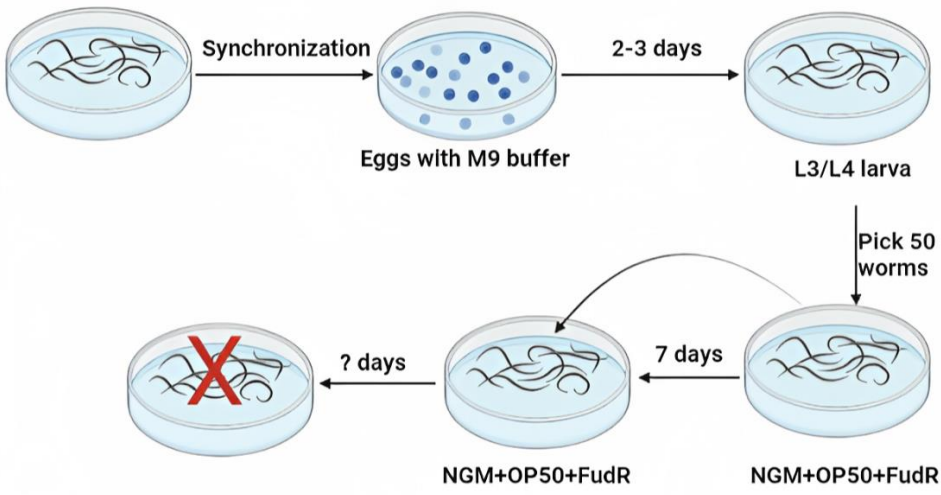

Fig. 30 The flow chart of survival assay of *C. elegans*. The different phenotypes of transgenic worm strains growing on one plate were synchronized;

after two days, eggs were hatched in the M9 buffer, and several of the same numbers of L3-L4 worms were picked up on an NGM medium with 150 mM floxuridine (FudR) and fresh OP50 *E. coli* as food resources. These worms were observed every two days until all of the worms died. To keep these worms at favorable condition, they should be transferred into the new plate every 5-7 days. The scheme was created with BioRender

Locomotion assay of *C. elegans*

To conduct a locomotion assay in *C. elegans*, the following steps were followed. First, NGM plates with OP50 *E. coli* bacterial lawns were prepared and allowed to dry at room temperature. The *C. elegans* worms were then synchronized using a bleach synchronization we described before. The synchronized L4 or young adult stage worms were carefully transferred onto the NGM plates using a worm pick. Subsequently, the NGM plate was placed under a microscope, and a suitable region where the worms were freely moving was focused on. The worm's movement was recorded for a desired duration using the microscope's camera, typically 1 minute or longer. The recorded video was then analyzed to quantify locomotion parameters, such as body bends, speed, or distance traveled, using appropriate software or manual tracking methods.

Nuclear staining of *C. elegans*

The cuticle and epidermis structure of *C. elegans* is impermeable, making it challenging to stain the worm bodies externally. To overcome this limitation, we fed *C. elegans* with Hoechst 33258-stained OP50 *E. coli*. Initially, 2 ml of OP50 culture cultivated overnight was obtained and centrifuged for 1 minute at 6,000 rpm. Subsequently, 4.4 µl of 1 mg/ml Hoechst 33258 was added to the 400 µl supernatant. The mixture was then kept in dark conditions at 20°C for 2 hours. 10 µl of the stained OP50 could be observed using microscopy during this time. Meanwhile, the worms were washed and transferred to NGM plates with stained OP50 as their food source overnight.

After feeding the worms with OP50, they were washed three times with 4 ml of 0.12 M NaCl to remove any excess staining. Finally, the worm pellet was anesthetized by adding 100 µl of a 5% urethane solution in water. The duration of sedation ranged from 20 to 40 minutes, depending on the size and number of worms. Staining of cell nuclei occurred 1-2 hours after the sedation process.

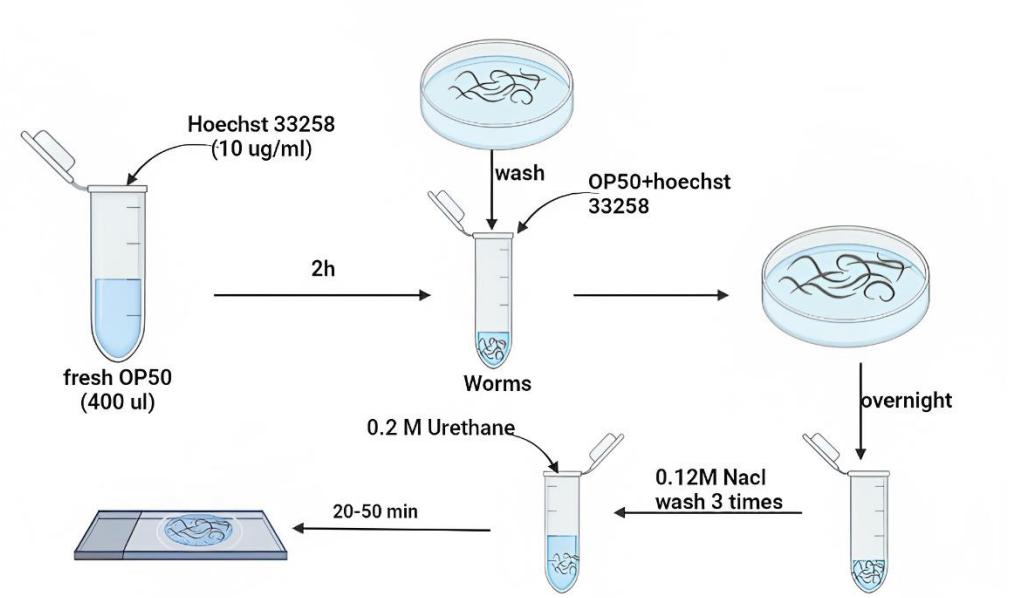

Fig. 31 Flow chart of nuclear staining with Hoechst 33258. 1-2 ml of fresh OP50 *E. coli* was centrifuged, and just 400 µl liquid was left. 4 µl of 10 µg/ml Hoechst 33258 was added into the liquid with OP50 stock for staining. After 2 hours, 1 µl OP50 was observed with microscopy to check whether they were stained or not. The worms that needed to be stained were collected without liquid as much as possible and added into stained successfully OP50 liquid for at least 6 hours, the mixture of worms and OP50 was centrifuged, and the supernatant was removed as much as possible, 1 ml of 0.2 M urethane was used to anesthetize worms, these paralyzed worms was observed with microscopy. The scheme was created with BioRender

Table 11: Media and buffers used for *C. elegans*.

Name	Composition/L
Nematode Growth Medium (NGM)	3 g NaCl 2.5 g Peptone 1 ml Cholesterol (5 mg/ml in Ethanol)

	17 g Agar 1 ml $CaCl_2$ (1 M) 1 ml $MgSO_4$ (1 M) 10.83 g KH_2PO_4 3.56 g K_2HPO_4
M9 Buffer	3 g KH_2PO_4 6 g Na_2HPO_4 5 g NaCl 1 ml $MgSO_4$ (1 M)
Low Nutrition Agar (LNA)	1 g KCl 0.2 g $MgSO_4 \cdot 7\ H_2O$ 0.4 mg $MnSO_4 \cdot 4\ H_2O$ 0.88 mg $ZnSO_4 \cdot 7\ H_2O$ 3 mg $FeCl_3 \cdot 6\ H_2O$ pH to 5.5 10 g Agar

4.4 Molecular microbiological methods

Polymerase chain reaction (PCR)

The PCR reaction was used for the amplification of specific double-stranded DNA fragments. The total volume of 50µl was shown as follows:

Content	
Template	100 ng DNA
Primer-forward	2.5 µl (10mM)
Primer-reverse	2.5 µl (10mM)
dNTPs	1 µl (10mM)
Q5 polymerase	2.5U
Q5 buffer	10 µl
ddH2O	To 50 µl

PCR program:

Temperature	Duration	cycle
98 °C	3 min	
98 °C	30 s	30-35 cycle
Tm ± 5 °C	30 s	
72 °C	30 s/kb	
72 °C	10 min	

DNA agarose gel electrophoresis and recovery

The DNA products were identified by a 0.8-2 % agarose gel concentration with 2ul Midori Green Advance (Biozym) as a detector. The suitable gel size was placed in an electrophoresis chamber filled with 0.5 x TAE buffer. DNA products mixture with 6 x loading dye was loaded into the gel's wells formed by a comb. The DNA ladder (1kb or 100bp, depending on the length of target DNA fragments) was also added to the standard. After 20-30 minutes at 100-130V, The DNA bands would be visualized by UV light. For the recovery of target DNA products, bands with the right size of DNA were cut off and put into an Eppendorf tube. It would be obtained with Zymoclean Gel DNA Recovery Kit (Zymo Research).

Table 12: buffers used for DNA agarose gel electrophoresis

Name	Composition
TAE buffer (50 x)	40 mM Tris/HCl pH8,3 20 mM NaAc 2 mM EDTA
1% agarose gel	4 g Agarose 400 ml TAE buffer (1 x)

Mini-preparation of plasmid DNA from *E. coli*: alkaline lysis method

This technique was used to obtain plasmid DNA from *E. coli*. 2 ml of *E. coli* culture for 16-18h was pelleted for 2 minutes at 13,000 rpm. After discarding the supernatant, the precipitate was resuspended with 200 µl suspend buffer. Afterward, 200 µl lysis buffer was added and mixed vigorously. 200 µl of 1.5M KAc buffer was added to pellet macromolecules, put on ice for 15-20 minutes, and centrifuged for 5 minutes and 13,000 rpm at 4 °C. The supernatant was transferred to reaction vessels, and 500 µl 100% isopropanol also was added for 20 minutes on ice. The plasmid DNA was precipitated after centrifuge for 15 minutes at 4 °C and 13,000 rpm. 500 µl 70% ethanol was used to remove residual proteins and centrifuge it again with the condition of 4 °C for 5 minutes. After removing ethanol as much as possible, the plasmid DNA as precipitate was collected and dissolved with 20 µl ddH2O.

Table 13: the buffers for mini-preparation of plasmid DNA.

Name	Composition
Suspend buffer	50 mM Tris-HCl (pH 7.5) 10 mM Na2EDTA
	100 µg/ml RNase A
Lysis buffer	0.2 M NaOH
KAc	1 % SDS 1.5 M KAc (pH 4.8)

Midi-preparation of plasmid DNA from *E. coli* with the kit and DNA sequence

The plasmid DNA requiring a high concentration or quality could be obtained with NucleoSpin Plasmid EasyPure Kit (Macherey Nagel).

The concentration measure and sequencing of the Plasmid DNA

The concentration of plasmid DNA was measured with Nanodrop. For sequencing, plasmid DNA and primers were mixed as the following system and sent to Eurofins MWG company.

Table 14. the buffers for sequencing of the plasmid DNA

Content	
Plasmid DNA	1-1.5 mg
Primer	2 µl
ddH2O	to 17 µl

Preparation of genomic DNA of *A. flagrans*

To extract of genomic DNA of *A. flagrans*, mycelia growing at PDA-agar media for 2-3 days were required. Agar with mycelia the size of a fingernail was crushed by the small grinding rod together with 750 µl of lysis buffer into 2 ml Epp. Tube. It was incubated on a shaking thermos heater; after 60-80 minutes, 350 µl of KAc buffer was added, inverted softly, and incubated on ice for 15 minutes, afterward, centrifuged at 4 °C and 13,000 rpm for 30 minutes to precipitate proteins and phenolic substances. And then, an equal volume of 100 % isopropanol was added in the tubes with supernatant (always 700 µl or so), inverted several times, and incubated for 20 minutes in the freezer. Subsequently, the DNA pellet was precipitated by centrifuging for 15 minutes and washed with 70 % ethanol. After removing all ethanol as much as possible, tubes were incubated for 3-5 minutes at 68 °C on the heater. Finally, the pellet was dissolved with 70 µl of ddH2O or TE buffer with 50 µl/ml RNase A. The concentration of gDNA could be measured by Nanodrop.

Table 15. the buffers used for extraction of gDNA

Name	Composition
Lysis buffer	0.2 % SDS 50 mM Na_2EDTA, pH 8.0
KAc buffer	1.5 M KAc, pH 4.8
TE buffer (10 X)	100 mM Tris-HCL, pH 7.9 10 mM Na_2EDTA

Isolation of RNA of *A. flagrans*

The extraction a high quantity of RNA from fungi is essential for detecting the expression level of genes. Therefore, for the preparation of RNA of *A. flagrans*. The mycelia growing for 2-day-old into the liquid PDA media were required at 28 °C. If the genes just expressed when fungi were induced by nematodes, 1 x 106 spores were collected and spread on the LNA media with the surface of sterile cellophane at 28 °C for 1 - 2 days. Then the appropriate number of nematodes rinsed from NGM plates were added; after three days, a microscope was used to check if there is any trap structure production. Mycelia with trap structure were scraped off the cellophane and collected. The mycelial pellet was frozen in liquid nitrogen and crushed with a grinding rod. The sample powder was put into 2 ml RNase-free Eppendorf tubes with 1 ml Trizol. After a short vortexing process (15 seconds), the samples were incubated for 5 minutes at room temperature. After centrifugation for 10 min, 4 °C. at 13000 rpm, the supernatant was transferred to a fresh reaction vessel. The sample was then mixed with 200 µl of chloroform and vortexed for a further 15 seconds. After an incubation time of 3 minutes at room temperature, another centrifugation process takes place (15 min, 4 °C, 13000 rpm). The aqueous phase was then transferred to a reaction vessel containing 500 µl of isopropanol and inverted. After incubation for 15 minutes at room temperature, the RNA was pelleted for 15 minutes at 4 °C and 13000 rpm and then washed with 500 µl of

70% (v/v) ice-cold ethanol. After a further centrifugation step (5 min, 4 °C, 9000 rpm), the remaining ethanol was removed, the RNA pellet was dried and then eluted in 30 µl DEPC H2O. The RNA was treated with the DNase Turbo DNA Free Kit (Thermo Fisher Scientific) to remove the remaining DNA.

RNA extraction from *C. elegans*

For the RNA extraction from *C. elegans*, an NGM plate with the desired population of *C. elegans* was rinsed with ddH2O. The worm pellet was frozen in liquid nitrogen and ground with a micropestle. After that, 500 µl of Trizol (Invitrogen) was added to the samples, and these were shaken on a vortex. The samples were frozen three times in liquid nitrogen, thawed again at 37 °C, and vortexed. The samples were then alternately incubated on ice for 30 seconds and vortexed for 30 seconds three times. After adding 100 µl of chloroform, the samples were inverted and incubated for three minutes at room temperature (RT). Then it was centrifuged at 13000 rpm and 4 °C for 15 minutes. The aqueous phase was transferred to a new reaction vessel containing 0.7 volume of 100% isopropanol, inverted, and then incubated at RT for 10 minutes. The RNA was precipitated at 13000 rpm and 4 °C. for 15 minutes and then washed with 500 µl of cold ethanol (70%). The pellet was dried for 5 minutes at 60 °C and then dissolved in 50 µl of DEPC H2O at 60 °C. The RNA was treated with the DNase Turbo DNA Free Kit (Thermo Fisher Scientific) to remove the remaining DNA.

Synthesis of cDNA from RNA and qRT-PCR

The SuperScript Double-Stranded cDNA Synthesis Kit (Thermo Fisher Scientific) was used as the manufacturer protocol for the synthesis of coding DNA. For the gene expression analysis with quantitative Real-Time RT-PCR, the Luna Universal One-Step RT-QPCR Kit (NEB) was used by the

manufacturer's instructions, and the reaction in the ICCLER IQ (Bio-Rad) was performed. The putative gamma actin gene was used as a reference for the quantification of relative expression. The expression was calculated with the formula $2^{-\Delta\Delta Ct}$.

Preparation of plasmid mix for microinjection into *C. elegans*.

For the efficient microinjection of plasmid with target gene into *C. elegans*. It is very important to linearize plasmid by using a restriction enzyme. After digestion overnight, the digested plasmid was then purified by gel electrophoresis. It could be obtained with DNA Recovery Kit, and the injection mix would be prepared according to the system as below. To check if the transformation succeeded or not, another plasmid with a marker gene also was injected at the same time as the control.

The total volume of 50 µl of the digestion system was showed as follows:

Content	
Plasmid	1 ug
Enzyme	1 µl
Reconstruction enzyme buffer	5 µl
ddH2O	To 50 µl

The total volume of 10 µl of injection system was showed as follows:

Content	
Plasmid	50 ng
Marker plasmid	50 ng
1 kb ladder	3 µl
ddH2O	To 10 µl

Cloning using Gibson Assembly

For cloning using Gibson assembly, the DNA fragments and vectors were amplified with primers containing overlapping (15-30 bp) complementary regions for the ligation. The fragments were purified and used in a 1:2 ratio in the reaction with 15 µl of Gibson assembly enzyme mix, bringing the total volume to 20 µl. The reaction was incubated for 30-60 minutes at 50 °C and then 10 µl transformed into *E. coli*.

Table 16: The composition of Gibson-Assembly-Enzyme-Mix.

Reagent	Concentration
Iso-Buffer (5 x)	26.6 % v/v
T5-Exonuclease (10 u/µl)	5.3 um/ml
Q5-Polymerase (2 u/µl)	33.3 u/ml
Taq Ligase (40 u/µl)	5333.3 u/ml
ddH2O	58.3 % v/v

Targeted deletion of genes using homologous recombination

A deletion cassette was created for the targeted deletion of genes using homologous recombination. Hygromycin resistance cassette (hph) was flanked by regions of about 1 kb in size, which were downstream and upstream of target genes in the *A. flagrans* genome. The fragments were cloned into the pJET1.2 vector using Gibson assembly. The plasmid DNA was isolated and confirmed by restriction digestion and sequencing. 6-8 µg of plasmid DNA was used to transform *A. flagrans*.

Southern Hybridization

Southern analyzes were performed to verify the genetically engineered *A. flagrans* strains. First, the gDNA was isolated, and the maximal amount was digested overnight with an appropriate restriction enzyme with 30 µl volume. After restriction, the DNA was separated by gel electrophoresis on a 0.8%

agarose gel at 100 V for about 2 hours. The DNA ladder was marked by punctures in the gel. The gel was then rocked in 0.25 M HCl for 30 min to make the DNA depurination and then incubated in a denaturation buffer for 30 min followed by 30 min in a renaturation buffer. The DNA was transferred from the gel to the nylon membrane (Roti-Nylon plus, Roth) via capillary forces. A glass plate was placed on a trough of 20x SSC buffer, and a bridge of Whatman paper was placed in contact with the buffer. The gel was now placed upside down on the bridge, and the nylon membrane was on top. Several layers of Whatman paper and paper towels were applied to create suction. The transfer was done overnight. After successful transfer, size markings and pockets were marked on the membrane with a pencil. The DNA was then fixed in a UV crosslinker. Subsequently, the prehybridization of the membrane takes place in Southern hybridization buffer for 30 min at 65 °C in a hybridization oven. DNA probes labeled with digoxigenin were used for detection. These were prepared by a PCR reaction using the DIG Probe synthesis kit (Roche, Mannheim, Germany) in a reaction volume of 25 µl according to the manufacturer's instructions. The probe was then purified by gel electrophoresis and isolated by freeze and squeeze. For this purpose, the corresponding band was cut out of the gel, frozen for 20 minutes at -80 °C, and then the DNA was pressed out of the gel into a reaction vessel. The probe was boiled at 98 °C for 10 minutes, dissolved in 15 ml Southern hybridization buffer and applied to the membrane. Hybridization was performed at 65 °C overnight. The membrane was then washed with SSPE buffer. For 15 minutes each with 2x SSPE + 0.1% SDS, 1x SSPE + 0.1% SDS and 0.1x SSPE + 0.1% SDS at 65 °C. All subsequent steps were performed at room temperature. The membrane was washed with DIG Wash for 5 min, and then vacancies of the membrane were blocked by incubation with 25 ml DIG2 for 30 min. The antibody solution was made up in DIG2 buffer (1:10000 dilution of the anti-DIG antibody), and the membrane was incubated with it for 30 min. The membrane was then washed twice with 40 ml DIG-Wash for 15 min and equilibrated with 40 ml DIG3 for 5 min. And then, the

membrane was incubated with 2 mL of CDP-Star solution and developed using the Chemi-Smart chemiluminescence system (Peqlab). If necessary, the probe was removed again by adding stripping buffer and incubating at 37 °C for 15 min so that the membrane could be prehybridized again and hybridized with another probe.

Table 16: buffers used for Southern hybridization

Name	**Composition / L**
0.25 M HCl	32 % HCl 28.4 ml ddH_2O 972 ml
DENAT Buffer	NaCl 87.6 g NaOH 16 g ddH_2O to 1 L
RENAT Buffer	87.6 g NaCl 44.4 gTris-HCl 26.5 g Tris-Base ddH_2O to 1 L
20 x SSC Buffer	175.3 g NaCl 88.2 g NaCitrate ·2 H_2O pH to 7.0
Southern Hybridization Buffer	500 ml 1 M Na-phosphate buffer 70 g SDS (7 %)
1M Na-phosphate Buffer	Solution 1/L: 177.99 g Na_2HPO_4 ·2 H_2O Solution 2/L : 156.01 g NaH_2PO_4 ·2 H_2O Pour solution 2 into 1 until pH 7.0
20 x SSPE Buffer	175.3 g NaCl 27.6 g Na_2HPO4 ·2 H_2O 7.4 g Na_2EDTA ·2 H_2O pH to 7.4
DIG1 Buffer	11.61 g Maleic acid

	8.77 g NaCl pH to 7.5
DIG wash Buffer	450 µl Tween 20 150 ml DIG1
DIG3 Buffer	5.84 g NaCl (0.1 M) 10.17 g$MgCl_2 \cdot 6 H_2O$ pH to 9.5
CDP-Star solution	2 µl CDP (1:500) DIG3 1 ml
Stripping Buffer	8 g NaOH 10 ml 10 % SDS

4.5 Microscope observation

A Zeiss AxioImager Z.1 with the objectives: 63x /1.4 oil immersion, 40x /0.75, 20x/0.50, 10x/0.30 was used for microscopic images. Detection was carried out using an MRM camera using the ZEN Blue software (2012).

A Zeiss LSM 900 with Airyscan 2 detector was used for high-resolution confocal microscopy.

A Zeiss SteREO Discovery.V12 and a Zeiss SteREO Lumar.V1 with fluorescence filters were used for work with C. elegans.

A Zeiss AxioObserver.Z1 with a Zeiss Multi Laser Module and a Spinning Disk Module CSU-X1M 5000 and Evolve 512 camera (Photometrics) was used for long-term recordings.

A NIKON Eclips E200 was used for the quantification of spores and protoplasts.

4.6 Data and image analysis

The program Fiji/ImageJ (Version 2.0) was used for image processing.

GraphPad Prism software was used for data plots and statistical analysis.

Illustrator for Biological Sequences (IBS) was used for schematic representations of proteins and genes.

ApE PlasmidEditor was used for DNA sequences visualization.

5. References

A. K. Corsi, B. Wightman, and M. Chalfie, A Transparent window into biology: A primer on Caenorhabditis elegans, The Online Review of C. elegans Biology [Internet]. Pasadena (CA): WormBook; 2005. Available from: https://www.ncbi.nlm.nih.gov/books/NBK299460/

Abd-Elgawad, M. M. (2020a). Biological control agents in the integrated nematode management of potato in Egypt. *Egypt. J. Biol. Pest Control,* **30**, 1-13.

Abd-Elgawad, M. M. (2020b). Plant-parasitic nematodes and their biocontrol agents: current status and future vistas. *Management of phytonematodes: recent advances and future challenges*, 171-203.

Abd-Elgawad, M. M. M. (2014). Plant-parasitic nematode threats to global food security. *J Nematol.,* **46(2)** 130-130.

Abd-Elgawad, M. M., & Askary, T. H. (2015). Impact of phytonematodes on agriculture economy. In *Biocontrol agents of phytonematodes* (pp. 3-49). Wallingford UK: CABI.

Ahren, D., Tholander, M., Fekete, C., Rajashekar, B., Friman, E., Johansson, T., & Tunlid, A. (2005). Comparison of gene expression in trap cells and vegetative hyphae of the nematophagous fungus *Monacrosporium haptotylum*. *Microbiology*, **151(3)**, 789-803.

Al-Ani, L. K. T., Soares, F. E. D. F., Sharma, A., de los Santos-Villalobos, S., Valdivia-Padilla, A. V., & Aguilar-Marcelino, L. (2022). Strategy of nematophagous fungi in determining the activity of plant parasitic nematodes and their prospective role in sustainable agriculture. *Front Fungal Biol.*, **3**, 17.

Allman, E., Johnson, D., & Nehrke, K. (2009). Loss of the apical V-ATPase a-subunit VHA-6 prevents acidification of the intestinal lumen during a rhythmic behavior in *C. elegans*. *Am J Physiol Cell Physiol.*, **297(5)**, C1071-C1081.

Amer-Zareen, Z. M. J., Abid, M., Gowen, S. R., & Kerry, B. R. (2004). Management of root knot nematode (*Meloidogyne javanica*) by biocontrol agents in two crop rotations. *Annu Rev Plant Biol.*, **1**, 67-73.

Anderson, S. M., Cheesman, H. K., Peterson, N. D., Salisbury, J. E., Soukas, A. A., & Pukkila-Worley, R. (2019). The fatty acid oleate is required for innate immune activation and pathogen defense in *Caenorhabditis elegans*. *PLoS Pathog.*, **15(6)**, e1007893.

Andersson, K. M., Kumar, D., Bentzer, J., Friman, E., Ahrén, D., & Tunlid, A. (2014). Interspecific and host-related gene expression patterns in nematode-trapping fungi. *Bmc Genomics*, **15(1)**, 1-15.

Andersson, K. M., Meerupati, T., Levander, F., Friman, E., Ahrén, D., & Tunlid, A. (2013). Proteome of the nematode-trapping cells of the fungus *Monacrosporium haptotylum*. *Appl Environ Microbiol.*, **79(16)**, 4993-5004.

Ansari, R. A., & Khan, T. A. (2012). Parasitic association of root-knot nematode, *Meloidogyne* incognita on guava. *eJ Sci Technol.*, **5**, 65-67.

Antebi, A. (2006). Nuclear hormone receptors in *C. elegans*. *WormBook*, **1**.

Asadulghani, M. D., Ogura, Y., Ooka, T., Itoh, T., Sawaguchi, A., Iguchi, A., ... & Hayashi, T. (2009). The defective prophage pool of *Escherichia coli* O157: prophage–prophage interactions potentiate horizontal transfer of virulence determinants. *PLoS Pathog.*, **5(5)**, e1000408.

Axmacher, N., Henseler, M. M., Jensen, O., Weinreich, I., Elger, C. E., & Fell, J. (2010). Cross-frequency coupling supports multi-item working memory in the human hippocampus. *Proc Natl Acad Sci.*, **107(7)**, 3228-3233.

Balbino, H. M., de Souza Gouveia, A., Monteiro, T. S. A., Morgan, T., & de Freitas, L. G. (2022). Overview of the nematophagous fungus *Duddingtonia flagrans*. *Biocontrol Sci Technol.*, ***32*(8)**, 911-929.

Baral, H. O., Weber, E., Gams, W., Hagedorn, G., Liu, B., Liu, X., ... & Weiß, M. (2018). Generic names in the Orbiliaceae (Orbiliomycetes) and recommendations on which names should be protected or suppressed. *Mycol Prog.*, **17**, 5-31.

Bargmann, C. I. (1993). Genetic and cellular analysis of behavior in *C. elegans*. *Annu Rev Neurosci.*, **16(1)**, 47-71.

Barksdale, K. A., Perez-Costas, E., Gandy, J. C., Melendez-Ferro, M., Roberts, R. C., & Bijur, G. N. (2010). Mitochondrial viability in mouse and human postmortem brain. *FASEB J.*, **24(9)**, 3590.

Barron, G. L. (2003). Predatory fungi, wood decay, and the carbon cycle. *Biodiversity*, **4**, 3-9.

Baumeister, R., Schaffitzel, E., & Hertweck, M. (2006). Endocrine signaling in *Caenorhabditis elegans* controls stress response and longevity. *J Endocrinol.*, **190(2)**, 191-202.

Beck, M., Zhou, J., Faulkner, C., MacLean, D., & Robatzek, S. (2012). Spatio-temporal cellular dynamics of the *Arabidopsis flagellin* receptor reveal activation status-dependent endosomal sorting. *Plant Cell*, **24(10)**, 4205-4219.

Birch, P. R., Boevink, P. C., Gilroy, E. M., Hein, I., Pritchard, L., & Whisson, S. C. (2008). Oomycete RXLR effectors: delivery, functional redundancy and durable disease resistance. *Curr Opin Plant Biol.*, **11(4)**, 373-379.

Block, D. H., Twumasi-Boateng, K., Kang, H. S., Carlisle, J. A., Hanganu, A., Lai, T. Y. J., & Shapira, M. (2015). The developmental intestinal regulator ELT-2 controls p38-

dependent immune responses in adult *C. elegans*. *PLoS Genet.*, **11(5)**, e1005265.

Bogaerts, A., Beets, I., Schoofs, L., & Verleyen, P. (2010). Antimicrobial peptides in *Caenorhabditis elegans*. *Inv Surv J.*, **7(1)**, 45-52.

Bourras, S., Kunz, L., Xue, M., Praz, C. R., Müller, M. C., Kälin, C., ... & Keller, B. (2019). The AvrPm3-Pm3 effector-NLR interactions control both race-specific resistance and host-specificity of cereal mildews on wheat. *Nat Commun.*, **10(1)**, 2292-2292.

Boyer, L., Magoc, L., Dejardin, S., Cappillino, M., Paquette, N., Hinault, C., ... & Stuart, L. M. (2011). Pathogen-derived effectors trigger protective immunity via activation of the Rac2 enzyme and the IMD or Rip kinase signaling pathway. *Immunity*, **35(4)**, 536-549.

Braga, F. R., Araújo, J. V., Soares, F. E., Geniêr, H. L., & Queiroz, J. H. (2012). An extracellular serine protease of an isolate of *Duddingtonia flagrans* nematophagous fungus. *Biocontrol Sci Technol.*, **22(10)**, 1131-1142.

Brand, D., Soccol, C. R., Sabu, A., & Roussos, S. (2010). Production of fungal biological control agents through solid state fermentation: a case study on *Paecilomyces lilacinus* against root-knot nematodes. *Micologia Appl Int.*, **22(1)**, 31-48.

Brefort, T., Tanaka, S., Neidig, N., Doehlemann, G., Vincon, V., & Kahmann, R. (2014). Characterization of the largest effector gene cluster of *Ustilago maydis*. *PLoS Pathog.*, 10(7), e1003866.

Brenner, S. (1974). The genetics of *Caenorhabditis elegans*. *Genetics*, *77*(1), 71-94.

Campbell, E. M., & Fares, H. (2010). Roles of CUP-5, the *Caenorhabditis elegans* orthologue of human TRPML1, in lysosome and gut granule biogenesis. *BMC Cell Biol.*, **11(1)**, 1-10.

Canonne, J., & Rivas, S. (2012). Bacterial effectors target the plant cell nucleus to subvert host transcription. *Plant Signal Behav.*, **7(2)**, 217-221.

Chalfie, M., & Sulston, J. (1981). Developmental genetics of the mechanosensory neurons of *Caenorhabditis elegans*. *Dev Biol.*, **82(2)**, 358-370.

Chalfie, M., Sulston, J. E., White, J. G., Southgate, E., Thomson, J. N., & Brenner, S. (1985). The neural circuit for touch sensitivity in *Caenorhabditis elegans*. *J Neurosci.*, **5(4)**, 956-964.

Chen, C., Fenk, L. A., & de Bono, M. (2013). Efficient genome editing in *Caenorhabditis elegans* by CRISPR-targeted homologous recombination. *Nucl Acid Res.*, **41(20)**, e193.

Chen, S. A., Lin, H. C., Schroeder, F. C., & Hsueh, Y. P. (2021). Prey sensing and response in a nematode-trapping fungus is governed by the MAPK pheromone response pathway. *Genetics*, **217(2)**, iyaa008.

Chiang, C. K., Mehta, N., Patel, A., Zhang, P., Ning, Z., Mayne, J., ... & Figeys, D. (2014). The proteomic landscape of the suprachiasmatic nucleus clock reveals large-scale

coordination of key biological processes. *PLoS genet.*, **10(10)**, e1004695.

Chin, C. S., Peluso, P., Sedlazeck, F. J., Nattestad, M., Concepcion, G. T., Clum, A., ... & Schatz, M. C. (2016). Phased diploid genome assembly with single-molecule real-time sequencing. *Nat Meth.*, **13(12)**, 1050-1054.

Choe, A., von Reuss, S. H., Kogan, D., Gasser, R. B., Platzer, E. G., Schroeder, F. C., & Sternberg, P. W. (2012). Ascaroside signaling is widely conserved among nematodes. *Curr Biol.*, **22(9)**, 772-780.

Coyne, D. L., Cortada, L., Dalzell, J. J., Claudius-Cole, A. O., Haukeland, S., Luambano, N., & Talwana, H. (2018). Plant-parasitic nematodes and food security in Sub-Saharan Africa. *Annu Rev Phytopathol.*, **56**, 381-403.

Culetto, E., & Sattelle, D. B. (2000). A role for *Caenorhabditis elegans* in understanding the function and interactions of human disease genes. *Hum Mol Genet.*, **9(6)**, 869-877.

Darby, C., & Falkow, S. (2001). Mimicry of a G protein mutation by pertussis toxin expression in transgenic *Caenorhabditis elegans*. *Infect Immun.*, **69(10)**, 6271-6275.

De Jonge, R., Peter van Esse, H., Kombrink, A., Shinya, T., Desaki, Y., Bours, R., ... & Thomma, B. P. (2010). Conserved fungal LysM effector Ecp6 prevents chitin-triggered immunity in plants. *science*, **329(5994)**, 953-955.

Dijksterhuis, J., Veenhuis, M., Harder, W., & Nordbring-Hertz, B. (1994). Nematophagous fungi: physiological aspects and structure–function relationships. *Adv Microb Physiol.*, **36**, 111-143.

Dimov, I., & Maduro, M. F. (2019). The *C. elegans* intestine: organogenesis, digestion, and physiology. *Cell Tissue Res.*, **377**, 383-396.

Djamei, A., Schipper, K., Rabe, F., Ghosh, A., Vincon, V., Kahnt, J., ... & Kahmann, R. (2011). Metabolic priming by a secreted fungal effector. *Nature*, **478(7369)**, 395-398.

Duddington, C. L. (1949). A new predacious species of Trichothecium. *Trans Br Mycol Soc.*, **32,** (3-4).

Dunbar, T. L., Yan, Z., Balla, K. M., Smelkinson, M. G., & Troemel, E. R. (2012). *C. elegans* detects pathogen-induced translational inhibition to activate immune signaling. *Cell Host Microbe*, **11(4)**, 375-386.

Duplessis, S., Cuomo, C. A., Lin, Y. C., Aerts, A., Tisserant, E., Veneault-Fourrey, C., ... & Martin, F. (2011). Obligate biotrophy features unraveled by the genomic analysis of rust fungi. *Proc Natl Acad Sci.*, **108(22)**, 9166-9171.

Edison, A. S. (2009). *Caenorhabditis elegans* pheromones regulate multiple complex behaviors. *Curr Opin Neurobiol.*, **19(4)**, 378-388.

Epe, C., Holst, C., Koopmann, R., Schnieder, T., Larsen, M., & von Samson-Himmelstjerna, G. (2009). Experiences with *Duddingtonia flagrans* administration to

parasitized small ruminants. *Vet Parasitol.*, **159(1)**, 86-90.

Ermolaeva, M. A., & Schumacher, B. (2014). Insights from the worm: the *C. elegans* model for innate immunity. *Semin Immunol.*, **26(4)**, 303-309.

Ermolaeva, M. A., Segref, A., Dakhovnik, A., Ou, H. L., Schneider, J. I., Utermöhlen, O., ... & Schumacher, B. (2013). DNA damage in germ cells induces an innate immune response that triggers systemic stress resistance. *Nature*, **501(7467)**, 416-420.

Estes, K. A., Dunbar, T. L., Powell, J. R., Ausubel, F. M., & Troemel, E. R. (2010). bZIP transcription factor *zip-2* mediates an early response to *Pseudomonas aeruginosa* infection in *Caenorhabditis elegans*. *Proc Natl Acad Sci.*, **107(5)**, 2153-2158.

Ewbank, J. J. (2002). Tackling both sides of the host–pathogen equation with *Caenorhabditis elegans*. *Microbes Infect.*, **4(2)**, 247-256.

Ezcurra, M., Benedetto, A., Sornda, T., Gilliat, A. F., Au, C., Zhang, Q., ... & Gems, D. (2018). *C. elegans* eats its own intestine to make yolk leading to multiple senescent pathologies. *Curr Biol.*, **28(16)**, 2544-2556.

Farman, M. L., & Leong, S. A. (1998). Chromosome walking to the AVR1-CO39 avirulence gene of *Magnaporthe grisea*: discrepancy between the physical and genetic maps. *Genetics*, **150(3)**, 1049-1058.

Ferreira, P. G., Muñoz-Aguirre, M., Reverter, F., Sa Godinho, C. P., Sousa, A., Amadoz, A., ... & Guigo, R. (2018). The effects of death and post-mortem cold ischemia on human tissue transcriptomes. *Nat Commun.,* **9(1)**, 490.

Ferreira, P. G., Muñoz-Aguirre, M., Reverter, F., Sa Godinho, C. P., Sousa, A., Amadoz, A., ... & Guigo, R. (2018). The effects of death and post-mortem cold ischemia on human tissue transcriptomes. *Nat Commun.*, **9(1)**, 490.

Figueroa, M., Ortiz, D., & Henningsen, E. C. (2021). Tactics of host manipulation by intracellular effectors from plant pathogenic fungi. *Curr Opin Plant Biol.*, **62**, 102054.

Fischer, R., & Requena, N. (2022). Small-secreted proteins as virulence factors in nematode-trapping fungi. *Trends Microbiol.*, **30(7)**, 615-617.

Ghahari, H., Lehr, P. A., Lavigne, R. J., Hayat, R., & Ostovan, H. (2007). New records of robber flies (*Diptera, Asilidae*) for the Iranian fauna with their prey records. *Far East. Entomol.*, **(179)**, 1-9.

Godfrey, D. (2010). Genome expansion and gene loss in powdery mildew fungi reveal tradeoffs in extreme parasitism. *Science*, **6010 (2010)**: 1543–46

Golden, J. W., & Riddle, D. L. (1982). A pheromone influences larval development in the nematode *Caenorhabditis elegans*. *Science*, **218(4572)**, 578-580.

Gout, L., Fudal, I., Kuhn, M. L., Blaise, F., Eckert, M., Cattolico, L., ... & Rouxel, T.

(2006). Lost in the middle of nowhere: the AvrLm1 avirulence gene of the Dothideomycete *Leptosphaeria maculans*. *Mol Microbiol.*, **60(1)**, 67-80.

Gravato-Nobre, M. J., Vaz, F., Filipe, S., Chalmers, R., & Hodgkin, J. (2016). The invertebrate lysozyme effector ILYS-3 is systemically activated in response to danger signals and confers antimicrobial protection in *C. elegans*. *PLoS Pathog.*, **12(8)**, e1005826.

Guo, X., & Lu, R. (2013). Characterization of virus-encoded RNA interference suppressors in *Caenorhabditis elegans*. *Uirusu.*, **87(10)**, 5414-5423.

Gürlebeck, D., Thieme, F., & Bonas, U. (2006). Type III effector proteins from the plant pathogen *Xanthomonas* and their role in the interaction with the host plant. *J Plant Physiol.*, **163(3)**, 233-255.

Hadj-Moussa, H., Watts, A. J., & Storey, K. B. (2019). Genes of the undead: hibernation and death display different gene profiles. *FEBS Lett.*, **593(5)**, 527-532.

Hagedorn, G., & Scholler, M. (1999). A reevaluation of predatory orbiliaceous fungi.

Haj Hammadeh, H., Serrano, A., Wernet, V., Stomberg, N., Hellmeier, D., Weichert, M., ... & Fleißner, A. (2022). A dialogue-like cell communication mechanism is conserved in filamentous ascomycete fungi and mediates interspecies interactions. *Proc Natl Acad Sci.*, **119(12)**, e2112518119.

Henderson, S. T., & Johnson, T. E. (2001). daf-16 integrates developmental and environmental inputs to mediate aging in the nematode *Caenorhabditis elegans*. *Curr Biol.*, **11(24)**, 1975-1980.

Heuer, H., Yin, Y. N., Xue, Q. Y., Smalla, K., & Guo, J. H. (2007). Repeat domain diversity of avrBs3-like genes in *Ralstonia solanacearum* strains and association with host preferences in the field. *Appl Environ Microbiol.*, **73(13)**, 4379-4384.

Hoang, C. V., Bhaskar, C. K., & Ma, L. S. (2021). A novel core effector Vp1 promotes fungal colonization and virulence of *Ustilago maydis*. *J Fungi (Basel)*. **7(8)**, 589-589.

Hoffmann, J. A. (2003). The immune response of *Drosophila*. *Nature*, **426(6962)**, 33-38.

Hsueh, Y. P., Mahanti, P., Schroeder, F. C., & Sternberg, P. W. (2013). Nematode-trapping fungi eavesdrop on nematode pheromones. *Curr Biol.*, **23(1)**, 83-86.

Huo, L., Hug, J. J., Fu, C., Bian, X., Zhang, Y., & Müller, R. (2019). Heterologous expression of bacterial natural product biosynthetic pathways. *Nat Prod Rep.*, **36(10)**, 1412-1436.

Hyde, K. D., Swe, A., & Zhang, K. Q. (2014). *Nematode-trapping fungi* (pp. 1-12). Springer Netherlands.

Ishii, K. J., Koyama, S., Nakagawa, A., Coban, C., & Akira, S. (2008). Host innate

immune receptors and beyond: making sense of microbial infections. *Cell Host Microbe*, **3(6)**, 352-363.

Jansson, H. B., Persson, C., & Odeslius, R. (2000). Growth and capture activities of nematophagous fungi in soil visualized by low temperature scanning electron microscopy. *Mycologia*, **92(1)**, 10-15.

Jiang, X., Xiang, M., & Liu, X. (2017). Nematode-trapping fungi. *Microbiol Spectr.*, **5(1)**, 5-1.

Jones, J. D., & Dangl, J. L. (2006). The plant immune system. *nature*, **444(7117)**, 323-329.

Jones, J. T., Haegeman, A., Danchin, E. G., Gaur, H. S., Helder, J., Jones, M. G., ... & Perry, R. N. (2013). Top 10 plant-parasitic nematodes in molecular plant pathology. *Mol Plant Pathol.*, **14(9)**, 946-961.

Kamoun, S. (2006). A catalogue of the effector secretome of plant pathogenic oomycetes. *Annu Rev Phytopathol.*, **44**, 41-60.

Kang, H., Nguyen, Q. M., Iswanto, A. B. B., Hong, J. C., Bhattacharjee, S., Gassmann, W., & Kim, S. H. (2021). Nuclear localization of HopA1Pss61 is required for effector-triggered immunity. *Plants*, **10(5)**, 888.

Khan, M., Seto, D., Subramaniam, R., & Desveaux, D. (2018). Oh, the places they'll go! A survey of phytopathogen effectors and their host targets. *Plant J.*, **93(4)**, 651-663.

Kim, D. H., Feinbaum, R., Alloing, G., Emerson, F. E., Garsin, D. A., Inoue, H., ... & Ausubel, F. M. (2002). A conserved p38 MAP kinase pathway in *Caenorhabditis elegans* innate immunity. *Science*, **297**, 623-626.

Kim, D. H., Liberati, N. T., Mizuno, T., Inoue, H., Hisamoto, N., Matsumoto, K., & Ausubel, F. M. (2004). Integration of Caenorhabditis elegans MAPK pathways mediating immunity and stress resistance by MEK-1 MAPK kinase and VHP-1 MAPK phosphatase. *Proc Natl Acad Sci.*, **101(30)**, 10990-10994.

Kiontke, K. C., Félix, M. A., Ailion, M., Rockman, M. V., Braendle, C., Pénigault, J. B., & Fitch, D. H. (2011). A phylogeny and molecular barcodes for Caenorhabditis, with numerous new species from rotting fruits. *BMC Evol Biol.*, **11(1)**, 1-18.

Kiontke, K., & Fitch, D. H. (2013). Nematodes. *Curr Biol.*, **23(19)**, 862-864.

Kiontke, K., & Sudhaus, W. (2006). Ecology of *Caenorhabditis species*. *WormBook*, **9**, 1-14.

Kloppholz, S., Kuhn, H., & Requena, N. (2011). A secreted fungal effector of *Glomus intraradices* promotes symbiotic biotrophy. *Curr Biol.*, **21(14)**, 1204-1209.

Kumari, S. (2017). Morphological and molecular characterizations of cereal cyst nematode Heterodera avenae Wollenweber, 1924 from the Czech Republic. *J Integr Agric.*, **16(3)**,

532-539.

Kurz, C. L., & Ewbank, J. J. (2003). *Caenorhabditis elegans*: an emerging genetic model for the study of innate immunity. *Nat Rev Genet.*, **4(5)**, 380-390.

Kurz, C. L., & Tan, M. W. (2004). Regulation of aging and innate immunity in *C. elegans. Aging Cell*, **3(4)**, 185-193.

Lanver, D., Tollot, M., Schweizer, G., Lo Presti, L., Reissmann, S., Ma, L. S., ... & Kahmann, R. (2017). *Ustilago maydis* effectors and their impact on virulence. *Nat Rev Microbiol.*, **15(7)**, 409-421.

Larsen, M., Faedo, M., & Waller, P. J. (1994). The potential of nematophagous fungi to control the free-living stages of nematode parasites of sheep: survey for the presence of fungi in fresh faeces of grazing livestock in Australia. *Vet Parasitol.*, **53(3-4)**, 275-281.

Larsen, M., Wolstrup, J., Henriksen, S. A., Dackman, C., Grønvold, J., & Nansen, P. (1991). In vitro stress selection of nematophagous fungi for biocontrol of parasitic nematodes in ruminants. *J Helminthol.*, **65(3)**, 193-200.

Laugé, R., Goodwin, P. H., De Wit, P. J., & Joosten, M. H. (2000). Specific HR-associated recognition of secreted proteins from *Cladosporium fulvum* occurs in both host and non-host plants. *Plant J.*, **23(6)**, 735-745.

Law, W., Wuescher, L. M., Ortega, A., Hapiak, V. M., Komuniecki, P. R., & Komuniecki, R. (2015). Heterologous expression in remodeled *C. elegans*: a platform for monoaminergic agonist identification and anthelmintic screening. *PLoS Pathog.*, **11(4)**, e1004794.

Lee, S. H., Omi, S., Thakur, N., Taffoni, C., Belougne, J., Engelmann, I., ... & Pujol, N. (2018). Modulatory upregulation of an insulin peptide gene by different pathogens in *C. elegans*. *Virulence*, **9(1)**, 648-658.

Li, W., Kennedy, S. G., & Ruvkun, G. (2003). daf-28 encodes a *C. elegan*s insulin superfamily member that is regulated by environmental cues and acts in the DAF-2 signaling pathway. *Genes Dev.*, **17(7)**, 844-858.

Li, X., Kang, Y. Q., Luo, Y. L., Zhang, K. Q., Zou, C. G., & Liang, L. M. (2017). The NADPH oxidase AoNoxA in *Arthrobotrys oligospora* functions as an initial factor in the infection of *Caenorhabditis elegans*. *J Microbiol.*, 55, 885-891.

Li, Y., Hyde, K. D., Jeewon, R., Cai, L., Vijaykrishna, D., & Zhang, K. (2005). Phylogenetics and evolution of nematode-trapping fungi (Orbiliales) estimated from nuclear and protein coding genes[J]. *Mycologia*, **97(5)**: 1034-1046.

Liang, L., Wu, H., Liu, Z., Shen, R., Gao, H., Yang, J., & Zhang, K. (2013). Proteomic and transcriptional analyses of *Arthrobotrys oligospora* cell wall related proteins reveal complexity of fungal virulence against nematodes. *Appl Microbiol Biotechnol.*, **97**, 8683-

8692.

Liang, M., Du, S., Dong, W., Fu, J., Li, Z., Qiao, Y., ... & Wang, R. (2019). iTRAQ-based quantitative proteomic analysis of mycelium in different predation periods in nematode trapping fungus *Duddingtonia flagrans*. *Biol. Control*, **134**, 63-71.

Lightle, S. A., Oakley, J. I., & Nikolova-Karakashian, M. N. (2000). Activation of sphingolipid turnover and chronic generation of ceramide and sphingosine in liver during aging. *Mech Aging Dev.*, **120(1-3)**, 111-125.

Liu, J. H., Yang, J. Y., Hsu, D. W., Lai, Y. H., Li, Y. P., Tsai, Y. R., & Hou, M. H. (2019). Crystal structure-based exploration of arginine-containing peptide binding in the ADP-ribosyltransferase domain of the type III effector XopAI protein. *Int J Mol Sci.*, **20(20)**, 5085.

Liu, K., Tian, J., Xiang, M., & Liu, X. (2012). How carnivorous fungi use three-celled constricting rings to trap nematodes. *Protein Cell*, **3**, 325-328.

Liu, Q., Li, D., Jiang, K., Zhang, K. Q., & Yang, J. (2022). AoPEX1 and AoPEX6 are required for mycelial growth, conidiation, stress response, fatty acid utilization, and trap formation in *Arthrobotrys oligospora*. *Microbiol Spectr.,* **10(2)**, e00275-22.

Lo Presti, L., Lanver, D., Schweizer, G., Tanaka, S., Liang, L., Tollot, M., ... & Kahmann, R. (2015). Fungal effectors and plant susceptibility. *Annu Rev Plant Biol.*, **66**, 513-545.

Lopez, V. A., Park, B. C., Nowak, D., Sreelatha, A., Zembek, P., Fernandez, J., ... & Tagliabracci, V. S. (2019). A bacterial effector mimics a host HSP90 client to undermine immunity. *Cell*, **179(1)**, 205-218.

López-Robles, J., Olalla, C., Rad, C., Díez-Rojo, M. A., López-Pérez, J. A., Bello, A., & Rodríguez-Kábana, R. (2013). The use of liquid swine manure for the control of potato cyst nematode through soil disinfestation in laboratory conditions. *Crop Prot.*, **49**, 1-7.

Luderer, R., Rivas, S., Nürnberger, T., Mattei, B., Van den Hooven, H. W., Van der Hoorn, R. A., ... & Joosten, M. H. (2001). No evidence for binding between resistance gene product Cf-9 of tomato and avirulence gene product AVR9 of *Cladosporium fulvum*. *Mol Plant Microbe Interact.*, **14(7)**, 867-876.

Luderer, R., Takken, F. L., Wit, P. J. D., & Joosten, M. H. (2002). *Cladosporium fulvum* overcomes Cf-2-mediated resistance by producing truncated AVR2 elicitor proteins. *Mol Microbiol.*, **45(3)**, 875-884.

Ma, N., Zhao, Y., Wang, Y., Yang, L., Li, D., Yang, J., ... & Yang, J. (2021). Functional analysis of seven regulators of G protein signaling (RGSs) in the nematode-trapping fungus *Arthrobotrys oligospora*. *Virulence*, **12(1)**, 1825-1840.

Mahoney, C. J., & Strongman, D. B. (1994). Nematophagous fungi from cattle manure in four states of decomposition at three sites in Nova Scotia, *Can. Mycol.*, **86(3)**, 371-375.

Martin, F., Aerts, A., Ahrén, D., Brun, A., Danchin, E. G. J., Duchaussoy, F., ... & Grigoriev, I. V. (2008). The genome of Laccaria bicolor provides insights into mycorrhizal symbiosis. *Nature*, ***452*(7183)**, 88-92.

Martin, F., Kohler, A., Murat, C., Balestrini, R., Coutinho, P. M., Jaillon, O., ... & Wincker, P. (2010). Périgord black truffle genome uncovers evolutionary origins and mechanisms of symbiosis. *Nature*, **464(7291)**, 1033-1038.

Matheu, A., Maraver, A., & Serrano, M. (2008). The Arf/p53 pathway in cancer and aging. *Cancer Res.*, **68(15)**, 6031-6034.

McElwee, J., Bubb, K., & Thomas, J. H. (2003). Transcriptional outputs of the *Caenorhabditis elegans* forkhead protein DAF-16. *Aging Cell*, **2(2)**, 111-121.

McGhee, J. D. (2007). The *C. elegans* intestine. *WormBook: The Online Review of C. elegans Biology [Internet]*.

Meerupati, T., Andersson, K. M., Friman, E., Kumar, D., Tunlid, A., & Ahren, D. (2013). Genomic mechanisms accounting for the adaptation to parasitism in nematode-trapping fungi. *PLoS Genet.*, **9(11)**, e1003909.

Meister, P., Towbin, B. D., Pike, B. L., Ponti, A., & Gasser, S. M. (2010). The spatial dynamics of tissue-specific promoters during *C. elegans* development. *Genes Dev.*, **24(8)**, 766-782.

Mele, M., Costa, R. O., & Duarte, C. B. (2019). Alterations in GABAA-receptor trafficking and synaptic dysfunction in brain disorders. *Front Cell Neurosci.*, **13**, 77.

Michálek, O., Walker, A. A., Šedo, O., Zdráhal, Z., King, G. F., & Pekár, S. (2022). Composition and toxicity of venom produced by araneophagous white-tailed spiders (*Lamponidae: Lampona sp.*). *Sci Rep.*, **12(1)**, 21597.

Millet, A. C., & Ewbank, J. J. (2004). Immunity in *Caenorhabditis elegans*. *Curr Opin Immunol.*, **16(1)**, 4-9.

Mittal, R., Sukumaran, S. K., Selvaraj, S. K., Wooster, D. G., Babu, M. M., Schreiber, A. D., ... & Prasadarao, N. V. (2010). Fcγ receptor I alpha chain (CD64) expression in macrophages is critical for the onset of meningitis by *Escherichia coli* K1. *PLoS Pathog.*, **6(11)**, e1001203.

Münter, S., Sabass, B., Selhuber-Unkel, C., Kudryashev, M., Hegge, S., Engel, U., ... & Frischknecht, F. (2009). *Plasmodium sporozoite* motility is modulated by the turnover of discrete adhesion sites. *Cell Host Microbe*, **6(6)**, 551-562.

Murphy, C. T., McCarroll, S. A., Bargmann, C. I., Fraser, A., Kamath, R. S., Ahringer, J., ... & Kenyon, C. (2003). Genes that act downstream of DAF-16 to influence the lifespan of *Caenorhabditis elegans*. *Nature*, **424(6946)**, 277-283.

Murray, D. S., & Wharton, D. A. (1990). Capture and penetration processes of the free-living juveniles of *Trichostrongylus colubriformis* (Nematoda) by the nematophagous

fungus, *Arthrobotrys oligospora*. *Parasitology*, **101(1)**, 93-100.

Mushegian, A. R., Bassett Jr, D. E., Boguski, M. S., Bork, P., & Koonin, E. V. (1997). Positionally cloned human disease genes: patterns of evolutionary conservation and functional motifs. *Proc Natl Acad Sci.*, **94(11)**, 5831-5836.

Nicholas, H. R., & Hodgkin, J. (2004). The ERK MAP kinase cascade mediates tail swelling and a protective response to rectal infection in *C. elegans*. *Curr Biol.*, **14(14)**, 1256-1261.

Niu, X. M., & Zhang, K. Q. (2011). *Arthrobotrys oligospora*: a model organism for understanding the interaction between fungi and nematodes. *Mycology*, **2(2)**, 59-78.

Nordbring-Hertz, B., & Mattiasson, B. (1979). Action of a nematode-trapping fungus shows lectin-mediated host–microorganism interaction. *Nature*, **281(5731)**, 477-479.

Nordbring-Hertz, B., & Stålhammar-Carlemalm, M. (1978). Capture of nematodes by *Arthrobotrys oligospora*, an electron microscope study. *Can J Bot.*, **56(10)**, 1297-1307.

Nordbring-Hertz, B., Jansson, H. B., & Tunlid, A. (2001). Nematophagous fungi. *eLS*.

O'Connell, R. J., Thon, M. R., Hacquard, S., Amyotte, S. G., Kleemann, J., Torres, M. F., ... & Vaillancourt, L. J. (2012). Lifestyle transitions in plant pathogenic *Colletotrichum* fungi deciphered by genome and transcriptome analyses. *Nat Genet.*, **44(9)**, 1060-1065.

Patterson, G. I., & Padgett, R. W. (2000). TGFβ-related pathways: roles in *Caenorhabditis elegans* development. *Trends Genet.*, **16(1)**, 27-33.

Pfister, D. H. (1994). *Orbilia fimicola*, a nematophagous discomycete and its *Arthrobotrys anamorph*. *Mycologia*, **86(3)**, 451-453.

Pires, D., Vicente, C. S., Menéndez, E., Faria, J. M., Rusinque, L., Camacho, M. J., & Inácio, M. L. (2022). The fight against plant-parasitic nematodes: Current status of bacterial and fungal biocontrol agents. *Pathogens*, **11(10)**, 1178.

Pozhitkov, A. E., Neme, R., Domazet-Lošo, T., Leroux, B. G., Soni, S., Tautz, D., & Noble, P. A. (2017). Tracing the dynamics of gene transcripts after organismal death. *Open biol.*, **7(1)**, 160267.

Prahlad, V., & Morimoto, R. I. (2009). Integrating the stress response: lessons for neurodegenerative diseases from *C. elegans*. *Trends Cell Biol.*, **19(2)**, 52-61.

Prahlad, V., Cornelius, T., & Morimoto, R. I. (2008). Regulation of the cellular heat shock response in *Caenorhabditis elegans* by thermosensory neurons. *Science*, **320(5877)**, 811-814.

Pukkila-Worley, R., & Ausubel, F. M. (2012). Immune defense mechanisms in the *Caenorhabditis elegans* intestinal epithelium. *Curr Opin Immunol.*, **24(1)**, 3-9.

Pungaliya, C., Srinivasan, J., Fox, B. W., Malik, R. U., Ludewig, A. H., Sternberg, P.

W., & Schroeder, F. C. (2009). A shortcut to identifying small molecule signals that regulate behavior and development in *Caenorhabditis elegans*. *Proc Natl Acad Sci.*, **106(19)**, 7708-7713.

Redkar, A., Hoser, R., Schilling, L., Zechmann, B., Krzymowska, M., Walbot, V., & Doehlemann, G. (2015). A secreted effector protein of *Ustilago maydis* guides maize leaf cells to form tumors. *Plant Cell*, **27(4)**, 1332-1351.

Rocafort, M., Fudal, I., & Mesarich, C. H. (2020). Apoplastic effector proteins of plant-associated fungi and oomycetes. *Curr Opin Plant Biol.*, **56**, 9-19.

Sánchez-Vallet, A., Saleem-Batcha, R., Kombrink, A., Hansen, G., Valkenburg, D. J., Thomma, B. P., & Mesters, J. R. (2013). Fungal effector Ecp6 outcompetes host immune receptor for chitin binding through intrachain LysM dimerization. *eLife*, **2**, e00790.

Saunders, D. G., Win, J., Cano, L. M., Szabo, L. J., Kamoun, S., & Raffaele, S. (2012). Using hierarchical clustering of secreted protein families to classify and rank candidate effectors of rust fungi. *PloS One*, **7(1)**, e29847.

Schenck, S., Chase Jr, T., Rosenzweig, W. D., & Pramer, D. (1980). Collagenase production by nematode-trapping fungi. *Appl Environ Microbiol.*, **40(3)**, 567-570.

Schneider-Poetsch, T., Ju, J., Eyler, D. E., Dang, Y., Bhat, S., Merrick, W. C., ... & Liu, J. O. (2010). Inhibition of eukaryotic translation elongation by cycloheximide and lactimidomycin. *Nat Chem Biol.*, **6(3)**, 209-217.

Schulze-Lefert, P., & Panstruga, R. (2011). A molecular evolutionary concept connecting nonhost resistance, pathogen host range, and pathogen speciation. *Trends Plant Sci.*, **16(3)**, 117-125.

Shi, Q., Mao, Z., Zhang, X., Ling, J., Lin, R., Zhang, X., ... & Xie, B. (2018). The novel secreted Meloidogyne incognita effector MiISE6 targets the host nucleus and facilitates parasitism in *Arabidopsis*. *Front Plant Sci.*, **9**, 252.

Silva, A. R., Araújo, J. V., Braga, F. R., Frassy, L. N., Tavela, A. O., Carvalho, R. O., & Castejon, F. V. (2009). Biological control of sheep gastrointestinal nematodiasis in a tropical region of the southeast of Brazil with the nematode predatory fungi *Duddingtonia flagrans* and *Monacrosporium thaumasium*. *J Parasitol Res*., **105**, 1707-1713.

Silva, B. F., Carrijo-Mauad, J. R., Braga, F. R., Campos, A. K., Araújo, J. V., & Amarante, A. F. (2010). Efficacy of *Duddingtonia flagrans* and *Arthrobotrys robusta* in controlling sheep parasitic gastroenteritis. *J Parasitol Res.*, **106**, 1343-1350.

Singh, S., Singh, B., & Singh, A. P. (2015). Nematodes: a threat to sustainability of agriculture. *Procedia Environ Sci.*, **29**, 215-216.

Singh, V., & Aballay, A. (2006). Heat-shock transcription factor (HSF)-1 pathway required

for *Caenorhabditis elegans* immunity. *Proc Natl Acad Sci.*, **103(35)**, 13092-13097.

Skibbe, D. S. (2000). *Ustilago maydis* Maize Tumors Caused by. *Development*, **127**, 725-725.

Sperschneider, J., Dodds, P. N., Gardiner, D. M., Manners, J. M., Singh, K. B., & Taylor, J. M. (2015). Advances and challenges in computational prediction of effectors from plant pathogenic fungi. *PLoS Pathog.*, **11(5)**, e1004806.

Sperschneider, J., Dodds, P. N., Gardiner, D. M., Manners, J. M., Singh, K. B., & Taylor, J. M. (2015). Advances and challenges in computational prediction of effectors from plant pathogenic fungi. *PLoS Pathog.*, **11(5)**, e1004806.

Srinivasan, J., von Reuss, S. H., Bose, N., Zaslaver, A., Mahanti, P., & Ho, M. C. O, Doherty, OG, Edison, AS, Sternberg, PW, and Schroeder, FC (2012) A modular library of small molecule signals regulates social behaviors in *Caenorhabditis elegans*. *PLoS Biol.*, **10**, e1001237.

Stergiopoulos, I., & de Wit, P. J. (2009). Fungal effector proteins. *Annu Rev Phytopathol.*, **47**, 233-263.

Stringham, E. G., Dixon, D. K., Jones, D., & Candido, E. P. (1992). Temporal and spatial expression patterns of the small heat shock (hsp16) genes in transgenic *Caenorhabditis elegans*. *Mol Biol Cell.*, **3(2)**, 221-233.

Syme, R. A., Hane, J. K., Friesen, T. L., & Oliver, R. P. (2013). Resequencing and comparative genomics of *Stagonospora nodorum*: sectional gene absence and effector discovery. *G3 (Bethesda)*, ***3*(6)**, 959-969.

Takai, Y., Sasaki, T., & Matozaki, T. (2001). Small GTP-binding proteins. *Physiol Rev.*, **81(1)**, 153-208.

Tan, K. C., Phan, H. T., Rybak, K., John, E., Chooi, Y. H., Solomon, P. S., & Oliver, R. P. (2015). Functional redundancy of necrotrophic effectors–consequences for exploitation for breeding. *Front Plant Sci.*, **6**, 501-501.

Tanaka, S., Brefort, T., Neidig, N., Djamei, A., Kahnt, J., Vermerris, W., ... & Kahmann, R. (2014). A secreted *Ustilago maydis* effector promotes virulence by targeting anthocyanin biosynthesis in maize. *eLife*, **3**, e01355.

Tarr, D. E. K. (2012). Distribution and characteristics of ABFs, cecropins, nemapores, and lysozymes in nematodes. *Dev Comp Immunol.*, **36(3)**, 502-520.

Thomas, J. H. (1990). Genetic analysis of defecation in *Caenorhabditis elegans*. *Genetics*, **124(4)**, 855-872.

Thorn, R. G., & Barron, G. L. (1984). Carnivorous mushrooms. *Science*, **224(4644)**, 76-78.

Tunlid, A., & Jansson, S. (1991). Proteases and their involvement in the infection and immobilization of nematodes by the nematophagous fungus *Arthrobotrys oligospora*.

Appl Environ Microbiol., **57(10)**, 2868-2872.

Tunlid, A., Jansson, H. B., & Nordbring-Hertz, B. (1992). Fungal attachment to nematodes. *Mycol Res.*, **96(6)**, 401-412.

Tzou, P., De Gregorio, E., & Lemaitre, B. (2002). How Drosophila combats microbial infection: a model to study innate immunity and host–pathogen interactions. *Curr Opin Microbiol.*, **5(1)**, 102-110.

Veenhuis, M., Nordbring-Hertz, B., & Harder, W. (1985). Development of fate of electron-dense microbodies in trap cells of the nematophagous fungus *Arthrobotrys oligospora*. *Antonie Van Leeuwenhoek*, **51(4)**, 399-407.

Vilela, V. L. R., Feitosa, T. F., Braga, F. R., de Araújo, J. V., dos Santos, A., de Morais, D. F., ... & Athayde, A. C. R. (2016). Coadministration of nematophagous fungi for biological control over gastrointestinal helminths in sheep in the semiarid region of northeastern Brazil. *Vet Parasitol.*, **221**, 139-143.

Vilela, V. L. R., Feitosa, T. F., Braga, F. R., de Araújo, J. V., de Oliveira Souto, D. V., da Silva Santos, H. E., ... & Athayde, A. C. R. (2012). Biological control of goat gastrointestinal helminthiasis by *Duddingtonia flagrans* in a semi-arid region of the northeastern Brazil. *Vet Parasitol.*, **188(1-2)**, 127-133.

Walker, A. A., Dobson, J., Jin, J., Robinson, S. D., Herzig, V., Vetter, I., ... & Fry, B. G. (2018). Buzz kill: Function and proteomic composition of venom from the giant assassin fly *Dolopus genitalis* (*Diptera: Asilidae*). Toxins, **10(11)**, 456.

Wang, B. B., Liu, W., Chen, M. Y., Li, X., Han, Y., Xu, Q., ... & Wang, Y. Y. (2015). Isolation and characterization of China isolates of *Duddingtonia flagrans*, a candidate of the nematophagous fungi for biocontrol of animal parasitic nematodes. *J Parasitol.*, **101(4)**, 476-484.

Wang, P., Jiang, H., Boeren, S., Dings, H., Kulikova, O., Bisseling, T., & Limpens, E. (2021). A nuclear-targeted effector of *Rhizophagus irregularis* interferes with histone 2B mono-ubiquitination to promote arbuscular mycorrhization. *New Phytol.*, **230(3)**, 1142-1155.

Wernet, N., Wernet, V., & Fischer, R. (2021). The small-secreted cysteine-rich protein CyrA is a virulence factor participating in the attack of *Caenorhabditis elegans* by *Duddingtonia flagrans*. *PLoS Pathog.*, **17(11)**, e1010028.

Wernet, V., & Fischer, R. (2023). Establishment of *Arthrobotrys flagrans* as biocontrol agent against the root pathogenic nematode *Xiphinema index*. *Environ Microbiol.*, **25(2)**, 283-293.

Wernet, V., Wäckerle, J., & Fischer, R. (2022). The STRIPAK component SipC is involved in morphology and cell-fate determination in the nematode-trapping fungus

Duddingtonia flagrans. Genetics, **220(1)**, iyab153.

Westerink, N., Roth, R., Van den Burg, H. A., De Wit, P. J., & Joosten, M. H. (2002). The AVR4 elicitor protein of *Cladosporium fulvum* binds to fungal components with high affinity. *Mol Plant Microbe Interact.*, **15(12)**, 1219-1227.

White, J. G., Southgate, E., Thomson, J. N., & Brenner, S. (1986). The structure of the nervous system of the nematode *Caenorhabditis elegans*. *Philos Trans R Soc Lond B Biol Sci.*, **314(1165)**, 1-340.

Whitfield, F. S. (1925) The Relation between the Feeding-habits and the Structure of the Month-parts in the Asilidæ (Diptera). *J Zool*., **95(2)**, 599-638

Wicker, T., Oberhaensli, S., Parlange, F., Buchmann, J. P., Shatalina, M., Roffler, S., ... & Keller, B. (2013). The wheat powdery mildew genome shows the unique evolution of an obligate biotroph. *Nat Genet.*, **45(9)**, 1092-1096.

Yaeno, T., Li, H., Chaparro-Garcia, A., Schornack, S., Koshiba, S., Watanabe, S., ... & Shirasu, K. (2011). Phosphatidylinositol monophosphate-binding interface in the oomycete RXLR effector AVR3a is required for its stability in host cells to modulate plant immunity. *Proc Natl Acad Sci.*, **108(35)**, 14682-14687.

Yamada, K., Hirotsu, T., Matsuki, M., Butcher, R. A., Tomioka, M., Ishihara, T., ... & Iino, Y. (2010). Olfactory plasticity is regulated by pheromonal signaling in *Caenorhabditis elegans*. *Science*, **329(5999)**, 1647-1650.

Yang, J., Wang, L., Ji, X., Feng, Y., Li, X., Zou, C., ... & Zhang, K. Q. (2011). Genomic and proteomic analyses of the fungus *Arthrobotrys oligospora* provide insights into nematode-trap formation. *PLoS pathog.*, **7(9)**, e1002179.

Yang, L., Li, X., Bai, N., Yang, X., Zhang, K. Q., & Yang, J. (2022). Transcriptomic analysis reveals that Rho GTPases regulate trap development and lifestyle transition of the nematode-trapping fungus *Arthrobotrys oligospora*. *Microbiol Spectr.*, **10(1)**, e01759-21.

Yang, L., Li, X., Xie, M., Bai, N., Yang, J., Jiang, K., ... & Yang, J. (2021). Pleiotropic roles of Ras GTPases in the nematode-trapping fungus *Arthrobotrys oligospora* identified through multi-omics analyses. *IScience*, **24(8)**, 102820.

Yang, Y., Yang, E., An, Z., & Liu, X. (2007). Evolution of nematode-trapping cells of predatory fungi of the Orbiliaceae based on evidence from rRNA-encoding DNA and multiprotein sequences. *Proc Natl Acad Sci.*, **104(20)**, 8379-8384.

Yochem, J., & Herman, R. K. (2005). Genetic mosaics. *WormBook: The Online Review of C. elegans Biology [Internet]*.

Youssar, L., Wernet, V., Hensel, N., Yu, X., Hildebrand, H.-G., Schreckenberger, B.,

Kriegler, M., Hetzer, B., Frankino, P., Dillin, A. *et al*. (2019). Intercellular communication is required for trap formation in the nematode-trapping fungus *Duddingtonia flagrans*. *PLoS Genet.*, **15**, e1008029.

Yu, X., Hu, X., Pop, M., Wernet, N., Kirschhöfer, F., Brenner-Weiß, G., ... & Fischer, R. (2021). Fatal attraction of *Caenorhabditis elegans* to predatory fungi through 6-methyl-salicylic acid. *Nat Commun.*, **12(1)**, 5462.

Zhang, H. X., Tan, J. L., Wei, L. X., Wang, Y. L., Zhang, C. P., Wu, D. K., ... & Niu, X. M. (2012). Morphology regulatory metabolites from *Arthrobotrys oligospora*. *J Nat Prod.*, **75(7)**, 1419-1423.

Zhang, L., Zhou, Z., Guo, Q., Fokkens, L., Miskei, M., Pócsi, I., ... & Lin, M. (2016). Insights into adaptations to a near-obligate nematode endoparasitic lifestyle from the finished genome of *Drechmeria coniospora*. *Sci Rep.*, **6(1)**, 1-15.

Zhang, W., Liu, D., Yu, Z., Hou, B., Fan, Y., Li, Z., ... & Wang, R. (2020). Comparative genome and transcriptome analysis of the nematode-trapping fungus *Duddingtonia flagrans* reveals high pathogenicity during nematode infection. *Biol. Control*, **143**, 104159.

Zhang, Y., Lu, H., & Bargmann, C. I. (2005). Pathogenic bacteria induce aversive olfactory learning in *Caenorhabditis elegans*. *Nature*, **438(7065)**, 179-184.

Zhu, G., Yin, F., Wang, L., Wei, W., Jiang, L., & Qin, J. (2016). Modeling type 2 diabetes-like hyperglycemia in *C. elegans* on a microdevice. *Integr Biol.*, **8(1)**, 30-38.

Zhu, M. C., Li, X. M., Zhao, N., Yang, L., Zhang, K. Q., & Yang, J. K. (2022). Regulatory mechanism of trap formation in the nematode-trapping fungi. *J Fungi (Basel).*, **8(4)**, 406.

Ziegler, K., Kurz, C. L., Cypowyj, S., Couillault, C., Pophillat, M., Pujol, N., & Ewbank, J. J. (2009). Antifungal innate immunity in *C. elegans*: PKCδ links G protein signaling and a conserved p38 MAPK cascade. *Cell Host Microbe*, **5(4)**, 341-352.

Zou, C. G., Ma, Y. C., Dai, L. L., & Zhang, K. Q. (2014). Autophagy protects *C. elegans* against necrosis during Pseudomonas aeruginosa infection. *Proc Natl Acad Sci U S A.*, **111(34)**, 12480-12485.

Acknowledgement

Twenty-four years old is the best time for a woman, and I came to beautiful Germany at this best time and started a new journey. My four-year doctoral journey is coming to an end. The setbacks, challenges, and triumphs during these four years have become the most cherished medals adorning my personal growth.

I am immensely grateful to my mentor, Prof. Dr. Reinhard Fischer, whose patience and understanding rescued me from the struggles I faced with my research project. His gentle and encouraging words instilled confidence in me to face not only scientific obstacles but also the challenges of life. I appreciate his demonstration of the significance of being an inspiring mentor to students. He treated each of us with equality and respect, always offering assistance in a patient manner, whether it was helping me revise my papers and my presentation slides. I extend my highest respect to him. I would also like to thank Prof. Dr. Jörg Kämper and Prof. Dr. Natalia Requena for their dedicated guidance and kind support during this journey.

I would like to express my gratitude to the members of the Worm Group, including Maria, Jenni, Marius, Anna-Lena, Satur, Xiaodi, and Jia, for their assistance with my research. I am thankful to Elke for her support and understanding, as well as her assistance in worm handling. I am grateful to all the colleagues in the lab who have been with me throughout these four years. I would like to thank my friends for standing by me during the most challenging initial years. Special thanks to my family for their unwavering support. I am grateful to the China Scholarship Council (CSC) for providing the funding that enabled me to successfully complete my doctoral journey. I will forever love my motherland. Thanks to my idol, Zhu Yilong, who taught me the meaning of

"accumulate steadily and accomplish great things."

These have been the most enriching four years of my life, during which profound changes have occurred within me. Within these four years, there were pain, confusion, and setbacks. But looking back now, I realize that everything happened for the sake of a better version of myself in the future. Such experiences have endowed me with the courage to face life's ever-changing nature. The time spent in the Germany will forever hold the most precious memories in my life. I hope that in the future, we will have the opportunity to meet again.

Supplementary data

Table S1: 50 upregulated genes associated with digestion pathways between transgenic worms expressing *einA* under the *hsp-16.48* promoter at RT, and 33 °C for three hours.

GeneID	Symbol	Up/Down-Regulation	log2Fold Change	Pvalue	Nr Description
179447	AC3.5	up	1.078685	1.86E-74	NP_001256214.1//Aminopeptidase-like protein AC3.5 [Caenorhabditis elegans]
179210	asp-12	Up	2.28802	1.50E-199	NP_505134.1//Peptidase A1 domain-containing protein [Caenorhabditis elegans]
180250	asp-17	Up	1.743819	0.00064	NP_741673.1//Aspartic protease 17 [Caenorhabditis elegans]
172324	C10G11.8	up	2.694535	1.54E-50	NP_001367497.1//AAA domain-containing protein [Caenorhabditis elegans]
177493	cest-10	up	1.354665	4.54E-07	NP_501133.3//COesterase domain-containing protein [Caenorhabditis elegans]
181493	cest-13	up	1.078003	3.06E-07	NP_741921.1//Carboxylic ester hydrolase [Caenorhabditis elegans]
182819	cest-7	up	3.421464	7.94E-05	NP_001367204.1//Carboxylic ester hydrolase [Caenorhabditis elegans];
173089	clp-3	up	1.468769	2.48E-05	NP_493052.3//Calpain catalytic domain-containing protein [Caenorhabditis elegans]
190738	clp-6	up	1.302078	1.18E-08	NP_500081.2//Calpain catalytic domain-containing protein [Caenorhabditis elegans]
185746	clp-8	up	6.554589	2.48E-09	NP_493327.2//Calpain catalytic domain-containing protein [Caenorhabditis elegans]
178612	cpr-5	up	2.137781	0	NP_503383.1//Cathepsin B-like cysteine proteinase 5 [Caenorhabditis elegans]
179645	cpr-9	up	1.116104	0	NP_001369965.1//Pept_C1 domain-containing protein [Caenorhabditis elegans]
174155	cth-2	up	1.514761	2.02E-254	NP_495449.1//Putative cystathionine gamma-lyase 2 [Caenorhabditis elegans]

173818	ctsa-1.1	up	1.161506	0	NP_494846.1//Serine carboxypeptidase ctsa-1.1 [Caenorhabditis elegans]
174802	ctsa-1.2	up	2.032452	0	NP_496507.1//Serine carboxypeptidase ctsa-1.2 [Caenorhabditis elegans]
177646	eppl-1	up	1.426339	1.12E-119	NP_001023346.1//Ethanolamine-phosphate phospho-lyase homolog 1 [Caenorhabditis elegans]
177314	gba-4	up	2.256505	2.19E-30	NP_500785.1//Putative glucosylceramidase 4 [Caenorhabditis elegans]
178129	hdl-1	up	3.110424	6.19E-09	NP_502265.2//Probable aromatic-L-amino-acid decarboxylase [Caenorhabditis elegans]
182464	hdl-2	up	3.889817	2.41E-17	NP_501539.3//Histidine Decarboxyase Like [Caenorhabditis elegans]
180928	ilys-5	up	3.970482	0	NP_001024594.1//Invertebrate LYSozyme [Caenorhabditis elegans]
171937	ipla-4	up	2.255501	2.38E-07	NP_491201.3//Intracelllar PhosphoLipase A family [Caenorhabditis elegans]
187683	lips-17	up	1.087463	6.15E-08	NP_495596.3//LIPaSe related [Caenorhabditis elegans]
179428	lys-1	up	1.127167	1.63E-221	NP_505642.1//Lysozyme-like protein 1 [Caenorhabditis elegans]
179429	lys-2	up	2.430508	0	NP_505643.1//Lysozyme-like protein 2 [Caenorhabditis elegans]
178086	lys-4	up	1.279978	9.76E-155	NP_502192.1//LYSozyme [Caenorhabditis elegans]
186491	lys-5	up	1.956673	1.91E-05	NP_502193.1//Lysozyme-like protein 5 [Caenorhabditis elegans]
178087	lys-6	up	2.03868	6.53E-19	NP_502194.1//LYSozyme [Caenorhabditis elegans]
187474	M110.7	up	2.947533	2.55E-06	NP_495734.3//Putative patatin-like phospholipase domain-containing protein M110.7 [Caenorhabditis elegans]
180426	nas-15	up	1.898386	1.09E-46	NP_508154.2//Zinc metalloproteinase nas-15 [Caenorhabditis elegans]
188420	nas-20	up	1.603378	1.31E-19	NP_505906.2//Zinc metalloproteinase nas-20 [Caenorhabditis elegans]
188423	nas-22	up	2.415037	0.000374	NP_505908.2//Zinc metalloproteinase nas-22 [Caenorhabditis elegans]

3565992	nas-23	up	1.608809	3.74E-08	NP_001022281.1//Zinc metalloproteinase nas-23 [Caenorhabditis elegans]
188809	nas-27	up	3.197939	7.85E-08	NP_493926.2//Zinc metalloproteinase nas-27 [Caenorhabditis elegans]
187045	nas-3	up	4.814697	1.21E-35	NP_505445.2//Zinc metalloproteinase nas-3 [Caenorhabditis elegans]
172506	nas-36	up	1.514573	1.08E-16	NP_492109.2//Zinc metalloproteinase nas-36 [Caenorhabditis elegans]
180407	nas-38	up	1.448724	5.91E-29	NP_001359993.1//Zinc metalloproteinase nas-38 [Caenorhabditis elegans]
173684	nep-10	up	3.5025	2.70E-08	NP_494532.2//NEPrilysin metallopeptidase family [Caenorhabditis elegans]
173672	nep-13	up	4.033423	1.62E-11	NP_001342017.1//NEPrilysin metallopeptidase family [Caenorhabditis elegans]
188176	nep-20	up	3.011973	4.92E-10	NP_001317749.1//NEPrilysin metallopeptidase family [Caenorhabditis elegans]
173933	nep-5	up	3.115477	1.06E-05	NP_001364754.1//NEPrilysin metallopeptidase family [Caenorhabditis elegans]
184628	nep-6	up	3.841302	1.06E-10	NP_494537.1//NEPrilysin metallopeptidase family [Caenorhabditis elegans]
184631	nep-8	up	4.049244	8.68E-12	NP_001309548.1//Peptidase_M13 domain-containing protein [Caenorhabditis elegans]
173683	nep-9	up	2.984893	8.07E-07	NP_494531.2//NEPrilysin metallopeptidase family [Caenorhabditis elegans]
180992	sur-5	up	2.265519	0	NP_509229.1//Acetoacetyl-CoA synthetase [Caenorhabditis elegans]
172557	suro-1	up	1.257123	5.07E-58	NP_492177.2//Putative carboxypeptidase suro-1 [Caenorhabditis elegans]
13181077	T28B8.4	up	2.61471	1.37E-08	NP_001263461.1//Uncharacterized protein CELE_T28B8.4 [Caenorhabditis elegans]
191201	try-7	Up	3.528379	1.69E-05	NP_491910.2//Peptidase S1 domain-containing protein [Caenorhabditis elegans]
179134	try-8	Up	4.058894	0.000193	NP_504916.1//Peptidase S1 domain-containing protein [Caenorhabditis elegans]
189809	Y40H7A.10	up	1.288129	9.53E-31	NP_502836.1//Uncharacterized protein

					CELE_Y40H7A.10 [Caenorhabditis elegans]
3565105	Y41E3.18	up	3.321928	7.94E-05	NP_001023462.2//Hydrolase_4 domain-containing protein [Caenorhabditis elegans]

Table S2: two upregulated genes associated with digestion pathways between N2 worms at RT, and 33 °C for three hours.

GeneID	Symbol	Up/Down-Regulation	log2Fold Change	Pvalue	Nr Description
179017	cest-24	Up	8.45E-161	5.17E-163	NP_504613.1//Carboxylic ester hydrolase [Caenorhabditis elegans]
179429	lys-2	up	7.86E-31	2.77E-32	NP_505643.1//Lysozyme-like protein 2 [Caenorhabditis elegans]

Table S3: 21 upregulated genes associated with digestion pathways between N2 worms and transgenic worms expressing *einA* under the *eft-3* promoter.

GeneID	symbol	Up/Down-Regulation	log2Fold Change	Pvalue	Nr Description
179210	asp-12	Up	3.130062	0	NP_505134.1//Peptidase A1 domain-containing protein [Caenorhabditis elegans]
191611	C10G11.8	up	2.667315	2.98E-71	NP_001367497.1//AAA domain-containing protein [Caenorhabditis elegans]
173884	cest-10	up	1.901595	6.86E-15	NP_501133.3//COesterase domain-containing protein [Caenorhabditis elegans]
185709	cpr-6	up	1.764573	0	OZG24397.1//hypothetical protein FL83_00324, partial [Caenorhabditis latens]
190221	ctsa-1.2	up	1.755763	0.000468	NP_496507.1//Serine carboxypeptidase ctsa-1.2 [Caenorhabditis elegans]
175569	F56F11.4	up	1.487813	1.53E-13	NP_001367906.1//AAA domain-containing protein [Caenorhabditis elegans];NP_001367905.1//AAA domain-containing protein [Caenorhabditis elegans]
172425	hdl-2	up	1.434284	3.75E-34	NP_501539.3//Histidine Decarboxyase Like [Caenorhabditis elegans]
259576	ilys-5	up	1.411576	4.75E-67	NP_001024594.1//Invertebrate LYSozyme [Caenorhabditis elegans]

245997	ipla-3	up	1.408873	2.81E-22	NP_001366900.1//Intracellular PhosphoLipase A family [Caenorhabditis elegans]
181957	ipla-4	up	1.408711	1.65E-80	NP_491201.3//Intracelllar PhosphoLipase A family [Caenorhabditis elegans]
188458	lys-1	up	1.357997	0.000711	NP_505642.1//Lysozyme-like protein 1 [Caenorhabditis elegans]
180232	lys-2	up	1.357409	1.84E-10	NP_505643.1//Lysozyme-like protein 2 [Caenorhabditis elegans]
182442	map-1	up	1.348522	6.25E-08	NP_001368273.1//Methionine aminopeptidase [Caenorhabditis elegans]
176171	NA	up	1.310206	0.000871	NP_493916.2//LIPaSe related [Caenorhabditis elegans]
177904	nas-20	up	1.278716	0.000115	NP_505906.2//Zinc metalloproteinase nas-20 [Caenorhabditis elegans]
175648	nep-10	up	1.275794	0.000316	NP_494532.2//NEPrilysin metallopeptidase family [Caenorhabditis elegans]
171641	nep-20	up	1.27565	1.09E-42	NP_001317749.1//NEPrilysin metallopeptidase family [Caenorhabditis elegans]
176471	nep-23	up	1.275555	0	NP_503004.2//NEPrilysin metallopeptidase family [Caenorhabditis elegans]
178054	nep-9	up	1.275476	0.000556	NP_494531.2//NEPrilysin metallopeptidase family [Caenorhabditis elegans]
173060	R03G8.6	up	1.221278	4.55E-10	NP_510175.1//Aminopeptidase [Caenorhabditis elegans]
173856	try-1	Up	1.833622	8.79E-73	NP_494910.2//Peptidase S1 domain-containing protein [Caenorhabditis elegans]